CHAPTER ONE

INTRODUCTION

1.1 Background to the Study

The earth's surface is affected by three main types of radiation from the sun: global solar (or total), beam (or direct), and longwave (or indirect) radiation. Global solar radiation is composed of direct and indirect radiation. Approximately 99% of the total radiation from the sun that reaches the earth is beam radiation, which has a wavelength range of 0.29 to 3.9 μm and is not subjected to interference from any interspatial matter. The remaining 1% is longwave radiation, which falls into the range of 4 to approximately 50 μm and encounters interference with matter on its way from the sun. Furthermore, downward longwave radiation (DLR) can be classified into three types: before, between, and after the DLR range of approximately 8 to 12 μm. The wavelength region between 8 to 12 μm is known as the atmospheric window that DLR comes directly from space. Additionally, there is net longwave radiation at the surface of the earth, which is caused by the difference between the downward and upward longwave radiations. Gases that absorb and radiate DLR include water molecule (H_2O), carbon dioxide (CO_2), ozone (O_3), nitrous oxide (N_2O), carbon monoxide (CO), oxygen (O_2), methane (CH_4), and nitrogen (N_2). The nature of the interaction between DLR and these gases and aerosols is dependent on the type of atmosphere, and the major absorbers of DLR are water molecules (Coulson, 1975; Niemela *et al.,* 2001; Liang *et al.,* 2012; Cotton *et al.,* 2010).

Although the beam radiation can only be received during a certain period of the daytime, and by extension, global radiation also has this limitation, downward longwave radiation is received 24 hours a day. By virtue of the diurnal disposition of DLR, DLR is an important parameter of both radiant and energy aspects of the atmosphere. Because DLR is primarily in

thermal form, it is responsible for the heat content without which the earth would be much cooler (Sellers, 1965; Ohmura, 2001). According to Soares *et al.,* (2004), data for DLR have the ability to replace data for cloud cover, and the radiation is a better index indicator of the climatic features of a region than any other meteorological parameter such as temperature, water vapour pressure and relative humidity.

Subsequently, DLR, as a part of the net longwave radiation (as depicted by equation 1.0 at the end of this paragraph), is a constituent of the surface energy of the radiation budget on the earth. DLR is an essential variable in land models used in prediction, in forecasting and in climate change evaluation. Furthermore, DLR is known have influence on the inducement of greenhouse gas-forced surface warming via its relation with water vapour (Culf and Gash, 1993; IPCC, 1996; Allan and Slingo, 1998; Allan, 2000). A direct linkage exists between DLR and the radiative cooling of the atmosphere, which, in turn, is also associated with the atmospheric hydrological cycle (Allan, 2006). Therefore, it is necessary that DLR be accurately calculated or simulated because DLR is also required for its role in radiant energy of the ocean dynamics in climate models (John *et al.,* 1997). Furthermore the knowledge of this component of the earth's surface energy budget is necessary for many meteorological studies e.g. forecasting of diurnal temperature variation, nocturnal frost and fogs. These aforementioned examples dwell on the agricultural uses of the knowledge of DLR. If the nighttime minimum threshold temperature that leaves can withstand before drying and subsequent dew formation can be effectively predicted then farmers would apply preventive fungicides to avert economic losses of crops and outbreaks of foliar disease (Diak *et al.,* 2000). Other methods to curb the effect of frost formation occasioned by low DLR by farmers include the breeding of low temperature resistance crops and the practice of special farming like terraces (Lhomme *et al.,* 2007). Also DLR is an important element of the energy balance of building especially for night time cooling, greenhouse and solar collectors. Its

quantification is necessary to estimate correctly the heat loses of these systems as well as for determination of climate variability and global warning (Catolonotti *et al.,* 1975; Crawford and Duchon, 1999).

$$R_n = S_n + L_n = DSR - USR + DLR - ULR \quad (1.0)$$

where R_n is the net radiation, S_n is the net shortwave radiation, L_n is the net longwave radiation, DSR is the downward shortwave radiation, USR is the upward shortwave radiation, DLR is the downward longwave radiation and ULR is the upward longwave radiation. Both USR and ULR are not directly from the sun but are secondary due to the consequences of reflection at the earth's surface.

Direct measurement of DLR is performed with an instrument known as a pyrgeometer. Generally DLR data are rare because of instrument complexities and high cost. As a result the instrument is not available in most weather stations and where present there are cases of small durations of measurement. Apart from their comparatively high cost as earlier mentioned, pyrgeometers are highly delicate instruments that require constant cleaning, shading, ventilation and in some instances, correction for the heating or cooling effects of the dome when in use for optimum precision. Furthermore, as a necessity to avoid malfunctioning, pyrgeometer requires regular calibration within two-year intervals because of the heating of the dome which influence may be as high as 30 W/m^2 (Miskolczi *et al.,* 1997). However, there is no standard for calibration because the instruments are undergoing changes in components that are eventually characterised by diverse testing methods. Although efforts have been regularly attempted for the standardisation and general improvement of these instruments, the field responses of calibrated pyrgeometers, which are distinct from laboratory observations, still pose vital limitations to the use of these instruments (Duarte *et*

al., 2006; Wang and Dickinson, 2013). With the issues affecting the pyrgeometers, its use has been limited to experts, and the instruments are not available in most weather stations.

Due to associated problems of the prygeometer, models are sometimes employed to circumvent the paucity of data. Most of the DLR models employ cloud cover and screen-level atmospheric parameters such as temperature and water vapor pressure, or temperature and water vapor pressure profiles (Niemela *et al.*, 2001). If profiles of atmospheric temperature and humidity are available, downward long wave radiation can easily be calculated. Evaluation can be done from many proposed models such as Schwarzchild equation (Berdahl and Fromberd, 1982; Heitor *et al.*. 1991) among other theoretical methods. However, these profiles are rarely available.

The longwave radiation equations are sometimes grouped into two types - the analytical methods and the empirical methods. The main difference between the two types is that while the analytical (or theoretical) are derived on a physical basis, the other are obtained by empirical correlations. Each group of models has advantages and disadvantages. For instance, models that need screen-level parameters are often location biased, which necessitates the calibration of coefficients when applied to a new location. Unlike data for screen-level parameters which are easily available and are commonly used for the empirical methods, data for temperature and water vapor pressure profiles needed for the analytical methods are generally lacking. Although these equations from both methods are known to work reasonably well on the daily or longer-term mean basis, yet hourly estimates often required in models of the surface energy balance are more prone to error (Arnfield, 1979).

In 1992, the World Meteorological Organization (WMO) through the Baseline Surface Radiation Network (BSRN) set out to measure DLR around the globe with the highest level of precision. Since 1992, about 40 ground stations have measured DLR even as more stations

are coming on board even though some stations are inactive. Presently four of the stations are located in Africa, namely De Aar, Pretoria (30.67°S, 23.99°E) in South Africa, Namib Desert (23.56°S, 15.04°E) in Namibia, Ilorin (8.53°N, 4.57°E) in Nigeria, and Tamanrasset (22.78°N, 5.51°E) in Algeria. While two of the four stations are situated below the equator, one is around the equator, and the other is above the equator, although none of them is on the longitudinal west of the continent (McArthur, 2005; König-Langlo *et al.,* 2013). The National Aeronautic and Space Administration (NASA) is one of the organizations that collect DLR satellite data. At the University of Ilorin, DLR measurement has been taken from September 1992 – August 1994 and from June 1995 – April 1998. It should be pointed out that the measurements of both global solar and shortwave radiations on this site far exceed that of DLR.

In Nigeria, previous studies using mostly the first period of measurement have established the DLR pattern at the University of Ilorin to be seasonally dependent, and the differences between the dry season and the rainy season are relatively small (Miskolczi e*t al.,* 1997; Udo and Aro, 1999; Wild *et al.,* 2001). For now, this site remains the only known location for ground measurements in Nigeria, and data from the site, along with data from other parts of the globe, have been used as inputs for global data reanalysis (Morcrette, 2002).

Another source of data acquisition is via remote sensing or satellite method, which tends to solve the problem of data scarcity, particularly concerning longevity and the simultaneous coverage of many locations. However, satellite data also have their attendant problems. The main issues that affect satellite method are techniques of retrieval for calculating DLR from satellite images, leading to differing readings from different satellites over same locations. As a result, DLR data from satellites are associated with varying degrees of detachment from ground truths (Nussbauser and Pinker, 2012; Ellington, 1995). Furthermore, there is another important source of DLR data, namely, reanalysis methods, which in most cases use satellite

data as inputs. Satellite-derived data have several advantages relative to ground measurements. These include the ability to record long-range data over time, wide space coverage and cost effectiveness (Diak *et al.,* 2000). Furthermore unlike pyrgeometers, satellites are less prone to malfunction. Satellite measurements are inputs in numerical weather prediction (NWP) models requiring prior knowledge of the amount of atmospheric gases such as CO_2. However satellite-based data may not be suitable for some applications because in some cases agreement with ground-truth data remains an issue. Although satellite-based data have greatly improved yet there is no universally accepted method for deriving data from the acquired images (Mc Millan and Govjindaraju 1983; Ellingson, 1995; Chou and Neelin, 1996; Kubuta *et al.,* 2002; Lee and Ellingson, 2002; Liu *et al.,* 2005; Zhou *et al.,* 2007; Wang and Liang, 2009a).

Another method of data acquisition is via the application of the artificial neural networks. Artificial neural networks (ANNs) which have the ability of recognizing hidden as well as clear pattern and information imbedded in a set of data given to it, are known to perform better than traditional methods (Kalogiron, 2000). The tasks that ANNs can perform include pattern classification, clustering or categorisation, function approximation, prediction/forecasting, optimization, content-addressable memory and control. Thus it finds applications in many areas of endeavours (Muller *et al.,* 1995; Basheer and Hajmeer, 2000) Primarily ANNs are algorithms that mimic the human nervous system and have various complex intricacies associated with it. Such include the network architecture/topology that fall under two main umbrellas of feedforward and feedback/recurrent and the diverse learning processes which are relatively complex (Jain *et al.,* 1996). ANNs surpass the Von Neumann model of basic computer by having parallel, distributed and self-learning as against serial, centralised and stored programme processing system, fault tolerance and poorly defined and unconstrained operating environment. It is expected that future development will make ANNs

have more abilities like massive parallelism and low energy consumption even as neural networks provide room for hybrid systems.

1.2 Statement of Problem

The earth would have been about 40^{o}C cooler than it is without DLR (Sellers, 1965) and the radiation is a parameter that better reveals the climatic features of a location than other atmospheric parameters (Soares *et al.*, 2004). However due to instrument associated problems the radiation has been measured on ground in Nigeria only at Ilorin even though satellite data for every location exist. Also most equations for DLR are locality biased and have to be tested in another location to ascertain their applicability, and if none is found adequate then a model fitting the location could be developed. Hence the questions are; How related are ground data and satellite data? How much of DLR do we know about in Nigeria, be it on yearly, monthly or daily basis? And can the radiation be effectively modelled in Nigeria? Our knowledge about DLR in Nigeria is relatively low since not much research on this radiation has been previously carried out in Nigeria owing to paucity of data. We do not know the extent of the variability of the radiation over Nigeria and if DLR can effectively be modelled in Nigeria.

1.3 Aim and Objectives

The overall aim of this work is to estimate DLR in the Nigerian environment using new clear skies empirical models and artificial neural networks.

The specific objectives of this study are to:

I. Examine the relationship between ground data and satellite data of DLR.

II. Establish the daily, monthly and yearly patterns of the radiation in Nigeria.

III. Segment the country into appropriate DLR categories.

IV. Evaluate the performance of existing DLR equations under clear skies in Ilorin and develop new equations using the data of the site.

V. And estimate DLR using artificial neural networks under different conditions.

1.4 Significance of the Study

The knowledge of DLR can be used for many purposes such as architectural design for heat conservation or otherwise in buildings, weather and meteorological forecasting for environmental protection and danger mitigation. It is also needed for agricultural and academic purposes amongst others. A good example can be in the area of greenhouse agriculture whereby plants that exist in one part of the country can effectively be grown in another part of the country. If the greenhouse effect is deployed based on the knowledge of the radiation in the north to grow and plant there trees found in the southern region of the country, then the problem of deforestation and desert encroachment can be solved. An international example is the fact that Malaysia, the number one producer and exporter of palm produce in the world actually came over to Nigeria and other West Africa regions, obtained the palm tree, went back and improved on the breed (Jalami *et al.,* 1997; Kajisak *et al.*, 1997; World Bank, 2006; Wu *et al.*, 2007). According to Yusoff (2006), the expansion of the palm industry in Malaysia started in the late 1950s and currently she is the world's largest producer and exporter of palm oil, replacing Nigeria as the chief producer since 1971.

Above all, in addition to providing more knowledge about the radiation patterns and the climatic conditions across Nigeria, this work will provide insight into the methods that are viable for modelling DLR particularly in Nigeria.

1.5 Definition of Terms

Artificial neural networks are algorithms that mimic the process found in the nervous system. Alternatively it is known as neural networks.

Bias is an additional input with constant value embedded in the mathematical model of an artificial neuron. Usually the constant value is unity.

Clearness index is the total solar radiation incident on a horizontal surface at the surface of the earth divided by incoming top-of-atmosphere insolation of the earth.

Clear skies are the state of the skies when mostly void of cloud formations.

Direct solar radiation on a horizontal surface is the quantity of solar radiant energy emitted from the solid angle subtended by the visible disc of the sun and passing through a unit area in the horizontal in unit time. This is also called the vertical component of the direct solar radiation.

Downward longwave radiation is the longwave radiation emitted downwards by the earth's atmosphere and passing through a unit horizontal area at the level of the instrument in unit time.

Weight can be defined as the connections between neuron *i* and neuron *j* which can be written as $w_{i,j}$

1.6 List of Abbreviations

ANNs; artificial neural networks

K_T: Clearness index

DLR: downward longwave radiation

BSRN: Baseline Surface Radiation Network

MBE: mean bias error

MABE: mean absolute bias error

NASA: National Aeronautics and Space Administration

NIMET: Nigeria Meteorological Services

RMSE: root mean square error

R: Correlation coefficient

$\mathbf{t_s}$: t statistic

SD: standard deviation

W/m^2: Watts per square meter

a: output of a neuron

b: bias

f: activation function

p: input vector in neural networks

n: net output of a neuron

W: matric vector of connected weights

s: sum of connected weights

IW: input weight matrix

LW: layer weight matrix

CHAPTER TWO

LITERATURE REVIEW

2.1 Downward Longwave Radiation

The entire atmospheric radiation comprises mainly two types namely the solar (or shortwave) regime and terrestrial (or longwave) regime. The demarcation between the two lies in the wavelengths range of both of them. While shortwave radiation is directly from the sun, whose surface temperature at about 6000K causes over 99% of the solar energy being at wavelengths of less than 4μm (starting from about 0.3μm). However the terrestrial radiation is from constituents of the earth's atmosphere at a much lower temperature (generally <300K), which yields most energy in wavelengths roughly in the region of 4 - 50μm. Thus, for overall energy considerations of wavelengths ranging from about 0 - 50μm, a division of the spectrum at about 4μm effectively separates the two (Duchon and Wilk, 1994; Coulson, 1975; Enz *et al.*, 1975). While others (e.g Jimenez *et al.*, 1987; Berger *et al.*, 1992) put it at 3μm, however WMO (1981) puts it between 3 - 5μm.

Longwave radiation generation is based on the concept of blackbody. A blackbody is a body that uniformly both absorbs and emits electromagnetic radiation at efficiency of 100%, though there is no such body in reality. In reality bodies can be referred to as grey bodies whereby the absorption and ability to emit radiation fall below 100%. Most of the energy of the earth is acquired from the sun and the earth's atmosphere re-radiates the energy from the sun. As shown in Fig 2.1.1, some part of the sun's radiation gets to the earth's surface without interaction with matter and the surface sends back radiation energy to the space. The earth's atmosphere interaction with radiation from the sun is in two directions; some are reflected back to space while some are transmitted downwards to the ground. Still on Fig 2.1.1, the radiation emitted from the earth's surface is termed upward longwave radiation and

could get back to space if it is within the range of the atmospheric window (8 - 12 µm) as indicted by the upwards dash arrow. Otherwise it interacts with the atmosphere. The difference between both upward and downward longwave radiation is known as net longwave radiation.

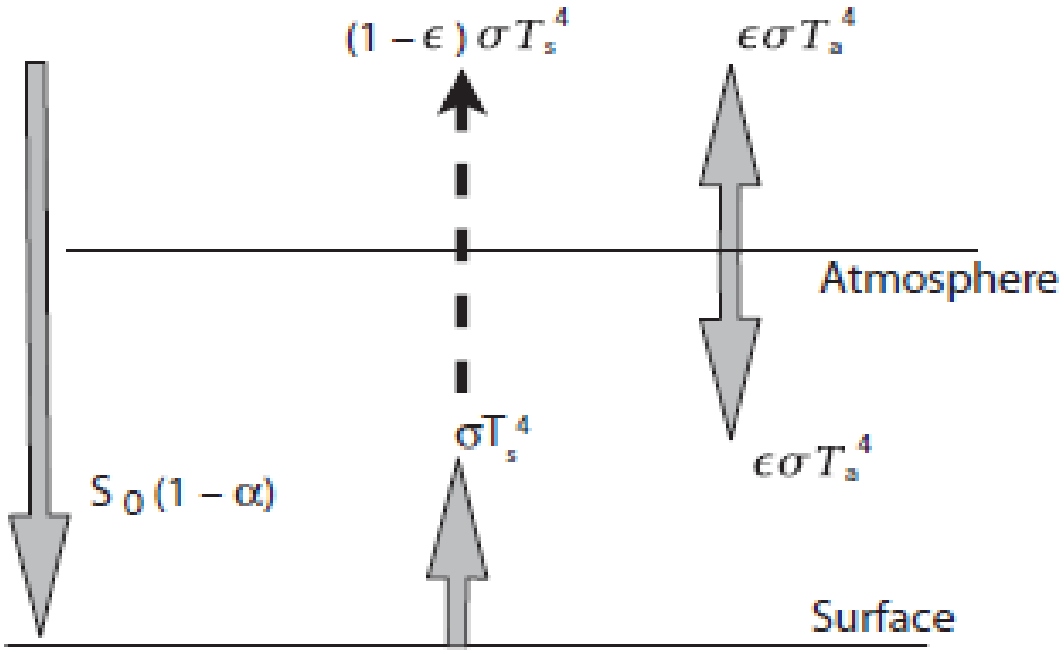

Fig 2.1.1: A two-level energy balance model which show the absorbed and reflected energy of the earth's atmosphere.

The earth's atmosphere is composed of gases like nitrogen, oxygen, argon, water vapour, carbon dioxide, neon, helium, methane and trace gases like krypton, hydrogen, nitrous oxide, carbon monoxide, xenon, ozone, chlorofluorocarbons (CFCs) etc. The major gases in the atmosphere are nitrogen, oxygen, carbon dioxide and water vapour. While most of the gases in the atmosphere are generally fixed, water vapour is not fixed but varies from time to time and from region to region, such that depending on temperature and wind, at critical values may cause rainfall.

The region of terrestrial or thermal radiation of the atmosphere surface system is in some respect more complicated than that of the solar radiation regime, although the same concepts and relationships are applicable to both. The greater complexity of the terrestrial regime is largely as a result of emission and absorption of such longwave radiation by all real materials – solids, liquids and gases which constitute the physical system of interest. The radiative processes of most interest in the solar regime are absorption, reflection and scattering by the constituents of the system, with emission of short wavelength radiation being entirely negligible by comparison. In the terrestrial regime, on the other hand, emission is a major factor, radiation being emitted by the solid and liquid materials of the earth surface, by dust and clouds in the atmosphere and by many atmospheric gases. Absorption by the same materials is always of prime concern in terrestrial range but the scattering of longwave radiation plays much less important role in terrestrial than in solar regime (Coulson, 1975). It also has been noted that longwave radiation from both ground (including ocean) and atmosphere continues during the night when no solar radiation is being received.

Longwave radiation is absorbed strongly by certain minor atmospheric gases. The radiation is absorbed in spectral bands which consist of many individual narrow spectral lines. The line absorption is caused by changes in the vibrational and rotational energies. An absorption gas is also an emitter of infrared radiation (at the absorbing wavelength) depending on its temperature and the temperature of the environment. Thus a given volume of the atmosphere both receives and emits infrared radiation and will cool and warm according to whether the net radiation input is negative or positive. Spectral radiometer measurements and theoretical studies of the atmosphere indicate that the downward sky radiation (also called counter radiation or down welling radiation) is a spectral division which departs from that of a blackbody (Quinn *et al.,* 1984). The spectral features in this sky radiation are largely attributable to emissions due to vibrational – rotational transmissions in atmospheric water

vapour, carbon dioxide, ozone and to a smaller extent by other asymmetrical molecules such as CH_4, CO, N_2O (Quinn *et al.,* 1984; Berger *et al.,* 1992). The contribution of water vapour is the most important (greater than 90%) (Berger *et al*., 1992). The spectral region from about 4 to approximately 100μm gives the distribution typical of the blackbody at ambient temperature. However, in the spectral region $8\mu m < \lambda < 13.5\mu m$ and to a much smaller extent in the 7 - 12μm region, the downward sky radiation intensity is generally weaker because of the absence of emission bands from carbon dioxide and water vapour in these regions. This is the so – called atmospheric window and as far as radiative cooling potential is concerned is significant (Quinn *et al.,* 1984). Experimental (Berdahl and Fromberg, 1982) and theoretical works (Berdahl and Martin, 1984) indicated that best cooling results are realized under clear sky and low humidity conditions. According to Berger *et al.,* (1988), the sky being a blackbody except at the region of the atmospheric window, serves as a cold radiative source in hot climates whereas it is avoided in temperate climates.

2.2 Review of DLR Modelling

Angstrom (1918) was the first to establish an expression for DLR in relationship with screen level atmospheric variables like temperature and water vapour pressure. After his pioneer work, other models have been tailored in such fashion (Brunt, 1932; Efimova, 1961; Swinbank, 1963; Idso and Jackson, 1969; Satterlund, 1979; Brutsaret, 1975; Idso, 1981; Alados-Arboledas, 1992; König-Langlo and Augstein, 1994; Plata, 1996; Guest, 1998; Crawford and Duchon, 1999; Iziomon *et al*., 2003; Wang and Liang, 2009b). The equations for DLR are mostly of two types namely the theoretical models and the empirical models and there are cases whereby both are combined.

Most of the models' coefficients are locations biased hence testing before adoption for another location is necessary and sometimes calibration is required for fitting (Aase and Idso, 1978; Jimenez *et al.*, 1987; Culf and Gash, 1993; Sridhar and Elliot, 2002; Udo, 2003; Lhomme *et al*., 2007; Choi *et al*., 2008; Sedlar and Hock, 2009). It has been established that DLR globally depends on latitude; that is decreasing from low latitude to mid latitude to high latitude (Wild *et al.*, 2001; Jonsson *et al*., 2006). Studies conducted at high latitudes have shown that the thickness of the atmosphere and heavy cloud lead to high DLR (Wendler and Eaton, 1990, Zhang *et al.*, 1997) and Maksimovich and Vihma (2012) have established that the radiation under certain conditions of cloud sizes instigate the onset and the duration of snowmelt. Furthermore, it is established that DLR varies inversely with altitude (Marty *et al.*, 2002). It is well known that DLR depends on atmospheric variables such as water vapour, temperature and cloudiness which vary from place to place and it also depends on different geographical composition such as water surface, agricultural surface etc (Choi *et al*., 2008). Particularly in the case of Nigeria, as earlier mentioned the first period of ground measurement at Ilorin, Nigeria from September 1992 to August 1994 has previously been studied whereby the seasonality of the radiation was established among others (Miskolczi *et al.*, 1997; Udo and Aro, 1999; Udo, 2000; Udo, 2003).

Explicating on some of the works already mentioned above and others, most equations whether empirical or analytical or both in form need be tested to ascertain their reliability in a particular location. Choi *et al.* (2008) tested these equations for Florida in USA under about 11 various sites like water surfaces, wetland and urban between January 2004 to December 2005. The study concluded that the Brunt (1932) model was more applicable for clear skies whereas for all skies conditions that of Crawford and Duchon (1992) was the best fit. However they recommended using the combination of both equations for optimum results in Florida by pairing the cloudiness factor in Crawford and Duchon (1992) to the clear skies

model of Brunt (1932) without the need for modification of the inherent constant. It is observed among other things that models with both water vapour pressure and temperature terms had optimum performance and that water bodies had more DLR than other land uses which was consistent for all the models evaluated.

Crawford and Duchon (1992) expression for cloud cover correction has also been noted by Lhomme *et al.* (2007) to be effective in the estimation of DLR for cloudy sky formation. However in the particular case of Lhomme *et al.* (2007), the cloudy term was paired with Brutsaert (1975) and also the constant was adjusted to fit the data of Andean Altiplano of Bolivia and Peru regions as against the earlier mentioned work of Choi *et al.* (2008) at Florida where the constants of Brunt (1932) were not adjusted. From the work of Lhomme *et al.* (2007), in order to obtain the constant of the Brutsaert (1975) expression, the emissivity was expressed in the form

$$\varepsilon_o = c\ \left(\frac{e_a}{T_a}\right)^{\frac{1}{7}} \qquad 2.1$$

where c is the constant (gradient), $e_a$is water vapour pressure and T_a is the air temperature.

By extension to cloudy sky condition, equation 2.1 assumes the form below

$$\varepsilon_c = F(s) \times\ \varepsilon_o \qquad 2.2$$

where ε_c is the effective emissivity and

$$F(s) = -\ 0.34s + 1.37 \qquad 2.3$$

s is the ratio between measured and potential solar radiation, a cloud correction term of the cloudy function *F(s)*, the ratio between solar radiation and the clear sky estimation.

For daytimes the new formulation fitted well but the nighttimes did not fit so well. As *s* cannot be evaluated during the night since no solar global radiation can be received by then, by trial and error the previous day's mean of between 14h and 16h 30mins were found to be adequate. The work by Crawford and Duchon (1992) clearly illustrates that the derivation procedures are relatively easy yet the dome heating effect was not accounted for. Although this effect is believed to about 5%, however Miskolczi *et al.* (1997) in the case of Ilorin noted that it could influence the readings by up to 30%. Probably the day time dome heating of the pyrgeometer may not have much influence in the temperate climate region or other regions of the globe. The data used in Lhomme *et al.* (2007) were taken in January 2005 – June 2005 at Condoriri in Bolivia and from November 2005 to February 2006 at Irpari in Peru. Both locations are at the high altitudes of about 4000m above sea level.

Niemela *et al.* (2001) made comparison between two classes of DLR models under clear skies and cloudy conditions of hourly data of 1997 and 1999 at Sodankyla ($67^{o}22^{l}$N, $26^{o}39^{l}$E), Finland. It was targeted at appraising the performance of some DLR models for a cool region particularly at nights whereby the temperatures ranged from -49^{o}C to 11^{o}C. The first group of models used were eight different simple equations which make use of screen level parameters like temperature and water vapour pressure and three models with parameters like cloud cover as well as both temperature and water vapour pressure for clear skies and all skies respectively. The second group was made up of four complex equations of radiation schemes for numerical weather predictions (NWP) such as Rapid Radiative Transfer Model (RRTM). Actually DLR was not directly measured but calculated from measurements of hourly averaged downward and upward shortwave radiation and net radiation as well. The first group of equations comprised clear skies models of Angstrom (1918) with localized calibrated coefficients, Brunt (1932) with northern hemisphere coefficients, Brutsaret (1975), Idso (1981), Prata (1996), Swinbank (1963) and Dilley and

O'Brien (1998). For the all skies models still within the first group of simple equations there are; Jacobs (1978), Maykut and Church (1973), and a third equation based on the net radiation model of Budyko (1974). In this category of simple equations, this work by Niemela *et al.* (2001) came forth with models for both the clear skies and the cloudy conditions. The equation put forward for the clear skies has two boundary conditions apparently for summer and winter whereas the new equation for the all skies is based on that of Budyko (1974), where it is extended to obtain a DLR model and localized coefficients from the initial net radiation model. The radiation schemes models for NWP tested are those of European Centre for Medium-Range Weather Forecast (ECMWF), Deutscher Wetterdien (DWD), High Resolution Limited Area Model (HIRLAM) and a new version of ECMWF model known as Rapid Radiative Transfer Model (RRTM). During summer, the models perform better than in the winter and except for Idso (1981) model that overestimated the radiation, all others for the clear skies including the NWP underestimated the radiation with various different degrees, though the second group of NWP models performed better than the first group. For the cloudy conditions the two models stood tall, both been the RRTM and that of Maykut and Church (1973). It is worth mentioning that their new model for the clear skies had acceptable results however there are issues of locality bias of the coefficients and that the fact that the study depicted only nighttimes. In addition, errors could be embedded in the process of obtaining DLR which was not directly measured. This work by Niemela *et al.* (2001) has further established the need to test the applicability of the models of DLR.

Jonsson *et al.* (2006) studied DLR in three African cities namely Ouagadougou ($12^{o}\ 12^{l}$ N, $1^{o}\ 40^{l}$ W), Dar es Salaam ($6^{o}\ 51^{l}$ S, $39^{o}\ 18^{l}$ E) and Gaborne ($24^{o}\ 40^{l}$ S, $25^{o}\ 55^{l}$ E). They agreed with Miskolczi *et al.* (1997) and Claquin *et al.* (1998) that seasonal dust particles loading of the aerosols contribute to decrease in DLR due to observation based on emissivity in Ouagadougou but pointed out that the notion was inconclusive if analysed from DLR itself.

It was also observed that DLR decreases away from the Equator and also that farther from the Equator, DLR depends more on temperature than it does closer the Equator. However, a critical view of this work reveals that measurements were not taken at the three sites simultaneously rather one site after another and the measurements were done within 2 weeks only, so their findings leave much to be that conclusive. Another source of error not considered is the fact that different months show different characteristic patterns and have variations from place to place (Wild *et al.,* 2001), thus the issue of seasonality poses a setback to this study since the movement from one location to another took place over months in the field study. Be that as it may, it was rightly highlighted by Jonsson *et al.* (2006) that Dar es Salaam in Tanzania being a Costal city had the highest DLR compared to Ouagadougou in Burkina Faso and Gaborone in Botswanna that are Inland and Inland Plateau sites respectively.

Still on works done in Africa, earlier Culf and Gash (1993) compared already existing models of DLR with measured data at a village called Damari (13^{o} 12^{l} N, 2^{o} 15^{l} E) about 45km South of Niamey in the Republic of Niger where the measuring instrument was mounted on a 12m tower. This work showed that the correction for the measured data is mostly necessary during the daytime periods of 7 to 16 hrs GMT and the correction factor for the location was given as;

$$L_{d,cor} = L_{d,obs} - 0.027S_d \qquad 2.4$$

where $L_{d,cor}$ is a shading formulation, $L_{d,obs}$ is the measured longwave radiation and S_d is the total downward solar radiation.

Five models tested are those of Brunt (1932), Swinbank (1963), Idso and Jackson (1969), Satterlund (1979) and Brutsaert (1975). Using hourly clear skies criterion that hourly ratio of diffuse solar to total solar radiation is less than or equal to 0.18 for the duration of 15^{th} July

1989 to 31st September 1990, a total of 165 hours of data were selected. On the other hand radiosonde profiles of wet and dry bulb temperatures and water vapour pressure were measured at 2 hours intervals for 11 days only during the DLR data measurement period. After matching the profiles measurement with the radiation measurement, only a day (25th October 1989) met the clear sky criterion and the night of 24 - 25 October was also used even though the criterion procedure cannot be evaluated at nighttimes. Brutsaert (1975) was calibrated to have a new constant of 1.31 as against the origin coefficient of 1.24. While Brunt, Swinbank, Idso and Jackson and Satterlund all had R^2 values of 0.77, 0.76, 0.91 and 0.81 respectively as against Brutsaert of 0.65, the (root mean square) rms values of these models accordingly were 36.5, 62.3, 74.9, and 24.1 as against 22.9. The calibrated Brutsaert (1975) still had $R^2 = 0.65$ but with rms reduced from 29.9 to 11.9. Though it is argued that the overestimation of Swinbank (1965) and Idso and Jackson (1969) are due to the fact that they assume an implicit relationship between temperature and water vapour, yet it would have been more appropriate to calibrate either one or both of them to find out if the overestimation could have been curbed since they correlated much better with the measured data than the calibrated Brutsaret (1975) model.

DLR dependency on latitude is further confirmed by Wild *et al.*, (2001), in which a total of 45 cities around the world are examined in an attempt to evaluate the radiation in General Circulation Models (GCMs). Clearly the low latitude locations (the Equatorial locations) have higher DLR, followed by the mid latitude and lastly the high latitude. And judging from the estimates from the GCMs, DLR was more adequate with few slight overestimations in the low latitudes as against less adequate with more high underestimations at both the mid-latitude and high-latitude sites. However out of the 45 cities, critical examinations and analyses were carried out on only 12 of them, 4 in each of the three latitude segmentations. Given the data availability at their disposal, if all or more locations were analysed, it would

have been better. The discrepancies in the GCMs models could be due to the low variability of higher DLR in the tropics as against high variability in the other locations of lower DLR noted in the study. The higher the latitude, the more the discrepancies in DLR. Wild *et al.*, (2001) reportedly used NASA data and observed that it did not differ in the outcome from data from other sources.

It seems that much work has been done in Brazil in recent times. Krut *et al.,* (2010) in their work on Sao Paulo, mentioned other recent works (eg Duarte *et al.,* 2006). Their own work in the clear skies category is tailored mainly after Brutsaert (1975) model of clear sky whereas in the original case of Brutsaert the constants were $\alpha = 0.642$ and $\beta = 1/7$ while in this particular case of Krut *et al.* (2010), $\alpha = 0.572$ and $\beta = 0.202$ in the equation below

$$DLR_{CL} = \left[\alpha \left(\frac{e_a}{T_a}\right)^{\beta}\right] \sigma {T_a}^4 \qquad 2.5$$

where σ is the Stefan Boltzmann constant (5.78×10^{-8} W/m^2.K^4)

From the results presented by Krut *et al.* (2010), the Brutsaert (1975) model was recalibrated because the closer fits to their data was those of similar formulation. The coefficient of determination R^2 was 0.841 and the bias error was 0.300 for the calibrated model whereas the original Brutsaert (1975) expression had $R^2 = 0.827$ and the bias error as 6.586.

For all sky conditions, to incorporate the cloud cover in the absence of cloud cover data, a formulation for it according to Crawford and Duchon (1999) model for cloud cover *c* was used which is given as;

$$c = 1 - \frac{S_d}{\widehat{S_d}} \qquad 2.6$$

where S_d is measured incoming shortwave radiation and $\bar{S}_d$ is the theoretical incoming shortwave radiation.

The drawback for the expression for *c* is that during the nighttimes, shortwave radiation is no longer received, so following other authors in obtaining the cloud cover for the nighttimes, a linear interpolation between the cloud cover at sunset (that is time t = a) and the following dawn (that is time t = b + 24) given below is used;

$$c(t) = \frac{c(b+24) - c(a)}{(b+24) - a}\ (t - a) + \ c(a) \qquad 2.7$$

whereby 24h is added to the time t after midnight.

The models tested in this work were those of Jacobs (1978), Maykut and Church (1973), Sugita and Brutsaert (1993), Konzelmann *et al.* (1994) and Crawford and Duchon (1993) in that order. Within these the prototype having the general form of;

$DRL_{ALL} = DRL_{Cl}\left(1 + \alpha C^{\beta}\right)$ are those of Maykut and Church (1973), and Sugita and Brusaret (1993). The formulation of Konzelmann *et al.* (1994) is of;

$$DRL_{ALL} = DRL_{Cl}\left(1 - C^{\beta}\right) + \ \alpha C^{\beta}\sigma T_a^4 \qquad 2.8$$

where specifically $\alpha = 0.952$ and $\beta = 4$.

By least square method, this study by Krut *et al.* (2010) obtained the constants α and β to be 0.576 and 0.202 for daytime while for all day the constants were 0.1007 and 0.9061 respectively. For the clear sky aspect of the expression, the calibrated model was adopted. The results for all sky section reveal better fitting for all the expressions during the daytime than for both daytimes and nighttime. For instance the coefficient of determination R^2 was 0.804 for daytime but 0.767 for diurnal when using the expressions promulgated for Sao Paulo. This study by Krut *et al*. (2010) establishes the trends of DLR during diurnal and

seasonal periods for the location under review. During diurnal period it is observed that not much difference exist between the calculated DLR and the measured DLR for all skies conditions. Also during the rainy season the error in calculating DLR for both clear sky and all sky conditions were more for the dry season despite the fact that all the coefficients for the expressions were adjusted accordingly. For the all sky conditions two sets of results were presented for the daytime and for both daytime and nighttime.

Morcrette (2002) studied the discrepancies on the forecasting in surface DLR in the ECMWF (European Centre for Medium-Range Weather Forecasts) for a 40 year reanalysis based on the global measurements for April - May 1999 for time scales of an hour to a day between the ground truth and other satellite models of DLR. The data were obtained from different agencies such as BSRN, SURRAD and ARM network that had data operational during the two months. The comparisons scattered over 27 stations is inclusive of Ilorin, Nigeria. Preference on the review of this work is given to Ilorin since it's the location of interest in this present research. By the order of different models that are reported on the basis of the DLR scheme on water cloud optical properties, the first being in 1991, the second being a revised version of the first and operated from December 1997 – June 2000 and lastly a third operating since 2000. The radiation code for the three models respectively for Ilorin had values for the first and the second codes of about the same. However the third code which gave values of difference of up to 7 W/m^2 in both clear skies and all skies, call for concern. The reason cited for the parity is that at the equatorial region it is quite difficult to infer DLR from the water cloud optical properties unlike in the high latitudes. Apparently this is somewhat true since the three codes in the high latitude of the South Pole gave reasonably close values.

Sridhar and Elliott (2002) showed the testing of three equations of Brutsaert (1975), Idso (1981) and Anderson (1954) for 9 sites in Oklahoma from June 1999 to May 2000. Using

data from only 4 sites for calibration, the original coefficient of Brutsaert (1975) changed from 1.24 to 1.31 and it was concluded that the adjusted Brutsaert (1975) model can be applied for all conditions of the skies including night and day times. The adjusted Brutsaert (1975) was statistically significant at 95% confidence level (this was only highlighted but not shown) and had very high correlation coefficient values in Oklahoma. However it is a bit surprising that Brutsaert (1975) model was calibrated instead of Idso (1981) model which was more promising, except that it is argued that the Brutsaert (1975) model is less complex.

2.3 Artificial Neural Networks

For so long ago and up till now man has been fascinated by nature and the desire to replicate it. Aeroplane came about after the thought of man flying as birds do. Just like birds in flight, so is the shape of the aeroplane, not just for copying sake, but nature seems to provide a better option. For instance, ships shaped like fishes move faster in water than those of any other shape. Nature is fascinating and has so much to offer if only we can tap from it. The study of nature has been used to make innovations and invention; for instance the hearing nature of birds has been used to make hearing aid machines for man (Bar-Cohen, 2006). Even after discoveries of certain processes by man, they are later found to be in use already in nature. Engineering process of system of valves that can alter the flow of fuel and air instantly as power needs change exist in fruit flies (Lehmann and Heymann, 2005). Sometimes, even other natural mechanisms found in animal are better than those made by man. Insect repellent for monkeys (a jungle millipede secretion) is stronger than repellent of humans (Weldon *et al.,* 2003).

Since the advent of the computer there have been serious desires to create a machine that can think like man that has made scientists. To make a machine or robot that can think then we have to replicate the thinking system of man. Various specialists like neurologists,

mathematicians, computer scientists etc have come up with terminologies like artificial intelligence, and artificial neural networks or neutral networks. Artificial intelligence (AI) according to Kalogiron (2001), in the broadest form can be regarded as the ability of a machine to perform the same tasks that are found in the human nervous system without using neural network as the computational architecture. An Artificial neural network (ANN) is sometime commonly called neural network (NN). Traditionally, the term neural network has been used to refer to a network of biological neurons. Neural network is a crude mimic of the processes found in the human nervous system which can be actualised by either electronic circuit or by mathematical algorithms.

To mimic the human nervous system in the artificial neural actualisation, attention is paid to the ability of the nervous system to learn, which involves the parallel processing of information as against the serial format of the von Neumann machine. A unique feature of neural networks is robust to tolerate error failure, because it can still perform its overall function even if some of the neurons are not functioning. Also, it is more readily adaptable to fuzzy logic computing tasks than Von Neumann machines. Neural networks have been applied in a lot of real world problems ranging from financial modelling (mostly for the prediction of the stock market), time series problems of climatic and weather studies and computer games like chess to medical diagnostic issues and data mining etc.

The tasks that ANNs can perform include classification, clustering or categorisation, prediction or forecasting, function approximation, optimisation, image association, content – addressable memory and control systems (Basheer and Hajmeer, 2000; Jain *et al.,* 1996). As highlighted by the Demuth and Beale (2002) the areas of applications include aerospace, security, industry, oil and gas, banking, electronics, medical, telecommunication, automotive, finance etc, and one could say that it can be adapted in any field of endeavour to suite specific objective.

2.3.1 The Nervous System

The nervous system body cells are referred to as neurons. The human body has numerous neurons everywhere and they differ in size and shapes. The nucleus cell of the nervous system is called soma. Linking one cell to another is the synapse. Synapse encompasses the receptor or (dendrite) and the motor (or axon) (Fig 2.1.2).

It is noteworthy to point out that the idea of neurons as structures that constitute the components of the brain were first highlighted independently by Camillo Golgi around 1880 and Santiago Ramon Y Cajal in 1888 whose works put to rest the controversy by medical doctors over the form of the human central nervous system. The two sides of the coin were; one- reticularist who believed the brain was a continuous uninterrupted network of nerve fibres and two- neuronists who proposed that the brain consisted of neural networks of nerves that are composed of a vast number of single interconnected cellular units (Muller *et al.,* 1995). The convincing method that gave the neuronists edge over the reticularists was the use of bichromate silver reaction to stain nerve fibres, which was invented and adopted by both scientists respectively.

After information is sent through a synapse of a nucleus to the synapse of another nucleus, the later will process it, be silent on it/not act on it, store it, send it to another nucleus etc. Each neuron may receive stimuli from about 10,000 other neurons. Nervous signals travel either electrically or chemically. Electrical transmission generally takes place more in the interior of a neuron whereas chemical transmission takes place between neuron and neuron i.e. at the synapses. The electrochemical media that transmit coded information are called neurotransmitters. Groups of neuron are organized into subsystem and the integration of these subsystems forms the brain (Muller *et al.*, 1995).

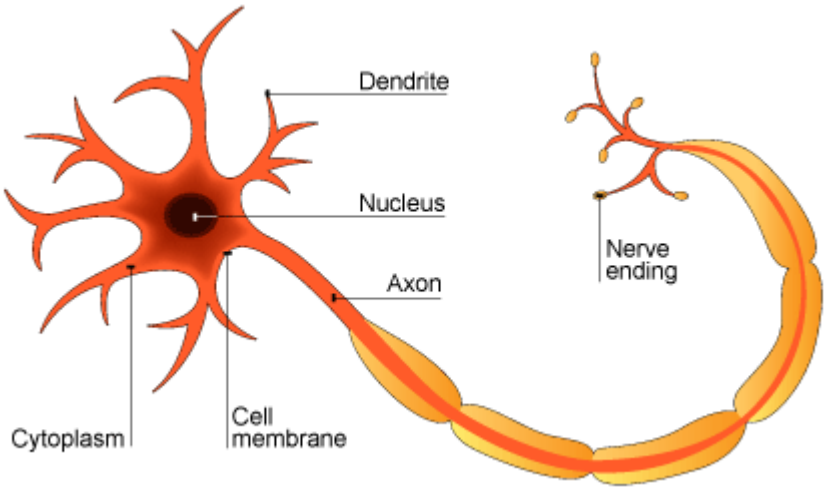

Fig 2.1.2: The biological neuron (courtesy of www.thedigitalmuse.net on the 10/01/2015)

2.3.2 Historical Development of Neural Networks

Incidentally the earliest studies in the neural network started with the studies on the working of the human brain. The historical period of the neural network lies in the eras of the 1950s and 1960s, though it appears to be the end thing and also expected to be the tool of the future. Neural networks imply mimicking the behavior pattern of the biological nervous system of humans. To achieve the goal of reproducing the behavior of a typical neuron, the electrical signal generated in the brain during a process of say remembering a past event will have to be written in mathematical form that would describe the signal. The accomplishers who first made an artificial neuron or say the pioneers in the construction of an artificial neuron or better still the first mathematical model of artificial neuron far back as in 1943 were Warren McCulloch, a neurophysiologist and Walter Pits, a logician. It is important to mention the work of Hebb (The organization of behavior) in 1949 that mainly emphasis that neural networks pathways grows stronger with every use. As at then there was little advancement in technology as compared to nowadays so they could not make much headway. However the

neuron model competed fiercely with the Von Neumann model of basic computing machine because it could as well perform all Boolean operations.

Later on in the 1950s the corporate world got interested and partnered with academies to develop the artificial neuron further. By such a partnership, Frank Rosenblatt in 1957 introduced the perceptron, now regarded as the predecessor to the modern neural network. The perceptron is a specific type of a simplified model of a biological neuron that has two stages, (the input and output), with information flow is in one direction. That is from the input to the output and never the order way round, whereby the neurons in same level do not communicate with each other. That make up is the feed forward network. This invention of the perceptron was that which caused a major setback in the field, as it was shown by Minsky and Papert (1969) that the perceptron could not handle the exclusive or case (XOR) whereby two cases of input are not linearly separable. The perceptron is a layer neural network and though Minsky and Papert (1969) incorrectly assumed that even the multilayer perceptron would not solve the problem of XOR, the introduction of back-propagation into the multilayer perceptron brought full life back to neural networks as the XOR issue was solved and further improvements came forth.

Due to the problem pointed out by Minsky and Papert (1969), the neural networks studies were thrown into darkness as investors in its research pulled out. However resurgence in the area of artificial neural networks was spear headed by Weebos, who actually in 1974 introduced the back propagation and later on in the 1980s many others like Hopfield, Remulhart, Lecun, Parker, McClelland and Kohonen at various occasions contributed to the development of the field of neural networks. The developments in the 1980s have given great boost to neural networks and ever since it has witnessed explosive breakthroughs (Kriesel, 2005)

2.3.3 A Neuron

An artificial neuron in its simplest form can be defined as a process that involves three stages of input, summation and activation, and the output (Fig 2.1.3). As earlier mentioned, these activities can be carried out by electronic circuit or by algorithm. It should be noted that only a brief description of the neuron networks is done here but in reality it entails a lot (Beale *et al.*, 2014). Mathematically a neuron is an element that realises the function;

$$y = f(\sum_{i=1}^{n} w_i x_i) \qquad 2.9$$

where f is activation function

w_i is weights for all inputs x_i

x_i is neuron input values

i is an input unit

The major attribute of the neuron when compared to the Von Neumann machine is the ability to learn. Learning, a common feature of the nervous system is regarded as training in neural networks and can be divided into two major segments which include the unsupervised learning and the supervised learning. Unsupervised learning is the procedure in the biological neuron whereby inputs are given to the network and on its own identifies the similarities as well as differences between the inputs and further puts those with similarities into groups. The training sets only consist of input patterns. On the other hand, supervised learning is by examples whereby the target is shown to the networks and approximating or exacting the target is required from the networks.

There are various designed functions that are incorporated in the training of neural networks. One of some of these functions involve is weighting factors. Since neural networks are rough mimicking process of the biological neuron, a weighted factor is typical of varying synaptic strengths which have to get to threshold value before firing is done. A neuron receives several inputs at the same time and depending on the impact the summation function is processed.

Weights are some adaptive coefficients that express the magnitude of inputs and are modified by various training sets, specific topology or learning rules.

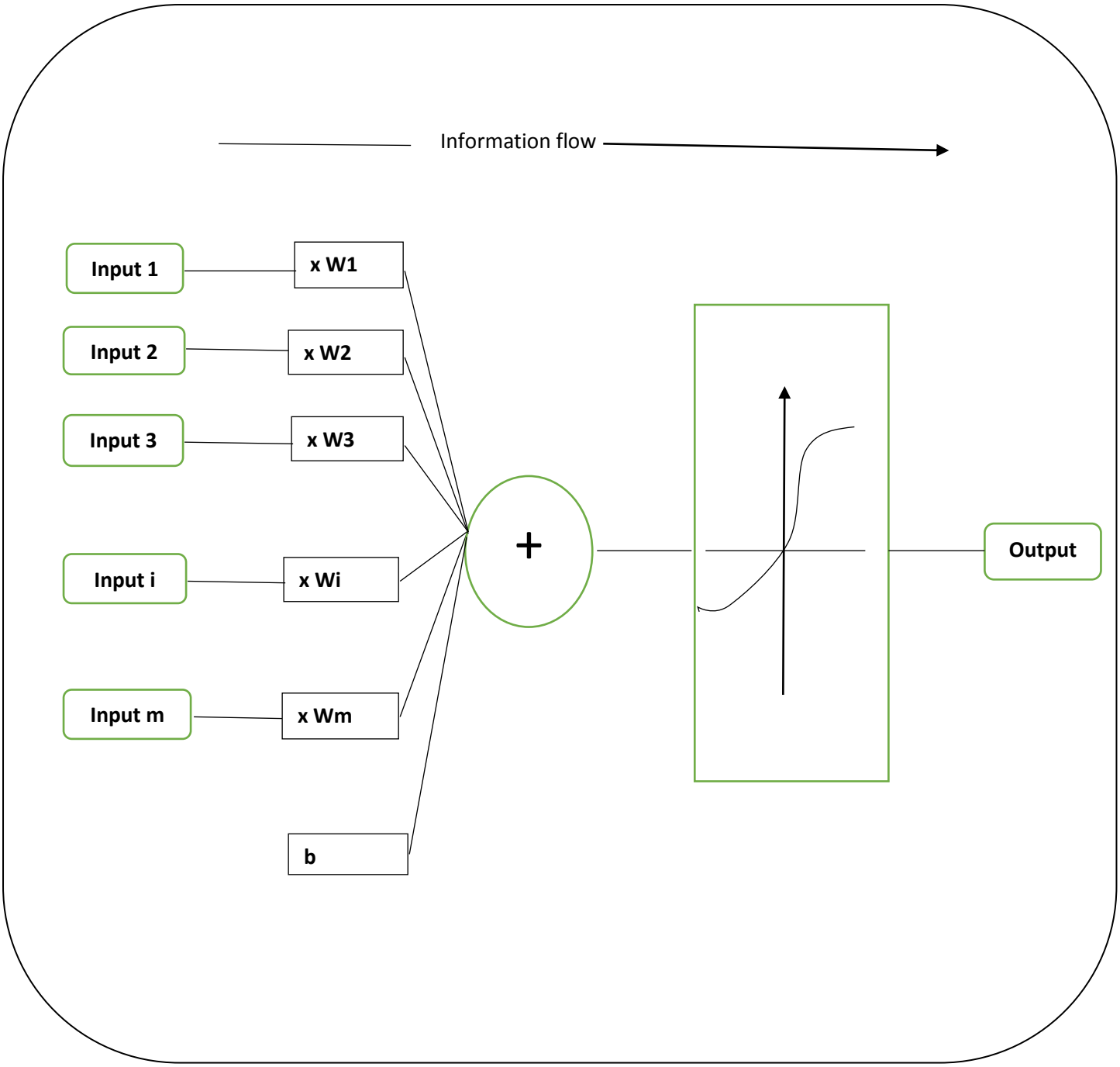

Fig 2.1.3: An artificial neuron system

A second factor is activation or summation function. After signals have been received by the neurons, the next activity is to compute the weighed sum of all inputs. The input vectors are multiplied by the weighted vectors of each input and the summation of the multiplications is taken. Several summation algorithms of minimum, maximum, product or normalisation of the entity of the inputs abound.

A third factor is transfer function: ANNs behaviours are determined importantly by the weights and the transfer function which are the input and output functions respectively. Both parameters are specified for each unit. The transfer functions are mostly of three categories namely linear, sigmoid and threshold. For a linear unit, the output activity is proportionated to the total weighted output. The function is technically known as purelin and it calculates the output of a layer from the net input within a range of -1 to +1.

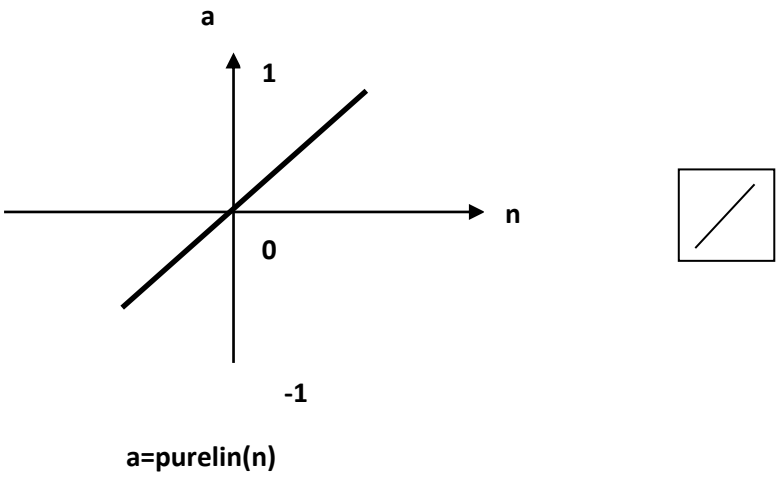

Fig 2.1.4a: Linear transfer function

The sigmoid unit has output varying in an S shape with changes in the input weights. Sigmoid are more typical of the biological neuron. The logsig or sigmoid transfer function

takes net inputs which may have any value from plus and minus infinity and forces the output into a range of 0 to 1.

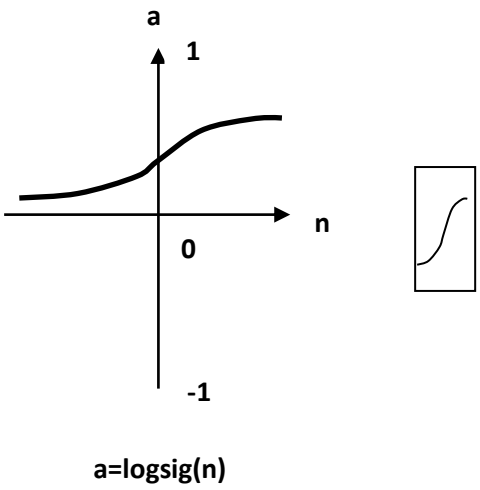

Fig 2.1.4b: Log-sig transfer function

A third type of transfer function is the Hard limit transfer function which ensures that a neuron is1 when the net input reaches a threshold, otherwise the output is zero. By that a neuron is able to take a decision on classification since it is works on either yes or no.

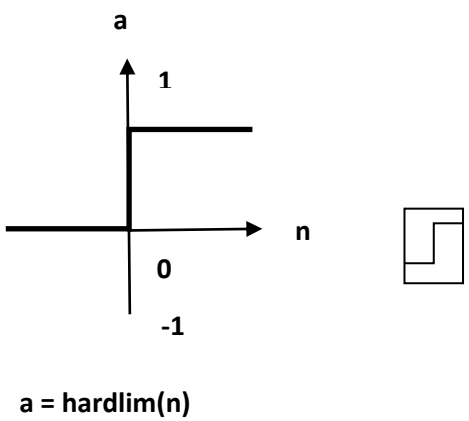

Fig 2.1.4c: Hard limit transfer function

A fourth factor is number of neurons. The number of neurons in the layer plays an important role. For the multi-layer feed forward neural networks, most times one hidden layer is sufficient; otherwise when a function is discontinuous then two layers are preferred. If the neurons are two few then neural networks cannot learn the necessary details and thereby result to under fitting the data. If the neurons are too many it leads to data over fitting in which case the networks learn unimportant details. The best method is to start small and increase the number while checking for optimum result.

The fifth factor is backpropagation. Backpropagation is a procedure that minuses the error network from the derivative of the error function. The algorithm of backprogation provides for clamped learning patterns whose values are propagated to the output units, such that the network output is compared with the desired output values and error terms between them is reduced to minimal level (Krose and Smart, 1996). The learning algorithm is known as the generalised delta rule. A major setback is the long time it takes in training or sometimes outright training failure.

Other functions that are incorporated in neural networks include the momentum factor, rate of iteration, layers, performance parameters which all have different algorithms help neural networks to function properly.

2.3.4 Types of Neural Networks

There are mainly two types, topologies or architectures of neural networks. The first group is the feed forward networks while the other group is the recurrent networks. For the feed forward neural networks the direction of movement of information is only in a forward direction and any other direction is forbidden. Hence data go through the input layer to the hidden layer (if any) and then the output (Fig 2.1.5). There are neither cycles nor loops in the

network. The feed forward neural networks can either be of single layer or multiple layers. Some examples of this include the perceptron, radial basis function, ADALINE, probabilistic neural networks, generalized neural networks etc. On the other hand recurrent networks are made up of topologies whereby a later stage can communicate with any of the previous stages (Fig 2.1.6), which is not allowed in the feed forward. Examples of the recurrent networks include Elman, Hopfield and Boltzmann machine.

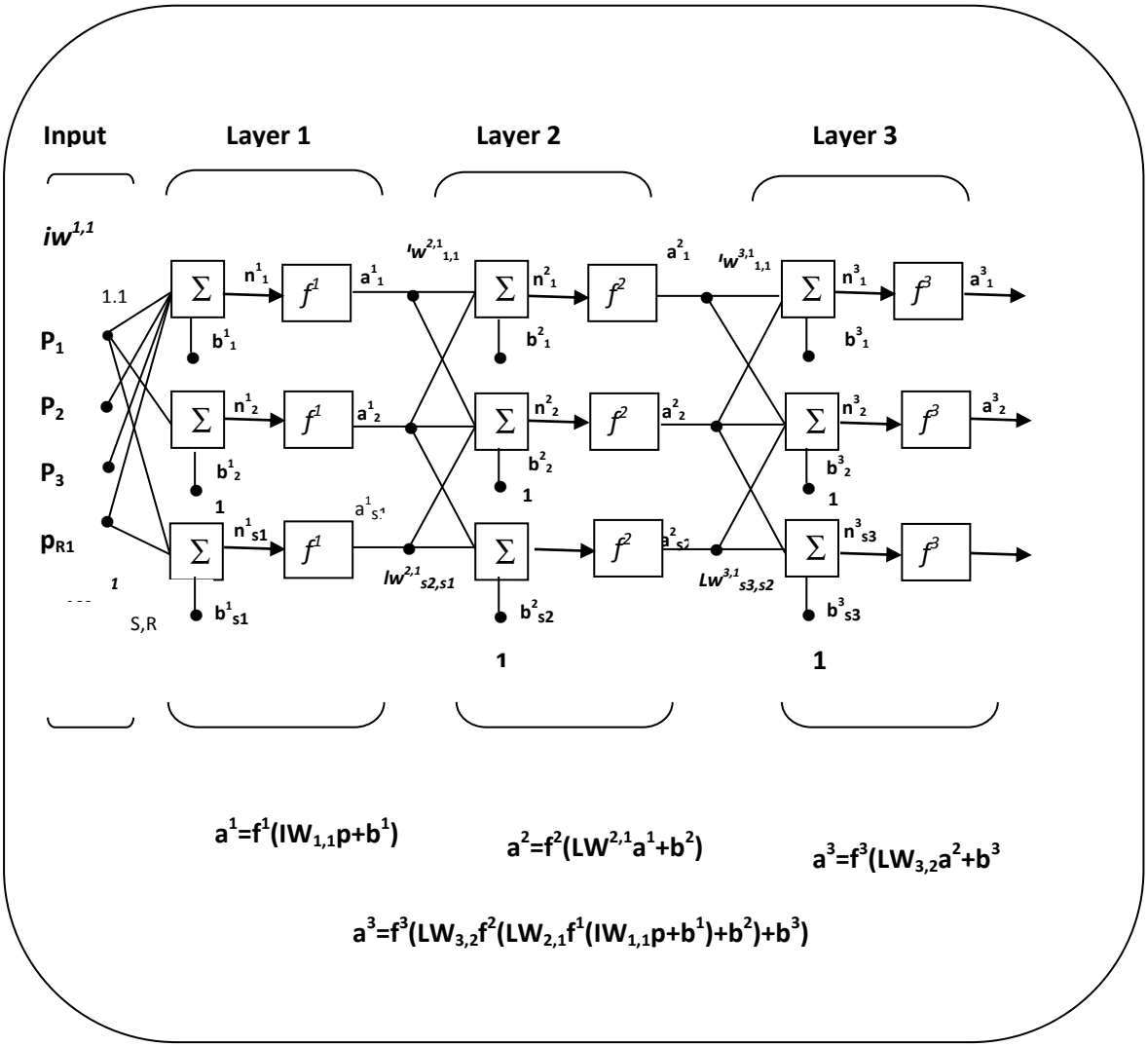

Fig 2.1.5: A feed forward neural networks system

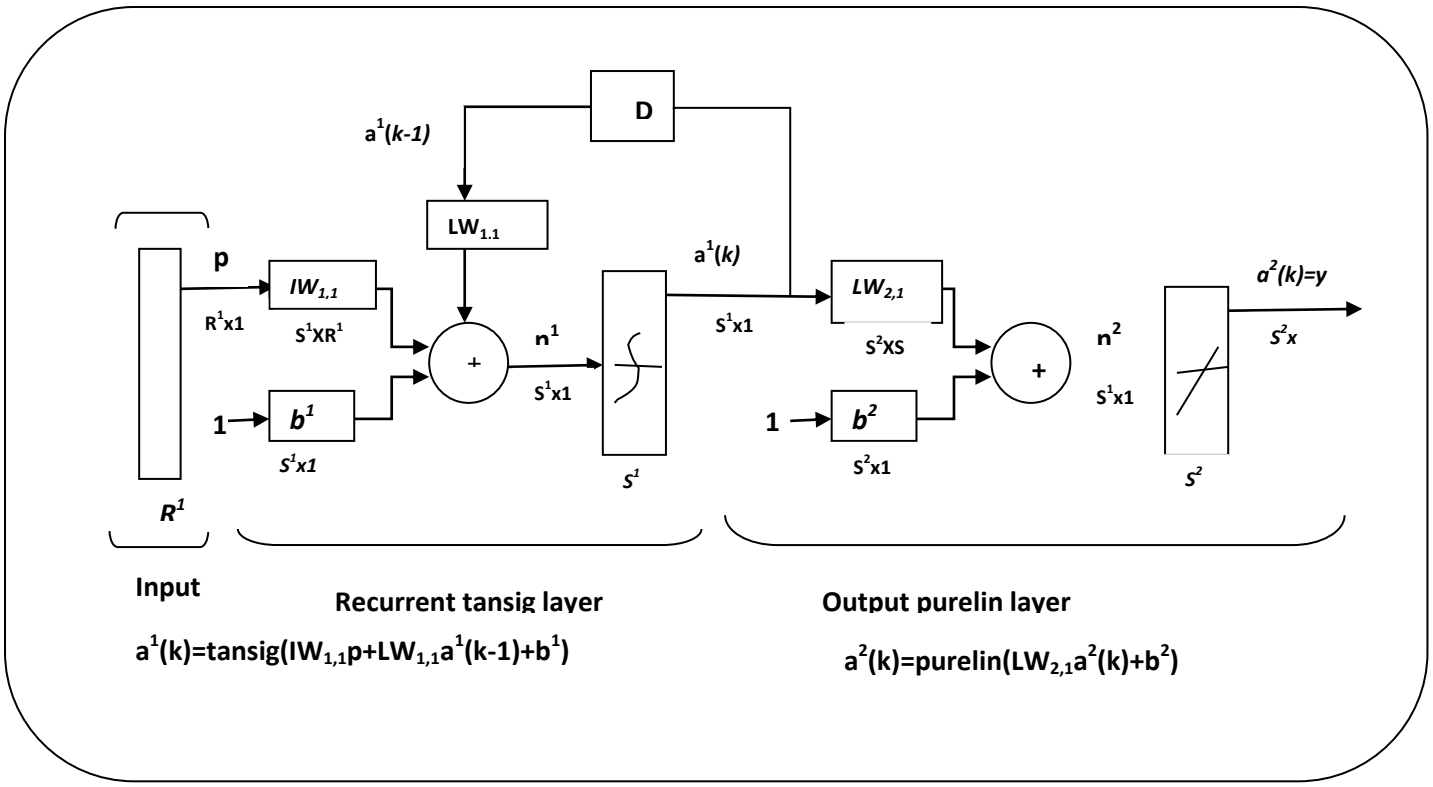

Fig 2.1.6: A recurrent neural networks system

2.4 Review of ANNs Application in Solar Radiation

ANNs employed in the general field of solar energy are mostly for optimisation, prediction or forecasting and system controls. Some specific areas of applications include modelling of solar steam generator, prediction of global radiation in locations with no direct measuring

instrument, analysis of power system harmonies, air bus conditioning, energy prediction in commercial buildings, wind speed prediction, identification of time parameters of solar collectors, and also for peak power tracking for PV-supplied D.C. motor etc (Kalogiron, 2000).

At the moment, the use of artificial neural networks seems to have taken center stage in modeling. And as already mentioned it is in use in almost every field of endeavor e.g. science, medicine, engineering, social science etc. ANNs have been used in solar radiations estimations in different locations around the world and in cases of comparison; it has been found to perform better than equations. Reddy and Ranjan (2003) used artificial neutral networks based models to estimate monthly mean daily and housefly values of solar global radiation in India. The multi-layer feed forward (MLFF) network was used and data of a total of 13 stations spreading over south and north India were used in their work. While 11 stations data were used to train the network, its predictive capability was tested with the ground data of the remaining 2 stations. The maximum mean deviation of prediction was found to be 4.07%, which was the highest occurring during the raining season. The result of the prediction was compared with three other empirical methods such as Angstrom, Hargreeve and Supit. ANNs were found to predict solar radiation values more closely than the rest. Similar work was later reported by Krishnaiah *et al.* (2007). Though in the earlier work no mention of the year(s) of data used, however the later reported the use of data of about four years (1989-1993) and it seems that in the later work, daily data were considered while in the former, hourly data were used. With a normalisation range of 0 to 1, the same input parameters such as latitude, longitude, wind speed, altitude, humidity, month, time, rainfall and temperature, the North and South partitioning of locations and three seasons of winter, summer and rainy were adopted in both works. The difference was that the later trained and tested the error of ANN with 7 stations as against 11 stations in the former work. However 2

stations were used to examine the predictability of ANN over unseen data in both cases. ANN was preferred to the traditional methods for adaptation more especially for places where measurements were not carried out but other atmospheric parameters are available in India (Reddy and Ranjan, 2003; Krishnaiah *et al.*, 2007). Therefore if ANN is in use, then no foreseen hindrances to solar energy technologies with respect to global solar radiation data.

Dorvlo *et al.*, (2002), while estimating solar radiation using artificial neural networks employed two different models - the radial basis function (RBF) and multiplayer perception (MLP) otherwise known as multiple layer feed forward (MLFF). These models were used to investigate data from eight stations in Omen. Both models performed well though the RBF model was recommended for the sake that it required less computing power. The MLP models were of three types depending on the number of hidden layers (from 1-3). Based on the computed RMSE's, the four networks performed very well. The ranges of errors for the RBF networks were from 0.83 to 10.08 $MJ/m^2/day$, while the range of errors for MLP networks as from 1.01 to 9.41 $MJ/m^2/day$. None of the networks seems to have an edge in terms of the mean absolute percentage error.

Lopez *et al.* (2005) used automatic relevant determination (ARD) to eliminate some parameters not really important as input in the estimation of rarely measured beam radiation from artificial neural network. Hourly data for about 4880hrs of a year from a specific location in USA were employed in this study. Out of a total of nine parameters like global irradiance, temperature, relative humidity, precipitation water, wind speed, surface pressure, cosine of zenith angle and optical air mass, as expected only two parameters were actually relevant.

The daily solar radiation data of Cordoba, Argentina from 1988 to 1991 were trained and validated from eight ANN models of varying combinations of inputs parameters like extra-terrestrial radiation, temperature range, precipitation, cloudiness and sunshine duration.

Multilayer perceptron backpropagation modelling of ANNs was adapted, whereby 1988 to 1989 were training sets of data with several modifications of the training parameters and 1990 to1991 data set were used for validation. It was observed that only a limited number of input variables are required for the neural networks to be effective. And although there were little variations in the estimated values of solar radiation a result of the different combinations of input parameters, but it was considered irrelevant. The availability of input parameters was deemed paramount in adaptation of properly trained ANN for the reproduction of solar radiation data (Bocco *et al.,* 2006).

Soares *et al.* (2004) used four years data (1998-2001) as training set and a year data (2002) as testing set to develop ANN for the city of Sao Paulo, Brazil. The aim was to verify the response of ANN to hourly data because it had been observed that developed expressions for diffuse fraction K_{DF}, performed poorly on hourly value as against the good performances when the hourly values are averaged to daily and monthly timescales. K_{DF} is the ratio of diffuse energy component at the earth's surface per unit of area and per hour to the total flux of energy received from the sun at the earth's surface per unit of area and per hour. The multilayer perceptron adapted ANN experiments were of three different sets and the third set having modified training parameters gave the best results. The inputs parameters used in the study were up to 15. Although all the models (that is both the traditional and the three MLPs) failed the t-test yet a MLP model in the experiment had a better fit to the measured data than the traditional equation that was developed from the measured data. The main observation of the study was that neural networks preserve the regional features of Sao Paulo better and that longwave radiation can serve as surrogate to cloud cover information on a regional scale and it more important than air temperature and atmospheric pressure.

Artificial intelligence techniques of neuro-fuzzy and neural networks were compared with statistically derived model known as Heliosat both for the calculation of cloud index from

satellite imaging for the estimation of hourly global irradiance (Zarzalejo *et al.*, 2005). For the neuro-fuzzy system the if-then rules were applied over four important influences of cloud index, latitude, solar declination and the slot to go alongside a trapezoidal membership function. Whereas for the neural networks a simple regression model was developed and other input variables like declination and latitude were later involved in the training of the artificial intelligence models. Data sets of 1994 to 1996 were employed over 15 stations across Spain and after validating with the ground truth, the artificial intelligence methods had better observed behaviour than the statistical model. The conclusion was drawn from the fact although all models tested failed the t-test for 10,000 data points at 95% confidence level, the other error statistics like MBE and RMSE respectively favoured the artificial intelligence models with colossal percentage of error occurring in the K_T range of 0.7 to 0.9. Specifically the mean bias error for the two traditional methods of simple regression model (SRM) and the extended regression model (ERM) were 0.0780 and 0.0779 respectively. However the MBE values for neuro-fuzzy and the neural networks were 0.0728 and 0.0727. Also the RMSE values for artificial intelligence techniques of fuzzy and neural networks were lower than those of the traditional methods. These values were 0.1079, 0.1078, 0.1034 and 0.1034 for SRM, ERM, neuro-fuzzy and neural networks respectively.

A more intensive approach to modelling solar radiation can be found in the study of Sfetsos and Coonick (2000). Though similar to Zarzalejo *et al.* (2005) in the sense that artificial intelligence technique of neural networks and fuzzy logic were adopted and comparison with the traditional model was made, however in this particular work of Sfetsos and Coonick (2000) three different neural networks types of feed forward, radial basis function (RBF) and Elman recurrent network (ERN) were experimented with as against just one in the case of Zarzalejo *et al.* (2005). Data of about 1512 hours of solar radiation for about 60 days period were used for the processes of training, evaluation and prediction from the artificial

intelligence methods and the time series comparisons were done with various forms of auto regression moving average (ARMA). The Levenberg Marquardt (LM) algorithm under the feed forward neural network gave the best result, particularly the multivariate LM case. Second was the neuro-fuzzy system carried out in the adaptive neuro fuzzy inference system (ANFIS) platform, and it was observed that the inclusion of wind direction improved the performance of both artificial intelligence techniques.

The closest in a few direct deployments of neural networks in the area of DLR are found mostly in applications in conjunction with climate models (Liu *et al.,* 1997; Chevallier *et al.,* 1998; Chevallier *et al.,* 2000; Kranopolsky *et al.,* 2004). Only the works of Kranopolsky *et al.* (2004) and Liu *et al.* (1997) are further discussed. Since an important source of data acquisition for DLR is via satellite, there are existing approaches whereby the retrieval of the DLR data from satellite images is executed with neural networks, which are better and faster than traditional methods. Kranopolsky *et al.* (2004) argues that since observational data have drifted from one-dimensional to three-dimensional, calculations previously based on the traditional methods are lagging behind in the eventual interpretation, thus giving room for possible errors. Given the dynamism in image observational data that the initial 1D processes gulped up to 70% calculation processes of the whole model computation, the present 3D stages may require up to 90%, therefore neural networks which take up less computational processes and time are of necessity in climate models and in the derivation of numerical data from images. Kranopolsky *et al.* (2004) went further to improve on an earlier neural network model for the retrieval of DLR by examining the outcome of varying the hidden neurons in about 10 input parameters of atmospheric temperature, humidity, ozone, CO_2, N_2O, CH_2, cloudiness etc for National Centre for Atmospheric Research Community Atmospheric Model, NCAR CAM-2. Various hidden neurons of 20, 90, 150, 200, 250 and 300 were tried and it was found that those of 90, 150 and 250 were appropriate for estimating DLR. the most

difficult parameter to evaluate in the said model to about 50-80 times faster with insignificant errors and efficiently upholding the climatic features of the original DLR data. This work however called for simulation of higher data size of over 100,000 records with ANN despite giving full assurances on the capabilities of ANN to cope with the already too sophisticated state-of-the-art of climate and weather simulation and prediction.

In similar vein Liu *et al.* (1997) used neural networks to estimate net longwave radiation over the sea for Special Sensor Microwave/Imager SSM/I. Theirs involves the use of an equation to train the neural networks for the estimation of the net longwave radiation over the sea in 1989. Comparison of their results with those of previously published works based on measurements on ship and satellite validated the neural networks model. Notably the neural networks reduced the standard error from 17 W/m^2 of a linear regression model to 5 W/m^2. Also poleward increase in net lonnwave radiation was shown, whereby supporting published works of such. However except for the clear sky cases, the work of Liu *et al.* (1997) did not have reasonable validation for cloudy sky cases due to large variability and limited validation data set. The combination of radiometer measurements and neural networks for improvement in the quality of data was recommended.

CHAPTER THREE

METHODOLOGY

3.1 Site and Climatology

Geographically and politically, Nigeria which is located in the West Africa sub-region of Africa is primarily divided into north and south. Furthermore, both the north and south are subdivided into three. Thus, there are six geopolitical zones in Nigeria, namely, north-east, north-west and north-central in the north, and south-east, south-west and south-south in the south (Fig 3.1.1). There are 36 states in Nigeria, excluding Abuja, the Federal Capital Territory, which is the capital of Nigeria and is situated in the centre of the country. The country occupies a total area of 923,768 km^2, of which 13,000 km^2 is covered with water. She is bounded by the Atlantic Ocean at the south and by other countries, such as Niger at the north, Benin at the west and Chad and Cameroon at the east. In Nigeria, there are approximately 160 million people, whose main occupation is agriculture, particularly those people living in rural areas.

Lying in the equatorial region, Nigeria is a tropical country that has two main seasons, namely, the dry season and the rainy season. However, there is the third season known as the Harmattan season, occurring as a cloudy and dusty period that sometimes can be regarded as or a subset of the dry season. Additionally, the country witnesses the occurrence of 'August break', which is a small dry period or reduction in rainfall that occurs amid the rainy season and lasts for one or two months predominantly in the south. Not all zones in the country have the same durations and patterns of the seasons. The dry season could last up to eight months in some parts of the north, whereas the rest of the period of the year would be the rainy season. In contrast, in the southern region, the dry season could last for less than four months, whereas the rest of the year would be the rainy season. In regions where the August break occurs, the rainfall pattern of such places in the south is such that the rainy season will occur

from March to the peak around July, before the August break occurs, after which the rainy season will have another peak in September before the dry season will begin. Nonetheless, in the north and in other places in the south where the August break does not occur, the rain could gradually peak and then quickly descend to the bottom.

From the south to the north, there are diversified geographical and meteorological attributes that cut across the entire land. The climate zones are primarily three types, namely, the rainforest climate or the equatorial monsoon, the savannah climate and the Sahelian climate (Omotosho and Abiodun, 2007). However, there is a fourth climate found within the other climates, namely, the mountain climate, because such locations are rare, are over 1,000 metres above sea level and are found to exhibit climatic features similar to a temperate climate. There are two types of wind associated with each season, namely, the tropical continental airmass coming from the north and dominating the dry season, and the tropical maritime airmass coming from the south and dominating the rainy season. The vegetation classifications of Nigeria are greater in number than the climate zones. There are seven vegetation zones, namely, Guinea savannah, Sudan savannah, Sahel savannah, fresh water swamp, high forest, mangrove swamp and montane vegetation.

3.2 Data Collection

This study covers all the capital cities of the 36 states and the Federal Capital Territory of Nigeria. However one of the 37 locations namely Ilorin (8.53°N, 4.57°E) is a peculiar location of interest because it has ground movements of DLR. Measurement details such as instrument calibrations and data correction due to dome heating effect of the pyrgeometer, climate data, and other types of data have been previously reported (Miskolczi *et al.,* 1997; Udo and Aro, 1999; Udo, 2000). The data covered the period from September 1992 to

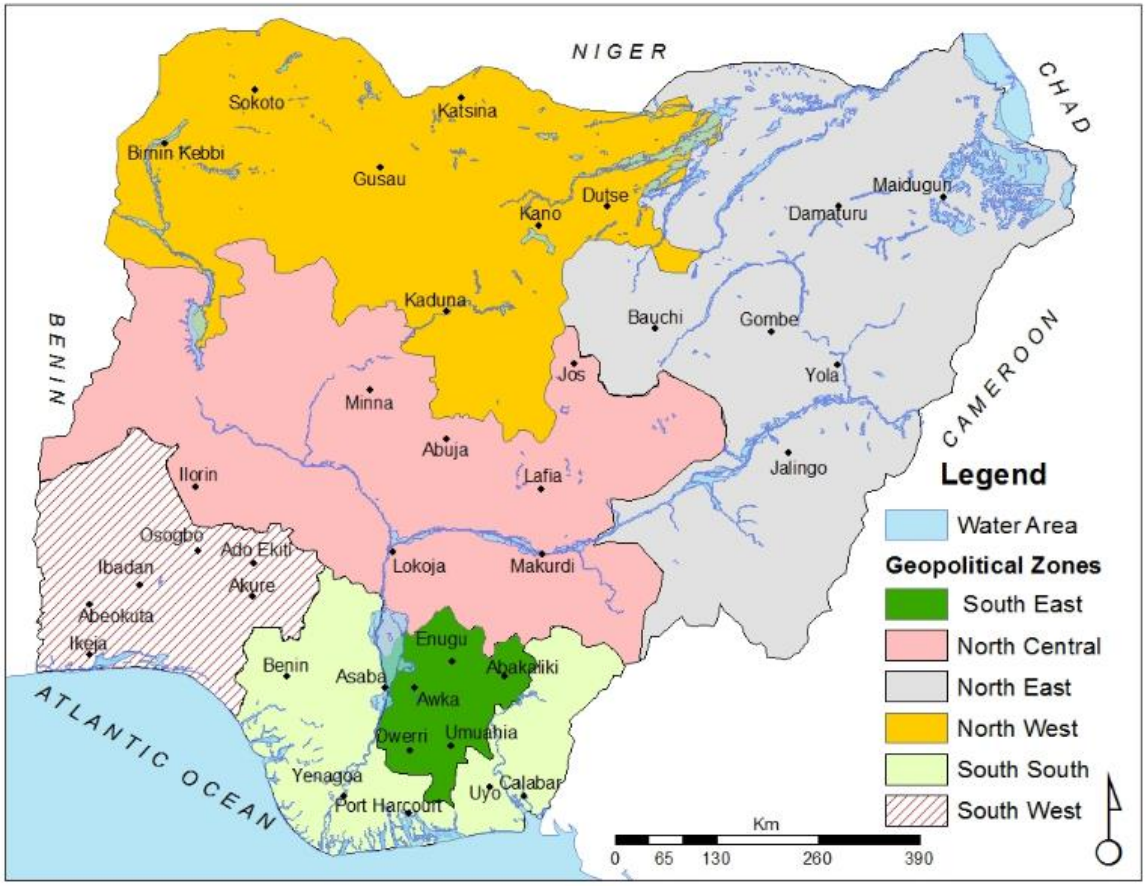

Figure 3.1.1: The six geopolitical zones in Nigeria showing the capital cities of the 36 states and Federal Capital Territory, which are the locations under study in this work.

August 1994 and June 1995 to April 1998 (e.g. Aro, 2007). To avoid any potential seasonal bias, a complete dataset from July 1995 to June 1997 was used in the subsequent analysis as the obtained one minute data were reduced to hourly averages. Because the earlier works (Miskolczi *et al.*, 1997; Udo and Aro 1999; Udo, 2000) covered the period of September 1992 to August 1994, this time around the focus is more on the second dataset. The selected months that represent the dry and rainy seasons are established using a 50-year rainfall dataset (1960–2010) from the Nigerian Meteorological Services (NIMET).

Satellite-derived data for the 37 locations were obtained from National Aeronautics and Space Administration (NASA) for the period of July 1983 to June 2005 (https://eosweb.larc.nasa.gov/sse). The downloaded all-sky data in KWh/m^2/day were converted into W/m^2, to agree with typical instrument readings. The satellite data (NASA, 2013) were obtained by specifying the geographical co-ordinates as given by Chineke *et al.* (2011). The NASA's online data system known as Goddard Earth Observing System version 4 (GOES-4) comprises more than twenty years of meteorological measurements, born out of developed processes including images from serial earth orbiting satellites, mathematical modelling techniques and computer simulations, quality control and validation with ground based instruments and remote sensors (Suarez, 2005; DAO, 1996; Colarco *et al.*, 2010; Liu, 2004). GEOS-4 data set spreads across the entire globe on equal angled grids of 64,800 regions on 1 degree latitude by 1.25 degree longitude. The satellite data were compared with ground data, and then used to evaluate the yearly radiation outlook over a 22-year period.

Ground measured DLR data for Ilorin were obtained from Baseline Surface Radiation Network (BSRN) for the periods of September 1992 - August 1994 and July 1995 – April 1998. Routinely 3-hourly measured records of meteorological parameters for Ilorin and monthly total rainfall data for cities in Nigeria, of various durations, were obtained from

NIMET Oshodi, Lagos. The obtained DLR data from BSRN were reduced to hourly averages from minutes readings and then to daily averages where necessary.

3.3 Statistical Tools

Some of the statistical measures used in this study include the class of descriptive statistics such as mean, maximum, minimum, standard deviation and range. Other statistical measures include correlation coefficient (*R*), mean bias error (*MBE*), mean absolute bias error (*MABE*), root mean square error (*RMSE*) and the t-statistics (t_s). Lastly for selection of clear skies days, the criterion by Aubinet (1994) was used. Some of the statistical measures are described below;

$$R = \frac{n(\sum V_c V_m) - (\sum V_c)(\sum V_m)}{\sqrt{[n\sum V_c{}^2 - (\sum V_c)^2][n\sum V_m{}^2 - (\sum V_m)^2]}} \quad 3.1$$

$$t_s = \sqrt{\frac{(n-1)MBE^2}{(RMSE^2 - MBE^2)}} \quad 3.2$$

$$MBE = \frac{\sum(V_C - V_m)}{n} \quad 3.3$$

$$RMSE = \sqrt{\frac{\sum(V_c - V_c)^2}{n}} \quad 3.4$$

$$MABE = \frac{\sum|(V_c - V_m)|}{n} \quad 3.5$$

where V_c is calculated value, V_m is measured value and *n* is the total number of cases.

It is desired that the magnitude of correlation coefficient *R* either positive or negative should fall into the highest range of 0.90 – 1.00 and at the same time that the compared two models be found to be statistically significant. Two solar radiation models are statistically significant if the calculated t-statistic t_s is lower than the critical *t* value at a particular confidence level,

alpha, (that is 1- alpha) and corresponding (n-1) degrees of freedom (Stone, 1993; Bashahu, 2003). In this study the adopted confidence level is 95%.

An R value rating is given below;

0.00 – 0. 29; little if any correlation

0.30 – 0.49; low positive / (negative) correlation

0.50 – 0.69; moderate positive / (negative) correlation

0.70 – 0.89; high positive / (negative) correlation

0.90 – 1.00; very high positive / (negative) correlation

The critical values at 90%, 95% and 99% confidence levels i.e. (1- alpha) for different degrees of freedom are given below;

df	.10	.05	.01
1	6.314	12.706	63.655
.	.	.	.
.	.	.	.
.	.	.	.
30	1.697	2.042	2.750
40	1.684	2.021	2.705
60	1.671	2.000	2.660
120	1.658	1.980	2.617
∞	1.647	1.960	2.576

The clear skies conditions are that (Aubinet, 1994); (1) the daily clearness index must be greater than or equal to 0.60 .i.e.

$$K_T = \frac{H}{H_o} \geq 0.60 \qquad 3.6$$

where H is the daily global solar irradiation (J/m^2) and H_o is the daily extraterrestrial solar irradiation intercepted by a plane parallel to the earth surface (J/m^2). (2) The earth-to-sky radiation deficit must be stable during the day. More particularly the equation below is used

$$(\Delta\Phi)_{24h} - (\Delta\Phi)_{night} < 10\text{W/m}^2 \quad 3.7$$

where the indexes (*24h, night*) refer to average values of the period considered and $\Delta\Phi$ refers to value of the radiation. These criteria ensure that no significant cloud passage occurs during the night and that no fog appears before the sunset.

3.4 Testing and Modeling Techniques for Clear Skies Equations at Ilorin

The general form for most expressions of clear sky downward longwave radiation is given as (Iziomon *et al.,* 2003; Sedlar and Hock, 2009):

$$DLR = F\varepsilon\sigma T^4 \quad 3.8^*$$

F is the cloud cover and is equal to unity for clear skies. Sometime it is incorporated into ε and the equation becomes:

$$DLR = \varepsilon\sigma T^4 \quad 3.8$$

where ε is emissivity, σ is Stefan Boltzmann's constant and T is ambient temperature.

Most equations of *DLR* are in the form of equation 3.8 with variations mostly in the forms in which the emissivity, ε are expressed. The clear skies estimates for DLR tested are listed below, with arrangement based on the year they were developed.

$Brunt$ (1932) $\left(0.605 + 0.048e^{1/2}\right)\sigma T^4$ 3.9

$Efimova$ (1961) $(0.746 + 0.0066e)\sigma T^4$ 3.10

$Swinbank$ (1963) $(5.31 * 10^{-13})T^6$ 3.11

$Idso\ and\ Jackson$ (1965) $(1 - 0.261\exp(-7.77 * 10^{-5}(273 - T)^2))\ \sigma T^4$ 3.12

Maykut *and Church* (1973) $0.7855\sigma T^4$ 3.13

Brusaret (1975) $1.24(\mathrm{e/T})^{1/7}\sigma T^4$ 3.14

Satterlund (1979) $1.08\left[1-\exp\left(-\mathrm{e}^{T/2016}\right)\right]\sigma T^4$ 3.15

Idso 1 (1981) $0.179\left[\mathrm{e}^{1/7}\exp(350/T)\right]\sigma T^4$ 3.16

Idso 2 (1981) $[0.70+5.95*10^{-5}\mathrm{e}\ \exp(1500/T^4)]\sigma T^4$ 3.17

König – Langlo *and Augstein* (1994) $0.765\sigma T^4$ 3.18

Plata (1996) $[1-(((1+46.7(\mathrm{e}/T))*$

$\exp(-(1.2+3*46.7*\mathrm{e}/T)^{1/2})]\sigma T^4$ 3.19

Guest (1998) $\sigma T^4-85.6$ 3.20

where *e* is water vapour pressure (mb), *T* is air temperature (K) and σ is Stefan Boltzmann's constant (5.67 x 10^{-8} $Wm^{-2}K^{-4}$).

Modelling techniques are of two main types; empirical and theoretical. Empirical technique is based explicitly on data while the theoretical technique is based on theory, pattern or behaviour inherent in the processes involved. In this work the empirical method was used while adopting the curve fitting procedures. In curve fitting, given two *n* numbers of points in pairs $(x_1, y_1) \ldots, (x_n, y_n)$ and such that a line is useful to fit through the points, then a good method for fitting through the points is a straight line via the method of least squares by Gauss (Kreyszig, 1999). Given a straight line of the form y = mx + c, the fitting will be such that the sum of the squares of the distances of those points from the straight line is minimum, where the distance is measured in the vertical direction (the y-direction).

The solution for the gradient *m* is given as;

$$m = \frac{n\sum x_j y_j - \sum x_j \sum y_j}{n(n-1)s_x^2} \quad 3.21$$

At times transformation of parameters, e.g. by taking the logarithm, makes the outcome of the fitting better (Edwards and Hamson, 1989). In this work, modelling is achieved by making the emissivity ε the subject of formula from equation 3.8. Since the obtained values of the emissivity were in fractions (average value was 0.84), the logs of water vapour pressure *e* and temperature *T* (such as log(*eT*), log(e^2T) etc), to conform to the corresponding nature of the values of the emissivity ε, were taken. Eventually the relationship of ln(eT^2), as the independent variable to the emissivity ε, as the dependent variable was expressed in the form of the well-known linear regression model of x and y, where y = mx + c. By empirical modelling technique as obtained in the least square method, the coefficients were assigned *a* and *b,* which corresponding to *m* and *c*, where *a* is the gradient and *b* is the intercept. Thus ε = *a* (lneT^2) + *b* and with respect to measured data a new model was found as;

$$\text{New 1} = (a\,(\ln eT^2) + b)\,\sigma T^4 \quad 3.22$$

The constants or coefficients were obtained to be;

$a = 0.058$ and $b = -1.48 \times 10^{-4}$

To verify the extent that the exponents of temperature in combination with water vapour pressure affect the estimation of DLR through the emissivity in Ilorin, the correlation between the emissivity and different combinations of atmospheric variables of temperature *T* in (K) and water vapour pressure *e* in (mb) was investigated. Based on the result of the correlation, another new equation in the form of ε = a + b(*eT*) was obtained and via the line of best fit, the values of the constants a and b were also obtained as 0.694 and 2.11×10^{-5} respectively. And the new equation is as expressed below:

$$New\ 2 = (a + b(eT))\sigma T^4 \quad 3.23$$

3.5 Neural Networks Actualisation

This work involved the usage of the ANNs for optimization and is not concerned with the development of the applications. In the course of the work, modelling with ANNs was undertaken using the Matlab® platform. As the neural networks are still developing, newer versions of Matlab® reflect innovations on neural networks. Incidentally during the course of this work different versions of the Matlab® (eg Matlab 6.5, Matlab 7.9.0.529/R2009b and Matlab7.13.0.564/ R2011b etc) have been brought out. Matlab 7.9.0.529/ R2009b was used in this work and consistency was maintained by using the feed forward backpropagation neural networks function for 1 hidden layer of 10 hidden neurons whereby the system on its own partitioned the data into training, validating and testing sets. The defaults parameters for transfer functions for hidden layers and output, learning rate, momentum, performance functions etc were adopted for the feed forward backpropagation neural networks. In the analysis carried out, the numbers of input parameters were investigated as well as the latitudinal impact of training of the neural networks for the satellite data, among others. Typically learning or training in ANNs is in two ways - one of it is to give the networks a proper formation of the problem (otherwise known as unsupervised learning) while the other is to allow the networks learn from examples (otherwise known as supervised learning). It should be pointed out that throughout all the experiments with ANNs in this work, the supervised learning was adopted, and the codes as contained in the released version for the training were used rather than the interface.

CHAPTER FOUR

RESULTS

4.1 Relationship between Ground and Satellite Data at Ilorin

The relationship between ground and satellite data could only be determined for Ilorin because that is the only station with ground measurements. Table 4.1.0 gives the descriptive statistical results for the comparison between ground measured data and satellite derived data of the station. For the first two years (that is between 1992 and 1994), the daily average ground DLR was 398 W/m^2, whereas the satellite value was 394 W/m^2. In the first year, the ground value was 395 W/m^2 and satellite value was 391 W/m^2, whereas in the second year, the ground value was 400 W/m^2 and satellite value was 396 W/m^2. For the non-seasonal case, the mean bias error (MBE) was approximately $-3.8 W/m^2$, which is within the experimental error of ± 5 W/m^2. Throughout Table 4.1.0, it is obvious that the both the satellite data and the ground data are relatively close.

At the 95% confidence level, the critical *t* value for any set of data having units more than 120 is 1.96. In Table 4.2.0, for the first period of measurements under the t-statistic column the only value less than 1.96 is that of the rainy season. However, despite the closeness of the values in Table 4.1.0 the rainy season shows low correlation (41%), whereas the dry season and combined seasons have correlation coefficients of 82% and 85% respectively despite not been statistically significant. With respect to parity with satellite data, because the experimental DLR measurements at Ilorin were performed in two phases and because of the slight differences between the results of the first and second phases, it was analyzed at both. Because the first phase showed seasonal dependency, only the full two-year period from July 1995 to June 1997 was considered to avoid the seasonal drift in the data from early June 1995 to late April 1998. The dry season showed consistently good correlation between satellite and

ground data as was the case earlier (0.82 and 0.79). Whereas the ground data were estimated to statistical significance in the rainy season during the first period, the reverse was the case during the period of July 1995 to June 1997 as the satellite data failed to estimate the ground data to statistical significance during the rainy season but rather during the dry season. It should be noted that throughout the comparison, none of the cases has correlation up to 0.90, which is the grade for the highest level of correlation though it is mostly during the dry seasons that the correlations are good.

Table 4.1.0; Summary statistics for both the ground measured data and the satellite derived data of DLR in W/m^2 for Ilorin, Nigeria

Period	Statistics	Ground measured data	Satellite derived data
Sept 1992 – Aug 1993 (1 year)	Mean (W/m^2)	395	391
	Maximum (W/m^2)	424	431
	Minimum (W/m^2)	334	307
	SD	21.7	30.0
Sept 1993 – Aug 1994 (1 year)	Mean (W/m^2)	400	393
	Maximum (W/m^2)	427	432
	Minimum (W/m^2)	343	318
	SD	15.5	25.1
Sept 1992 – Aug 1994 (2 years)	Mean (W/m^2)	398	394
	Maximum (W/m^2)	427	433
	Minimum (W/m^2)	334	307
	SD	19.0	27.8
July 1995 – June 1996 (1 year)	Mean (W/m^2)	392	403
	Maximum (W/m^2)	419	430
	Minimum (W/m^2)	335	333
	SD	21.4	19.6
July 1996 – June 1997 (1 year)	Mean (W/m^2)	395	393
	Maximum (W/m^2)	421	430
	Minimum (W/m^2)	342	303
	SD	17.9	27.7
July 1995 – June 1997 (2 years)	Mean (W/m^2)	393	398
	Maximum (W/m^2)	421	430
	Minimum (W/m^2)	335	303
	SD	19.8	24.4

Table 4.2.0: Statistical analysis between ground measurement and satellite derived DLR at Ilorin.

Periods of Observations	Seasons	R	MBE	RMSE	t_s
Sept 1992 – Aug 1994	All seasons	0.85	-3.80	16.03	2.20
	Dry season	0.82	-11.83	22.40	5.59
	Rainy season	0.41	1.82	9.24	1.81[b]
July 1995- June 1997	All seasons	0.67	4.66	18.96	2.28
	Dry season	0.79	-1.92	17.87	0.97[b]
	Rainy season	0.17	9.32	19.69	4.84

[b] the satellite data estimated the ground data to statistical significance

4.2 Trends of DLR in Nigeria

4.2.1. Diurnal Trends of DLR

The hourly pattern of DLR could only be established for a single station, Ilorin due to the fact that the ground data obtained extended through the respective hours of the day, while the satellite data were for daily values only. The average diurnal behavior of DLR was found to increase gradually (with some inherent fluctuations) from 01:00 to a maximum around 14:00 hrs local time, and then gradually decreased to minimum (Fig 4.1.1). During the rainy season (Fig 4.1.2), DLR showed the same pattern as described above, though the values were much higher and the pattern was maintained during the dry season (Fig 4.1.3) but at lower values. Furthermore, the diurnal patterns of four important solar periods were studied. The September equinox diurnal DLR (Fig 4.1.4) is similar to the existing pattern, whereas in the March equinox (Fig 4.1.5) the radiation maintains almost a steady value from 01:00 to 07:00 hrs before starting to increase from 08:00 hrs and thereafter follows the normal pattern. However comparing the diurnal DLR for the two equinoxes, one seems to be a lateral inversion of the other. While the radiation is lower at the beginning hours of the day than at the ending hours for the March equinox, the situation is reversed for the September equinox.

Differing scenarios were observed during the months of June and December. Examining the June solstice (Fig 4.1.6) , the values are rather low, even lower than the dry season (Fig 4.1.3), despite the fact that June is part of the rainy season with typically high DLR values. The December solstice produced a cyclic pattern within a 24 h period, as seen in Fig 4.1.7; it increases from 01:00 hrs, dims slightly from 07:00 to 10:00 hrs, rises until 15:00 hrs, and then gradually decreases to a minimum.

To examine the uncommon patterns of the two diurnal extremes witnessed during June and December, the respective two months for all the periods of ground measurements were further investigated. Not only are June and December further considered, but also their respective preceding and succeeding months. When the Junes were studied, it was discovered to have such varying random patterns (Figs 4.1.9, 4.1.12 and 4.1.17) with exceptions of June 1995 (with six days of missing data) of Fig 4.1.14 which showed little of such character and that of June 1997 (Fig 4.1.20) which had the normal pattern similar to Fig 4.1.1. The irregular Junes pattern when averaged caused the unexpected too low radiation effect of Fig 4.1.6. Thus most times, the diurnal pattern in June is unpredictable. At that point in time, the sun–earth distance is the longest and the experience of a long day and short night is prevalent while the sun is overhead, especially on June 21. Though the erratic diurnal DLR patterns of June have not been consistently found to occur in that month, yet the patterns could also occur in other months around June and last for months as well. While in 1993 the pattern did not occur in May (Fig 4.1.8) but in June (Fig 4.1.9) and July (Fig 4.1.10), in 1994 it was predominately observed from May to July (Figs 4.1.11 - 4.1.13). However in 1995, the irregular pattern could not be investigated for May due to no measurement, and even though the pattern did not occurred in June (Fig 4.1.15), yet it occurred in July (Fig. 4.1.15). In 1996, the irregular pattern occurred from May down to July (Figs 4.1.16 - 4.1.18). Throughout May

(Fig 4.1.19) and June (Fig 4.1.20) of 1997 the pattern did not occur, even though it showed some degree of it in July (Fig 4.1.21) of that year.

Except December 1993, which had a different graphical output somewhat similar to that of the March equinox of Fig 4.1.5, those of Decembers1992 (Fig 4.1.23), 1995 (Fig 4.1.29), 1996 (Fig 4.1.32), and 1997 (Fig 4.1.35) are typical of the already established pattern of Fig 4.1.7; that is, rising to a peak value and then decreasing before rising to a second peak value before finally returning to a minimum. Leaving out 1994 in the case of the December diurnal pattern due to unavailable data, the double peak diurnal DRL pattern that dominates at the end of the year was found to always occur in diverse magnitudes lasting various durations. Just like in the case of the established June pattern, at times it would also stay on for three to two months. In the case of 1992 when it lasted from November to December (Figs 4.1.22 - 4.1.23), the diurnal curves displaced about three peaks. In January of 1993 (Fig 4.1.24) the pattern did not occur, though it came back in November of 1993 (Fig 4.1.25). But even though it did not occur throughout December of 1993, (Fig 4.1.), January of 1994, and November of 1995, however it occurred in December (Fig 4.1.29) of 1995 and lasted to January (Fig 4.1.30) of 1996. In 1997, the end of the year diurnal pattern of DLR occurred in January, November and December. It did not occur in January of 1998. If the patterns established for the diurnal variation of DLR both at the mid of the year and at the end of the year were to occur throughout the rainy and dry seasons respectively, then it would have been attributed to seasonal effects. However the periods the patterns did not occur as expected could be due to normal variation imbedded in climatic parameters.

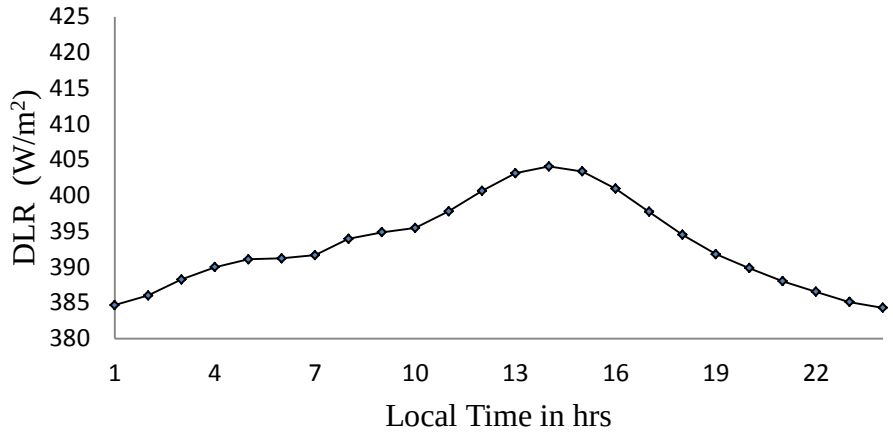

Fig 4. 1.1: Daily DLR between 1995 and 1997

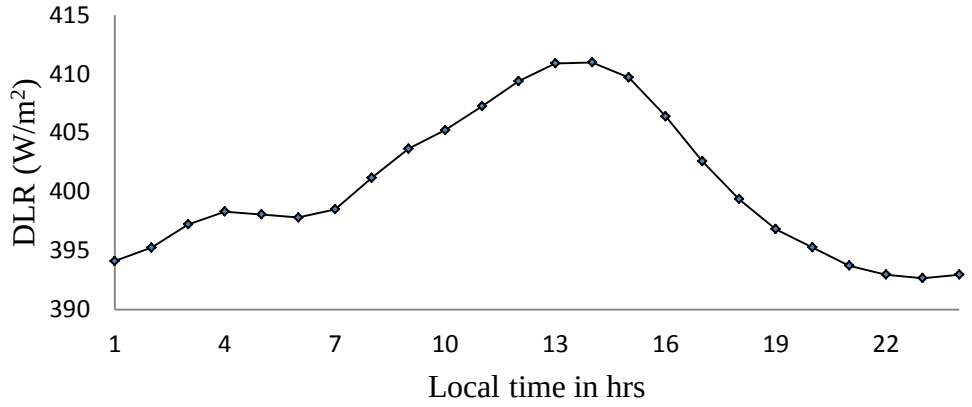

Fig 4. 1.2: Rainy season diurnal DLR between 1995 and 1997

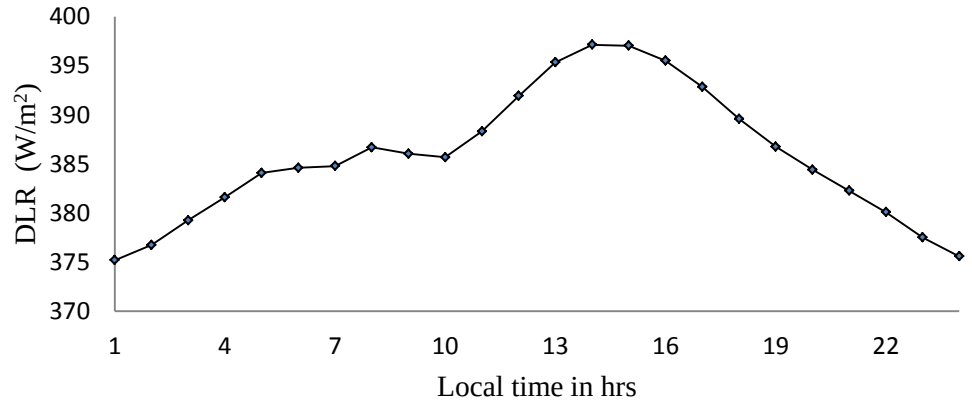

Fig 4. 1.3: Dry season DLR between 1995 and 1997

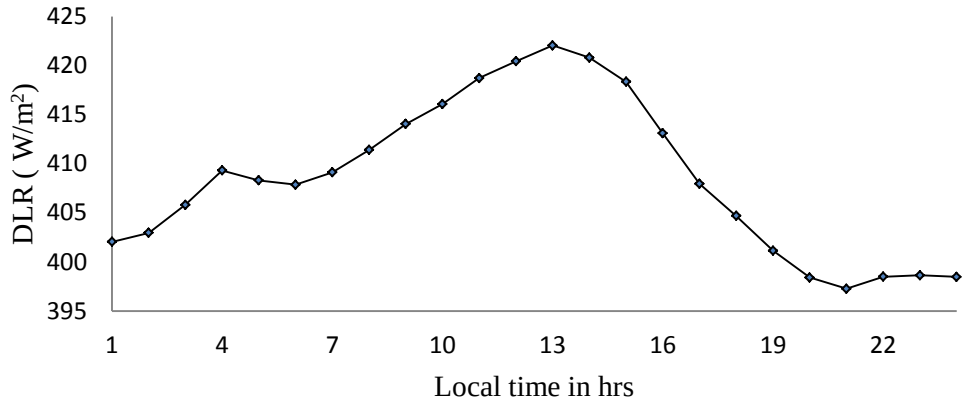

Fig 4. 1. 4: September equinox diurnal DLR between 1995 and 1997

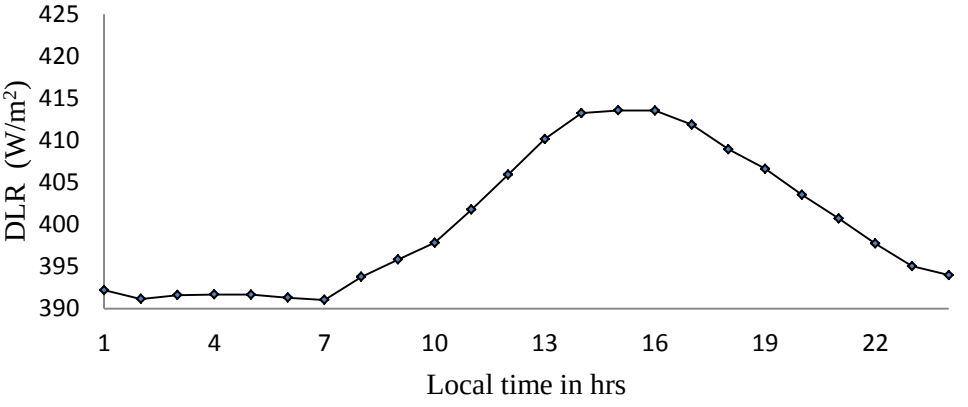

Fig 4. 1.5: March equinox DLR between 1995 and 1997

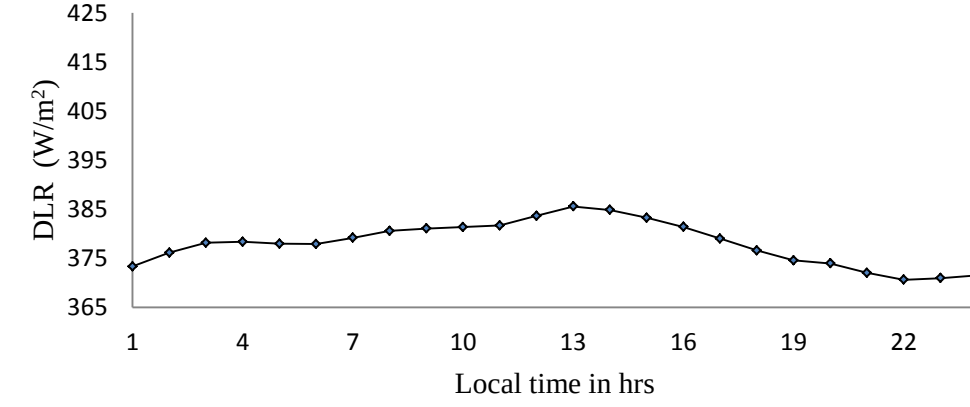

Fig 4. 1.6: June solstice DLR between 1995 and 1997

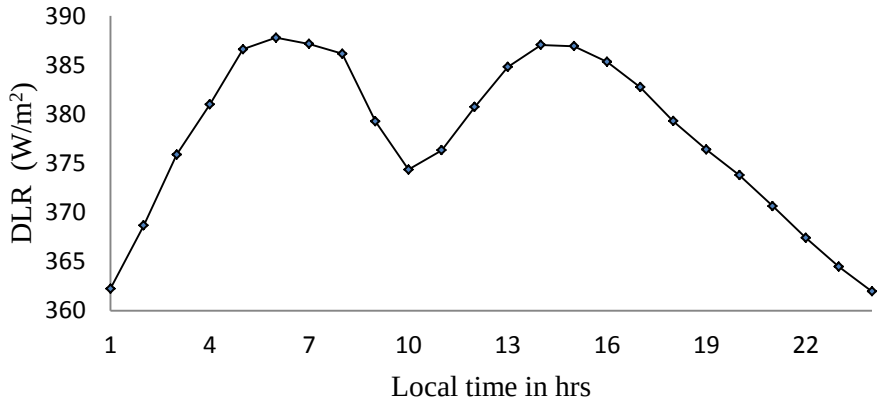

Fig 4.1.7: Average December between 1995 and 1997

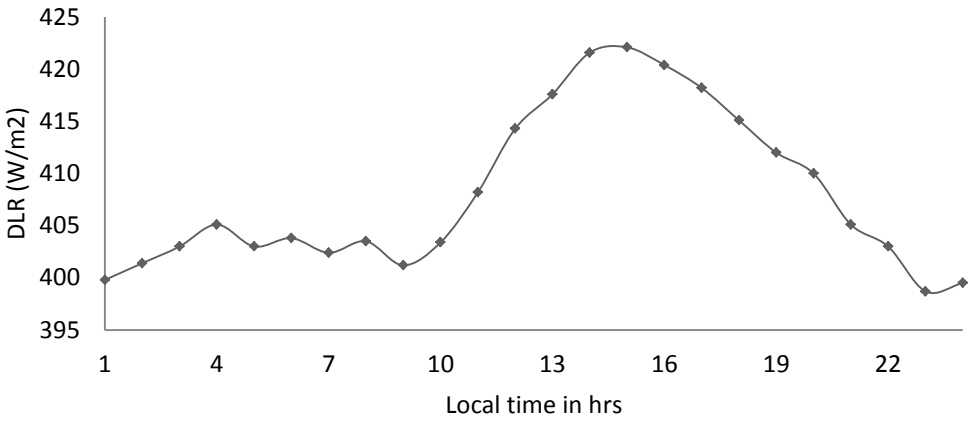

Fig 4.1. 8: May 1993

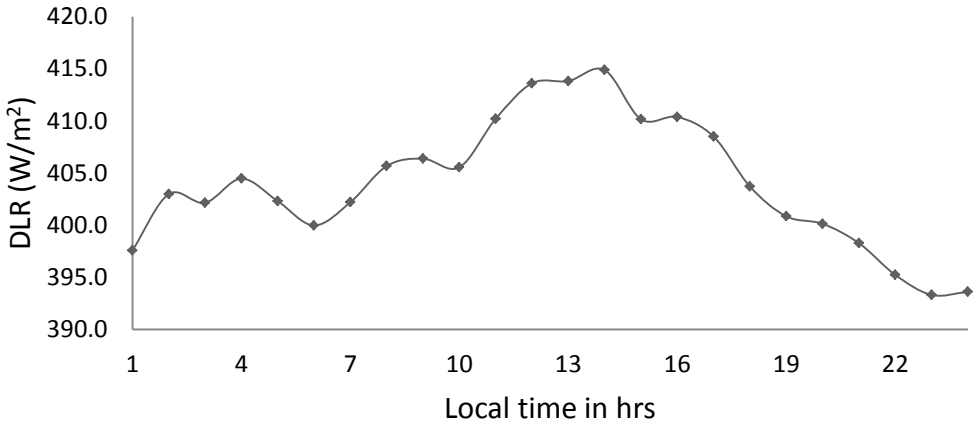

Fig 4.1.9: June 1993

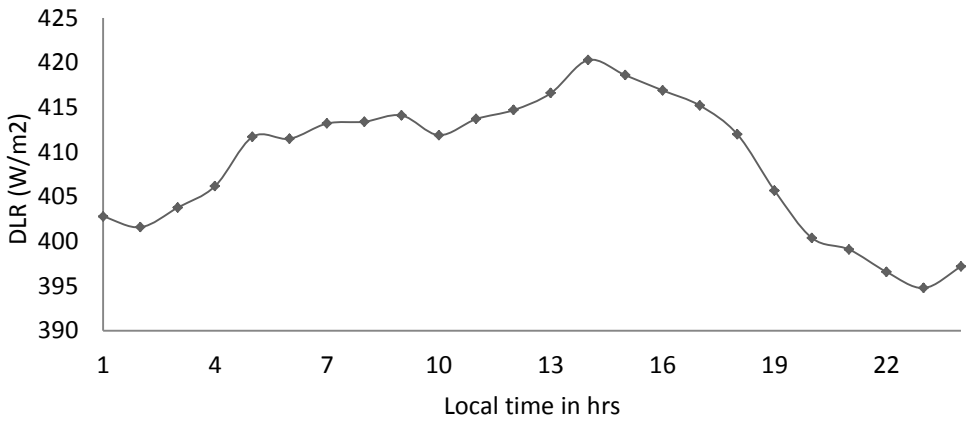

Fig 4.1.10 : July 1993

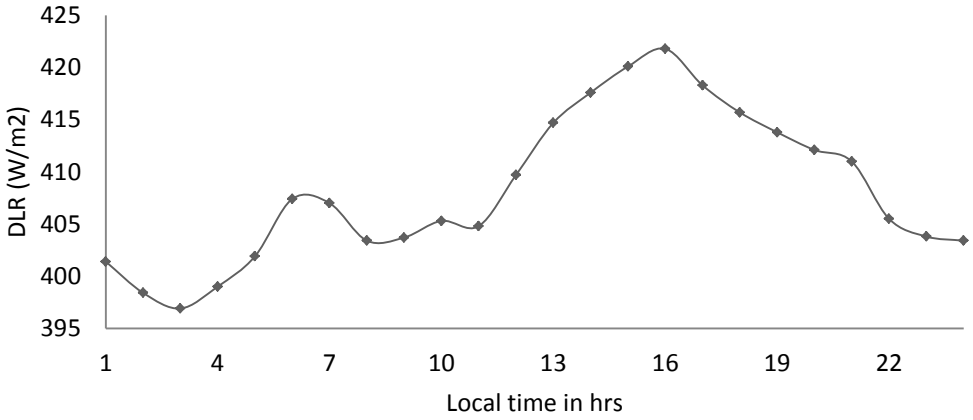

Fig 4.1.11 : May 1994

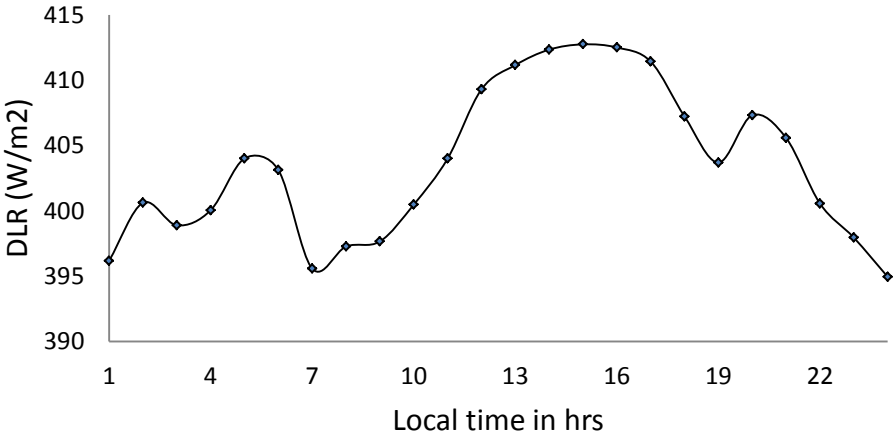

Fig 4.1.12: June 1994

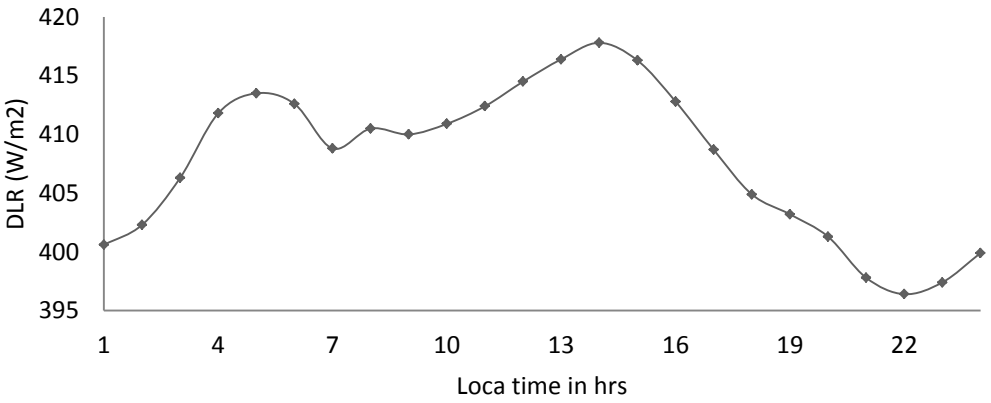

Fig 4.1.13 : July 1994

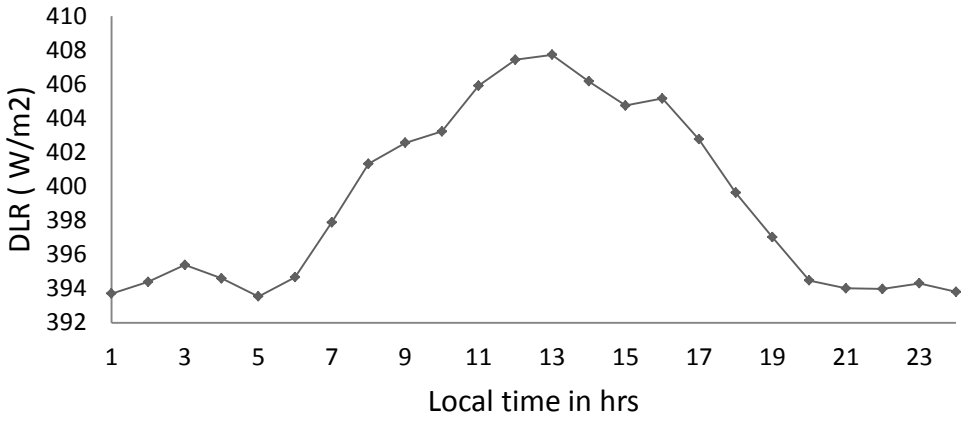

Fig 4.1.14: June 1995

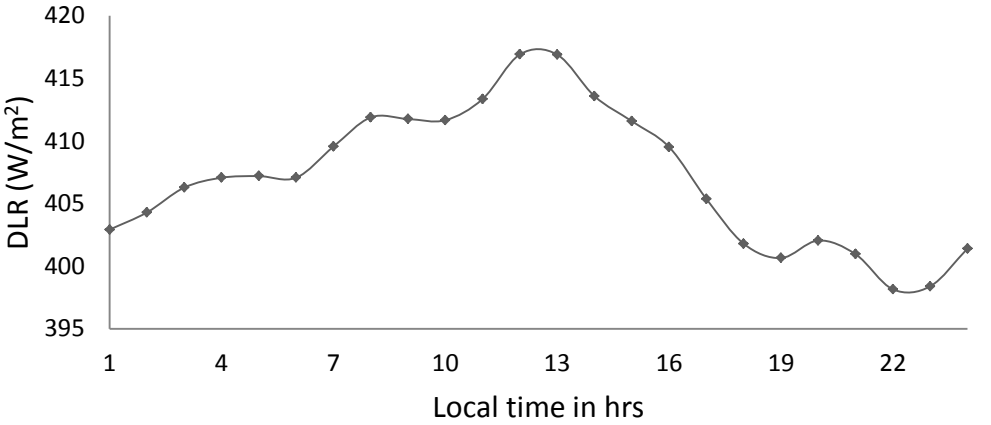

Fig 4.1.15: July 1995

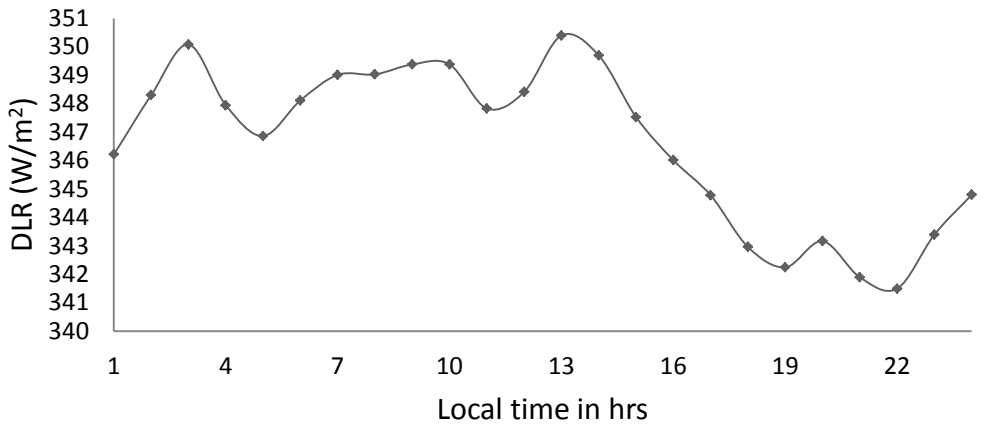

Fig 4.1.16: May 1996

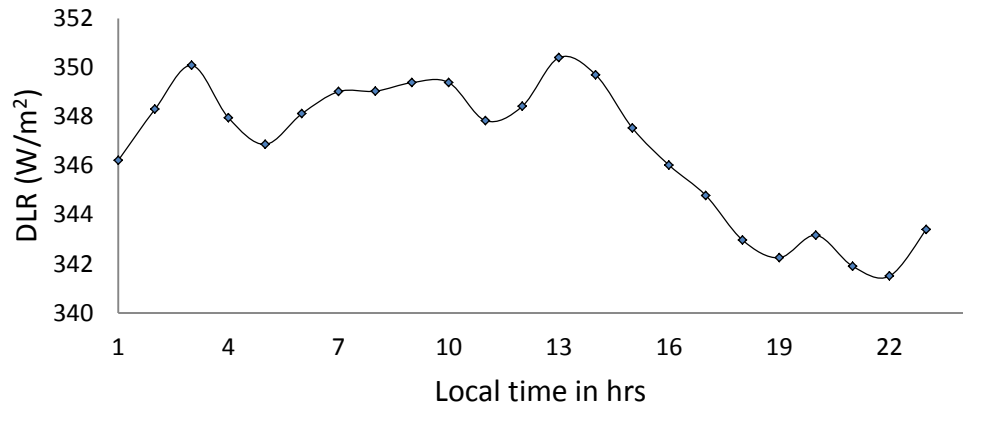

Fig 4.1.17: June 1996

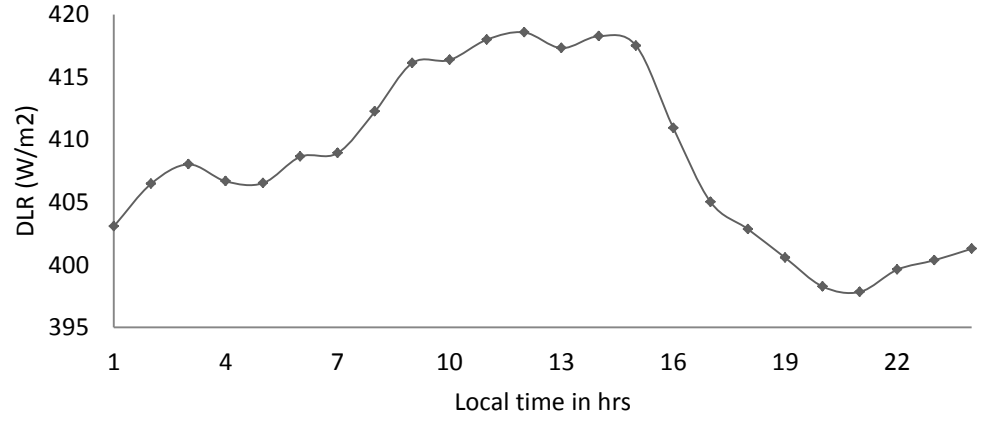

Fig 4.1.18: July 1996

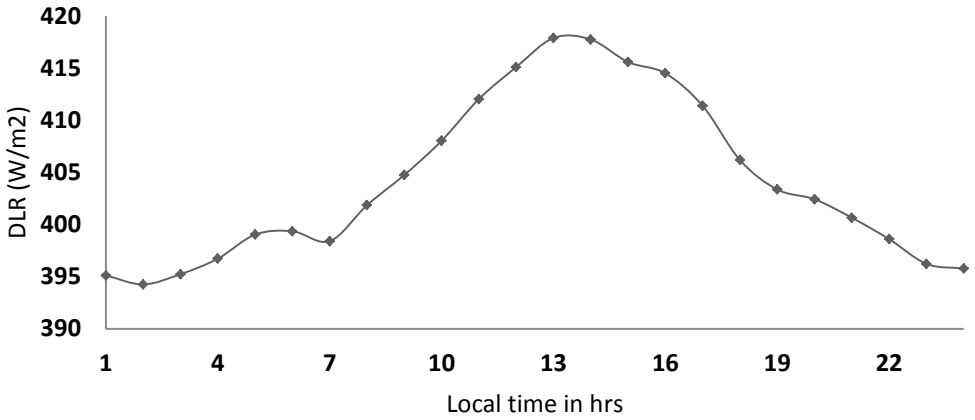

Fig 4.1. 19: May 1997

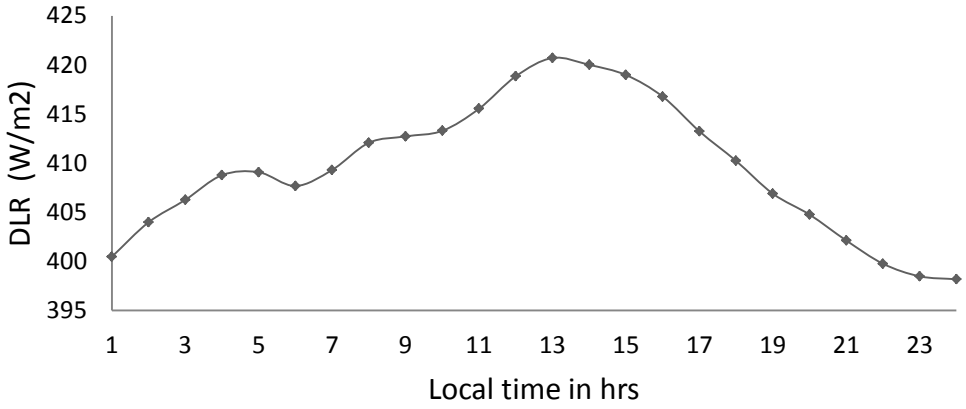

Fig 4. 1.20: June 1997

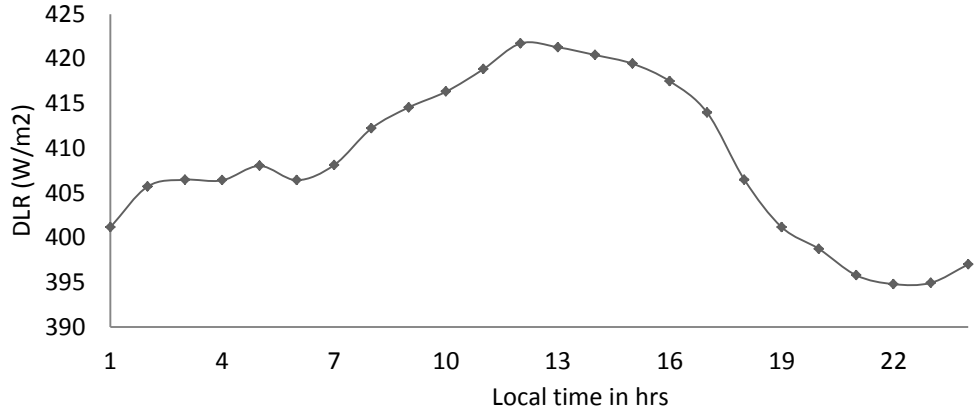

Fig 4.1.21 : July 1997

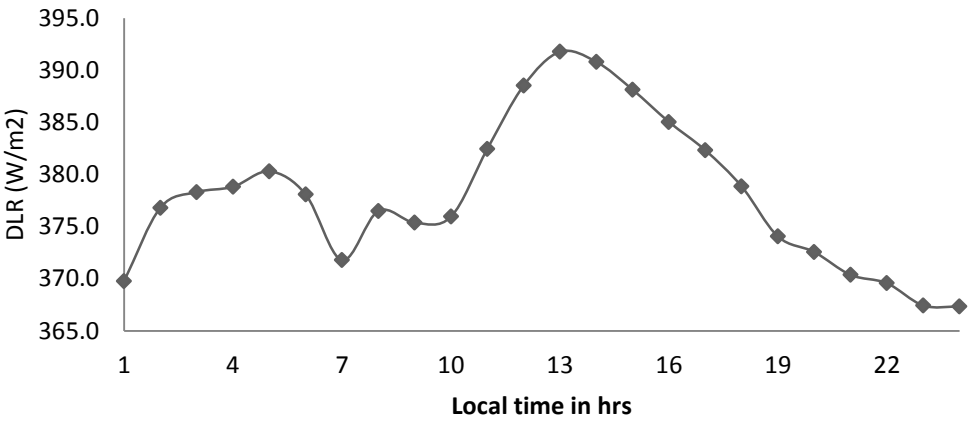

Fig 4.1.22: November 1992

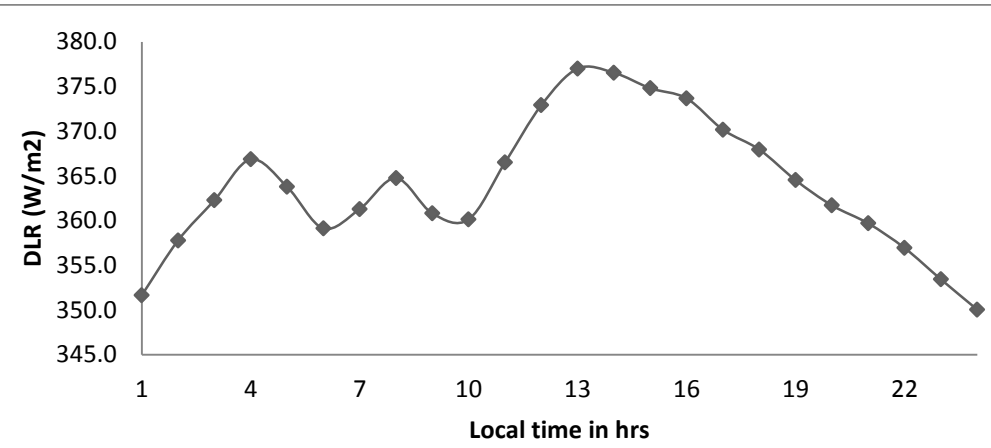

Fig 4.1.23: December 1992

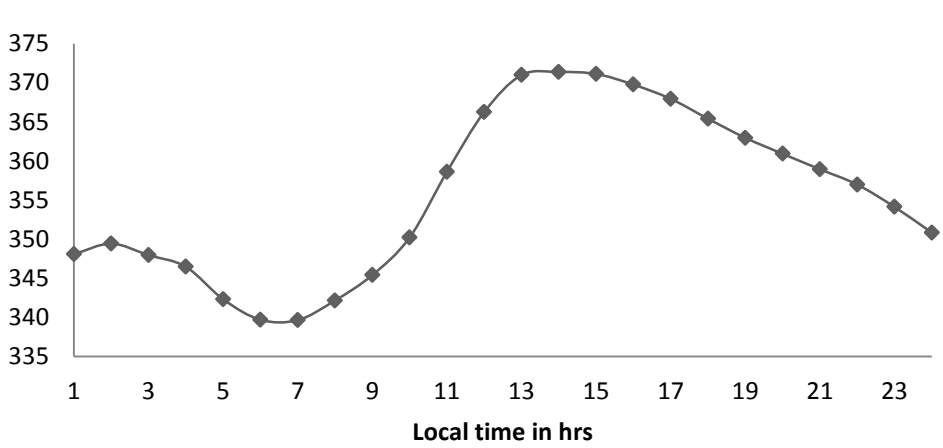

Fig 4.1.24: January 1993

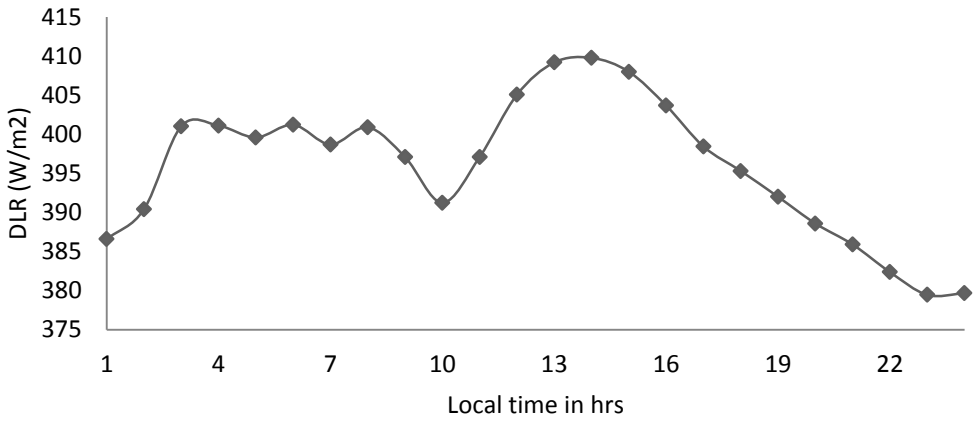

Fig 4.1.25: November 1993

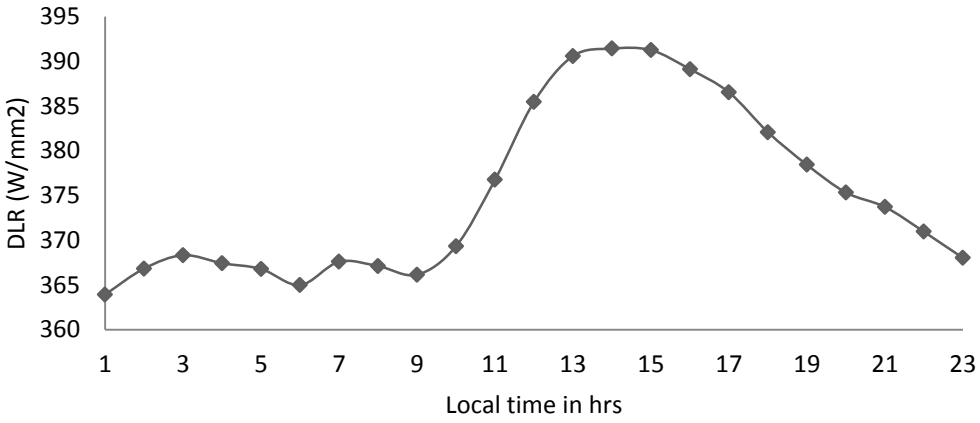

Fig 4.1.26: December 1993

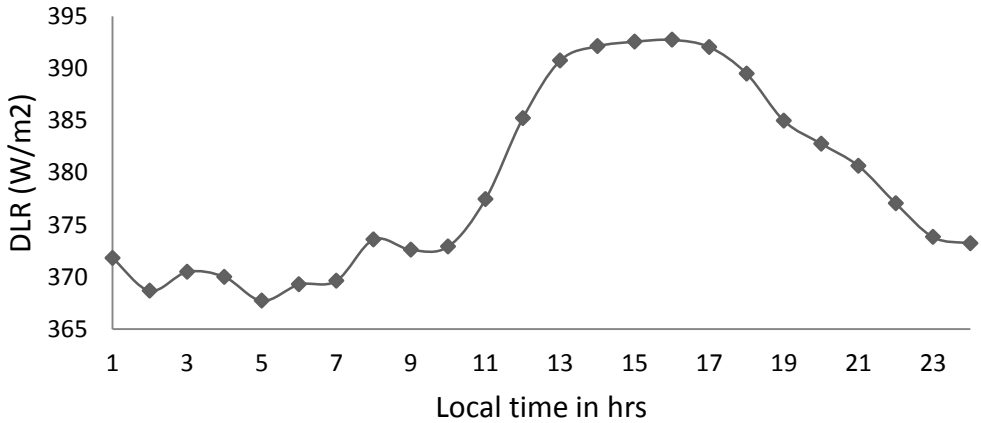

Fig 4.1.27: January 1994

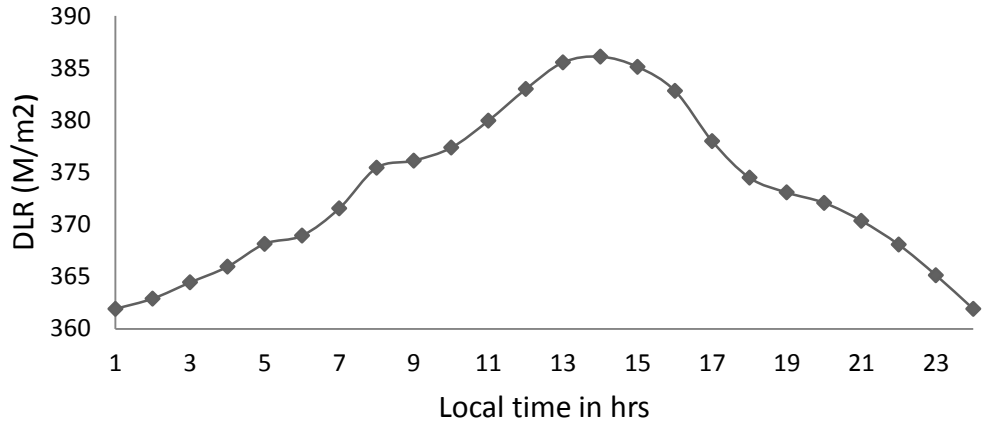

Fig 4.1.28: November 1995

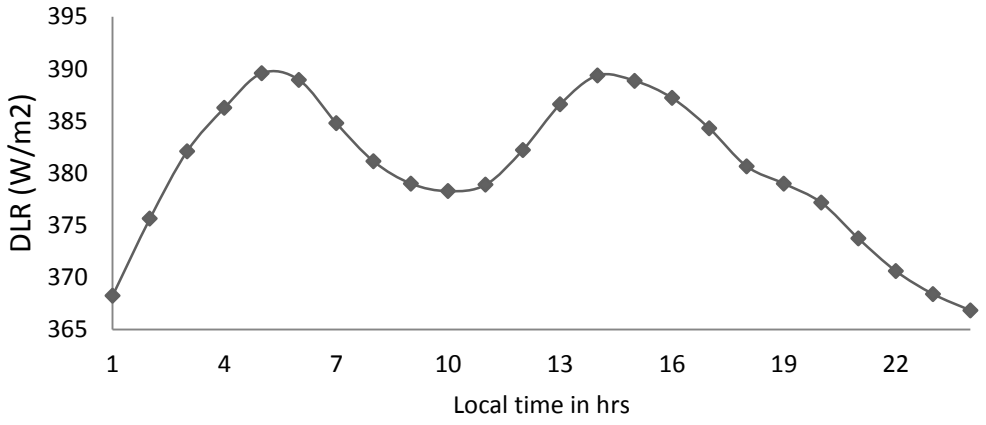

Fig 4.1.29 : December 1995

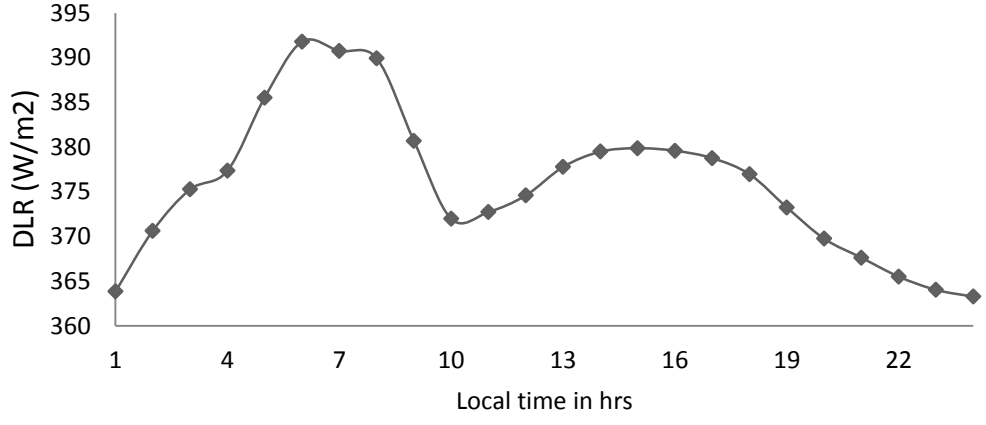

Fig 4.1.30: January 1996

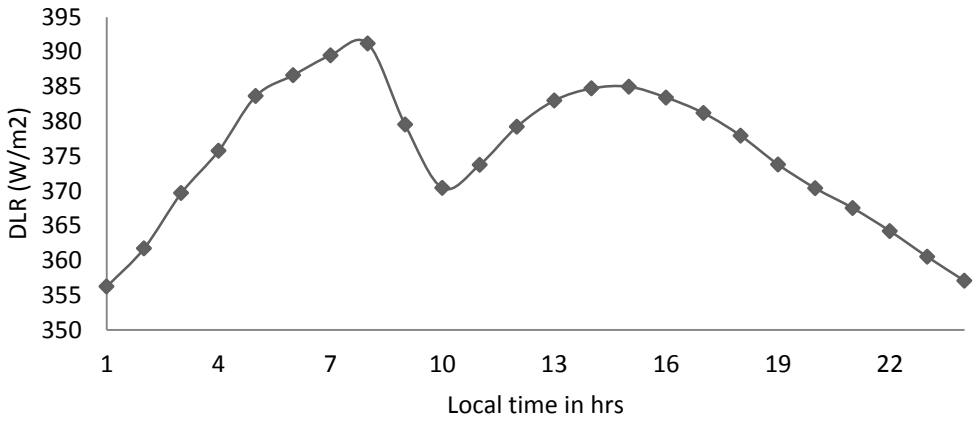

Fig 4.1.31: November 1996

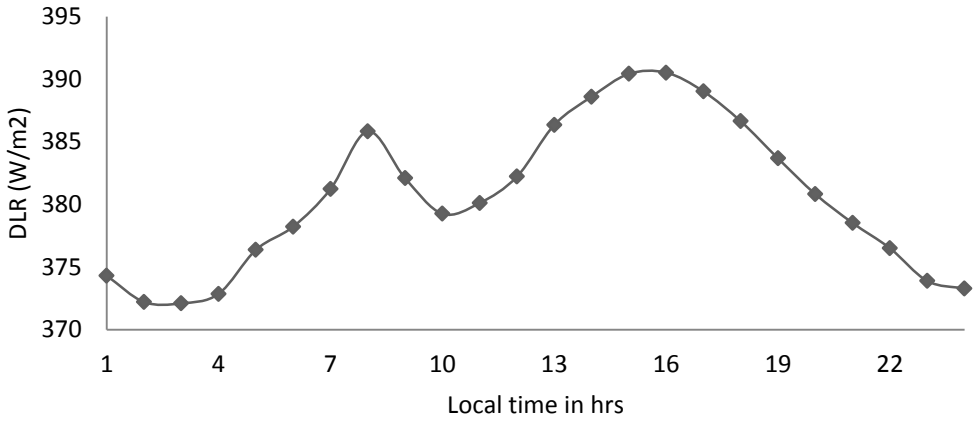

Fig 4.1.32: December 1996

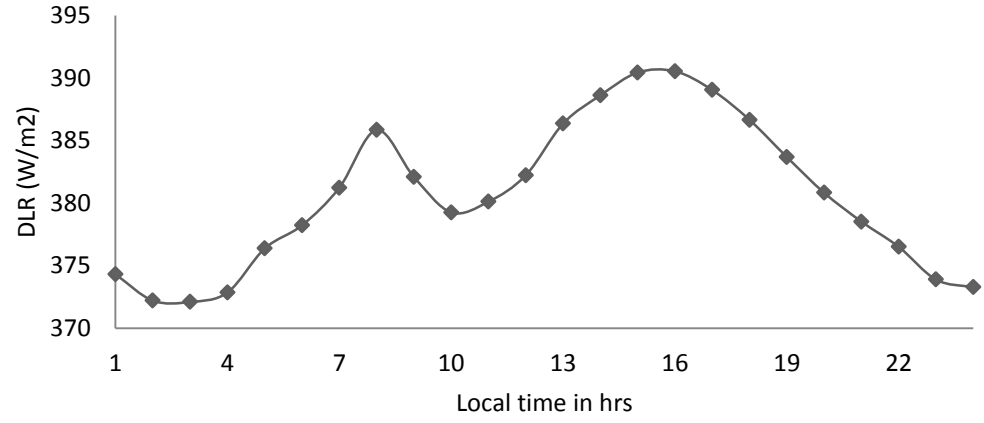

Fig 4.1.33 :January 1997

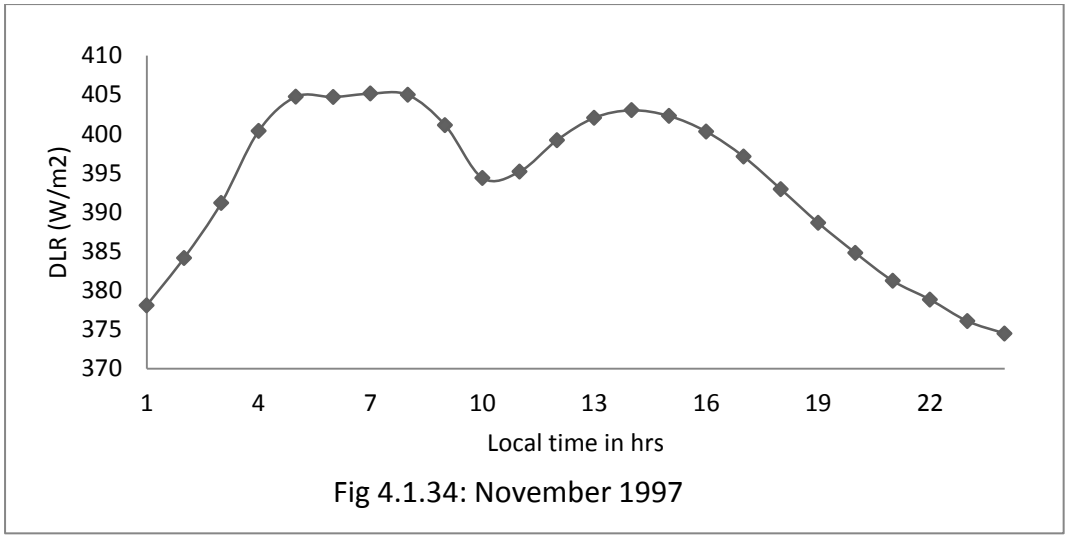

Fig 4.1.34: November 1997

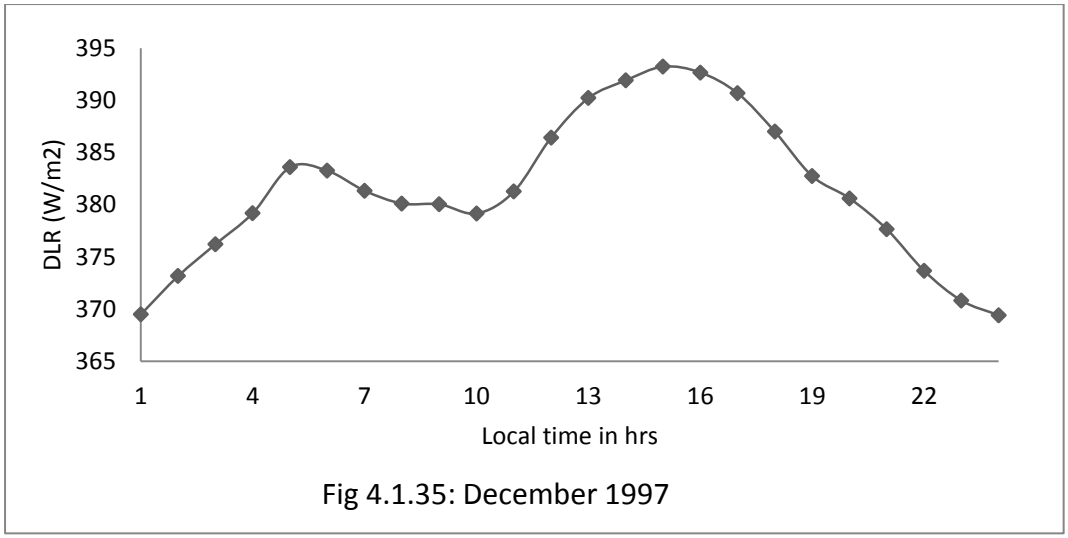

Fig 4.1.35: December 1997

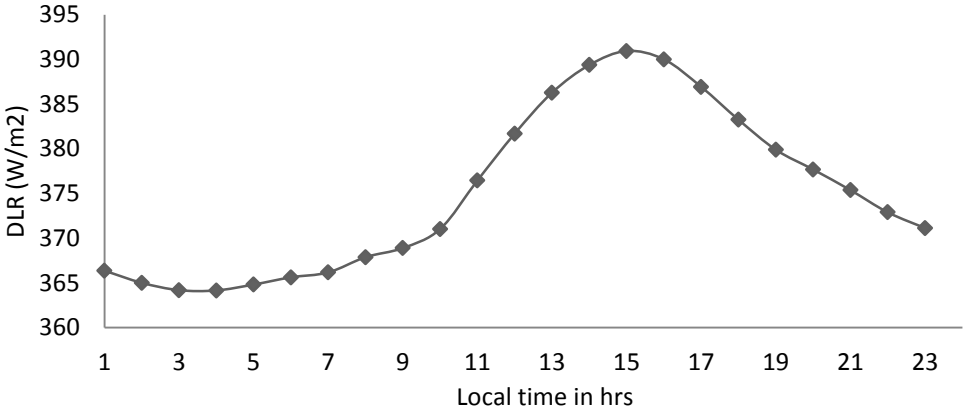

Fig 4.1.36: January 1998

Figs 4.1.1 – 4.1.36: Average Diurnal patterns of DLR based on ground taken data in Ilorin, Nigeria.

4.2.2 Daily Trends of DLR

There are different cases of two or more cities closely situated that have exact values of DLR and other parameters from the satellite data (Table 4.3.0). One set is Ado Ekiti (7.62^{o}N, 5.22^{o}S) and Akure (7.25^{o}N, 5.20^{o}S) and another set is Owerri (5.02^{o}N, 7.93^{o}S), Umuahia (5.48^{o}N, 7.02^{o}S) and Uyo (5.53^{o}N, 7.48^{o}S). Others are Awka (6.20^{o}N, 7.73^{o}S) with Enugu (6.50^{o}N, 7.50^{o}S) and Abeokuta (7.15^{o}N, 3.33^{o}S) with Ibadan (7.38^{o}N, 3.90^{o}S). Incidentally these locations are in the southern part of the country. As earlier mentioned in section 3.2, NASA Goddard Earth Observing System - Version 4 (GEOS 4) Multiyear Assimilation Time Series Data is on a 1 degree longitude by 1 degree latitude equal-angle grid covering the entire globe (64,800 regions). The GEOS 4 data set has a spacing of 1.25 degrees longitude by 1 degree latitude. Bilinear interpolation is used to produce 1 by 1 degree regions. Hence, when the latitude and longitude for a specific region are specified, the values received by the system are for a 1 degree by 1 degree box containing the location. Therefore, if the coordinates are close, then the outputs will be identical.

The identical cases recorded in this study are most likely due to the co-ordinates of the locations falling into the same grip box, and therefore, identical data are obtained for the affected locations. These locations may not necessarily have identical meteorological variables and all satellite outputs of every type of data may not be equal (Nwokocha *et al.,* 2012; Chineke *et al.*, 2011; Okonkwo and Mbajiorgu, 2010; David-Okoro *et al.,* 2009). However, as already highlighted, this situation is particularly the case due to the adopted technique. In this study, whenever one of the locations is mentioned, the other locations are also implied, except when otherwise stated. Still on that, the rainfall patterns for affected locations where data were obtained from NIMET in this study are not the same. For instance Fig 4.3.38c for Uyo and Fig 4.3.38d for Owerri are different.

The daily mean DLR for the study period ranged from 374.7 W/m^2 for Kano in the extreme north to approximately 411.1 W/m^2 for Yenagoa in the extreme south, which is a difference of approximately 36 W/m^2 (Table 4.3.0). The highest daily maximum DLR values are Sokoto (475.0 W/m^2), Birnin Kebbi (471.7 W/m^2), and Damaturu (470.4 W/m^2), which are all in the north, while the lowest daily maximum DLR values are Calabar (432.9 W/m^2), Yenagoa (436.3 W/m^2), and Port Harcourt (437.5 W/m^2), which are all in the south. Incidentally, these locations with lowest daily DLR are coastal cities and have the lowest latitudes. The range of the daily maximum DLR is approximately 42 W/m^2. In contrast, the highest minimum value was approximately 339 W/m^2 for Port Harcourt in the south, and the smallest was approximately 272 W/m^2 for Kano in the north. Between the south and the north, the range of the minimum values was 67 W/m^2, as against the maximum range of 42 W/m^2 and the mean values range of 36 W/m^2.

As the latitude increases, the daily mean radiation decreases, as shown in Fig. 4.2.1. Without the use of any specific systematic segmentation according to latitude, but an interval of approximately 11 W/m^2, it was found that from a latitude of 4.75°N (Port Harcourt) to

7.77°N (Osogbo), the means were approximately between 399 and 411 W/m^2; from 8.48°N (Lafia) to 10.28°N (Gombe), the means were from 387 to 398 (W/m^2); and from 10.32°N (Bauchi) to 13.07°N (Sokoto), the means were from 375 to 386 (W/m^2).

However, this inverse proportionality between latitude and DLR does not completely explain the differences, because the elevation also has an influence. Like in the case of latitude variability with daily mean DLR, also the daily mean DLR is inversely proportional to elevation (Fig 4.2.2). It is found that there are instances whereby the difference in daily mean DLR between two locations is rather determined by difference in elevations instead of difference in latitudes. Specifically where a location A is at slightly lower latitude to another location B and the daily mean DLR should be higher at A due to the influence of latitude, rather if the elevation at A is higher than B, then the daily mean DLR at A is lower than B. Precisely, this occurrence was found within the last division of latitudinal coordinates from 10.32°N to 13.07°N, whereby the locations at lower latitudes have their elevations lower than 500 m and the locations at higher latitudes are at altitudes greater than 500 m above sea level.

Generally, regarding the height distributions of locations across the country, latitudes lower than 8.00°N have small elevations approximately between 70 and 250 m above sea level, whereas latitudes above 8.00°N to 13.07°N have altitudes ranging from 270 to 580 m. Thus, the northern elevations are more than twice the southern elevations and as such the daily mean DLR decreases moving from the south to the north.

Consider Yenagoa and Calabar, which have a latitude of 4.95°N but longitudes of 6.26°E and 8.32°E, respectively. When comparing these locations, the mean and maximum for Yenagoa are larger than for Calabar (Table 4.3.0), but not the minimum. However, Calabar is 163 m higher than Yenagoa. Therefore, if consider the influence of the altitude on the DLR, one

Table 4.3.0: The geographical coordinates of the 37 locations and the states found. The arrangement is in order of increasing latitude (Chineke *et al.*, 2011), and the basic statistics are for the daily DLR for approximately 8036 days starting from July 1983 to June 2005

Location	State	Latitude (^oN)	Longitude (^oE)	Elevation (m)	Mean (W/m^2)	Max (W/m^2)	Min (W/m^2)	SD(Standard Deviation)
Port Harcourt	Rivers	4.75	7.00	117	410.8	437.5	338.8	11.203
Yenagoa	Bayelsa	4.95	6.26	83	411.1	436.3	331.3	11.553
Calabar	Cross River	4.95	8.32	246	407.1	432.9	335.8	10.846
Uyo [S1]	Akwa Ibom	5.05	7.93	176	400.6	438.3	300.0	22.042
Owerri [S1]	Imo	5.48	7.02	176	400.6	438.3	300.0	22.042
Umuahia [S1]	Abia	5.53	7.48	176	400.6	438.3	300.0	22.042
Awka[S2]	Anambra	6.20	7.73	183	404.4	440.4	306.7	21.095
Benin	Edo	6.32	5.60	135	405.6	438.8	310.8	18.051
Abakaliki	Ebonyi	6.33	8.10	227	399.7	442.5	302.9	22.273
Enugu[S2]	Enugu	6.50	7.50	183	404.4	440.4	306.7	21.095
Ikeja	Lagos	6.58	3.33	73	408.0	440.4	326.7	15.119
Asaba	Delta	6.75	6.18	159	405.0	453.3	308.8	19.506
Abeokuta[S3]	Ogun	7.15	3.33	183	403.0	450.4	308.3	19.939
Akure [S4]	Ondo	7.25	5.20	233	400.5	438.3	300.5	22.042
Ibadan [S3]	Oyo	7.38	3.90	183	403.0	450.4	308.3	19.939
Ado Ekiti [S4]	Ekiti	7.62	5.22	233	400.5	438.3	300.5	22.042
Makurdi	Benue	7.73	8.53	249	397.3	456.2	300.4	26.278
Lokoja	Kogi	7.75	6.82	216	400.8	460.4	300.8	23.297
Osogbo	Osun	7.77	4.57	223	401.1	452.9	307.1	21.004
Lafia	Nasarawa	8.48	8.52	374	389.4	449.6	300.8	29.490
Ilorin	Kwara	8.50	4.55	274	396.4	462.9	296.7	24.965
Jalingo	Taraba	8.90	11.37	476	384.7	448.8	280.0	32.170
Abuja	Abuja	9.00	10.00	421	383.9	447.1	283.3	33.011
Minna	Niger	9.62	6.55	319	390.7	448.3	293.3	30.678
Yola	Adamawa	9.91	11.93	406	384.9	450.8	283.6	33.280
Jos	Plateau	9.92	8.90	587	377.6	443.3	277.1	34.355
Gombe	Gombe	10.28	11.17	416	382.5	465.4	279.6	37.239
Bauchi	Bauchi	10.32	9.83	559	374.8	445.4	274.6	37.773
Kaduna	Kaduna	10.52	7.43	575	375.2	440.0	277.5	35.944
Kano	Kano	11.50	8.50	545	374.7	449.6	271.7	39.841
Dutse	Jigawa	11.73	9.28	480	378.6	463.3	272.5	40.639
Damaturu	Yobe	11.73	11.95	397	380.8	470.4	273.8	41.348
Maiduguri	Bornu	11.83	13.15	377	381.1	465.8	276.3	41.473
Gusau	Zamfara	12.17	6.67	415	378.1	464.6	274.6	41.277
Birnin Kebbi	Kebbi	12.45	4.20	271	386.4	471.7	282.5	41.050
Katsina	Katsina	12.98	7.60	492	375.6	458.3	268.8	41.997
Sokoto	Sokoto	13.07	5.23	331	381.4	475.0	272.9	43.638

[S1, S2, S3 S4]; Regions with the same grid and same values of meteorological parameters

cannot conclude any relationship between DLR and longitude using Calabar and Yenagoa. Table 4.3.0 shows that Dutse and Damaturu have the same latitude of 11.73°N and Dutse is only 3 m higher. Dutse is at 9.28°E and Damaturu is at 11.95°E, and all the daily mean, min, and max DLR values at Damaturu are higher than those of Dutse. This suggests that an increase in longitude corresponds to an increase in radiation.

Incidentally, the two cases examined based on longitudinal variation with daily mean DLR gave conflicting results. In the first case, eastward analysis from 6.26°E to 8.32°E produced reduction in the daily mean radiation whereas moving from 9.28°E to 11.92°E in the second case produced increase in the same radiation. Therefore, the investigation is further extended by using data around the Gulf of Guinea. The longitude is increased by 1 degree and the latitude kept constant. The daily mean values in Table 4.3.1 show that an increase in the longitude corresponds to an increase in the radiation. Moving from a longitude of 4.00°E to 5.00°E (with zero elevation), there is slight increase in radiation, which can be attributed to the increasing longitude. However, importantly, when the longitude increases from 5.00°E to 8.00°E it is accompanied by an increase in elevation from 0 to 34 m, and the moment the land appears maximum radiation decreases. With regards to longitudinal impact, similar to the maximums, the minimums in Table 4.3.1 show no systematic pattern, and it is believed that the uncharacteristic trends are most likely a result of many factors that influence the radiation. Initial the increasing longitudes produced corresponding effect on the minimums; however as the altitude increased from 2 to 4 and to 34 m, the minimums DLR are seen to consistently regress irrespective of the continuous increase in longitude.

Based on the confirmation from Table 4.3.1 that DLR increases with eastward increase in longitude except when influenced by other factors like elevation, the decrease found in the case between Yenagoa and Calabar is most probably due to the large difference in elevation between both locations. Hence the factors that affect DLR show interlinking relationship and

at some instances one singular factor could have an overwhelming grip on the totality of the radiation.

Areas of high daily mean radiation are consistently relatively stable, because they do not experience large variations, unlike areas of lower mean radiation. Coincidentally, the locations with high mean DLR are in the south of the country and close to the Atlantic Ocean.

Fig. 4.2.3 shows that locations with high elevations experience wide ranges of DLR. Consequently as the latitude increases the DLR range becomes wider, because for the locations in this study latitude is directly proportional to elevation (Fig. 4.2.4). Reconsider two locations namely Calabar and Yenagoa that were earlier examined on increasing longitudinal basis; these locations are on the same latitude, but Calabar has a latitude of 246 m and Yenagoa has a latitude of 83 m. Because elevation is directly proportional to the size of the DLR range, one can expect that Calabar has a wider DLR range than Yenagoa. Nonetheless, the reverse is true, as shown in Fig. 4.2.5. The DLR range at Yenagoa is significantly wider than at Calabar. Fig.3.1.1 shows that Calabar is closer to the Atlantic Ocean than Yenagoa. This suggests that, for two locations at the same latitude, the climate is more stable closer to a water body even though the height difference should make it otherwise.

To further establish the enormous effect of a water body on DLR , locations at relatively similar latitudes are examined. Another example of this phenomenon can be seen at Ikeja, which is a costal location and has the narrowest range for locations lying between 6.20°N to 7.77°N (see Fig. 4.2.6).

Because H_2O is a major gas contributor to DLR, its abundance at any region ensures that DLR values do not get low. To further establish the influence of water bodies on DLR, we considered the DLR ranges for locations between the latitude of 9°N to 11.89°N. Minna has

the lowest range (as shown in Fig 4.2.7), and is close to a water body. The contributory source rivers from the south of the country to the Atlantic Ocean comprise many creeks and deltas (this region is known as the Niger delta). The confluence is at Lokoja, where the river divides into two, the major Niger River and minor Benue River (Ojoina, 2014). The Niger River is mostly in Niger state (with capital Minna), and the Benue River is in Benue state (with capital Makurdi). Minna most likely falls into the same grid as most of the electricity generation damns. There are three hydroelectricity dams in Niger state, Kanji, Jebba, and Shiroro (Olukanni and Salami, 2012; Aliyu *et al.,* 2013). Fig 4.2.7 shows that the location with the next smallest range is Kaduna. Interestingly, Kaduna is also a well know river area in the northern part of Nigeria, and Kaduna River is one of the Niger River's tributaries (Laë *et al.,* 2003; Ezeabasili *et al.,* 2014).

Although very low DLR ranges are associated with water bodies, locations with water bodies do not always have very narrow ranges. For example, Lokoja and Makurdi are close to the Niger and Benue Rivers (Fig. 3.1.1), and do not have very narrow ranges within the latitudinal division in Fig 4.2.6. This could be because of grid related issues, i.e., their coordinates could be in a grid that does not contain the water source.

Table 4.3.1: Descriptive statistics to investigate the longitudinal trend of DLR around the Gulf of Guinea for 8036 days starting from July 1983 to June 2005.

Latitude (^{o}N)	Longitude (^{o}E)	Elevation (m)	Mean (W/m^2)	Max (W/m^2)	Min (W/m^2)	SD
1.00	4.00	0	417.28	443.33	350.00	11.160
1.00	5.00	0	417.62	447.08	357.08	10.807
1.00	6.00	2	417.98	444.58	364.17	10.369
1.00	7.00	4	418.14	444.48	363.33	9.700
1.00	8.00	34	418.15	441.25	357.50	9.320

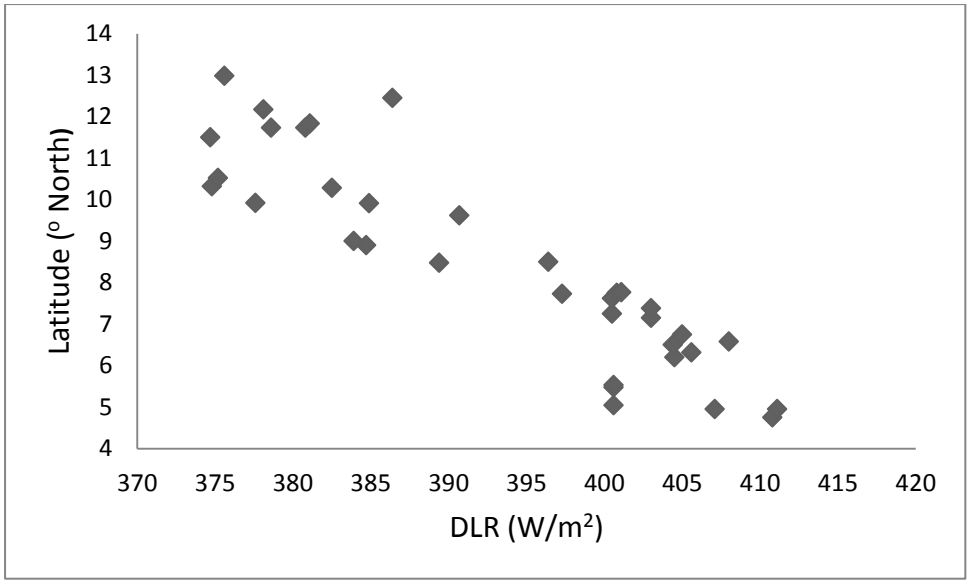

Figure 4.2.1: Scatter plot of latitude versus daily mean DLR, which shows that an increase in latitude is inversely proportional to the daily mean DLR.

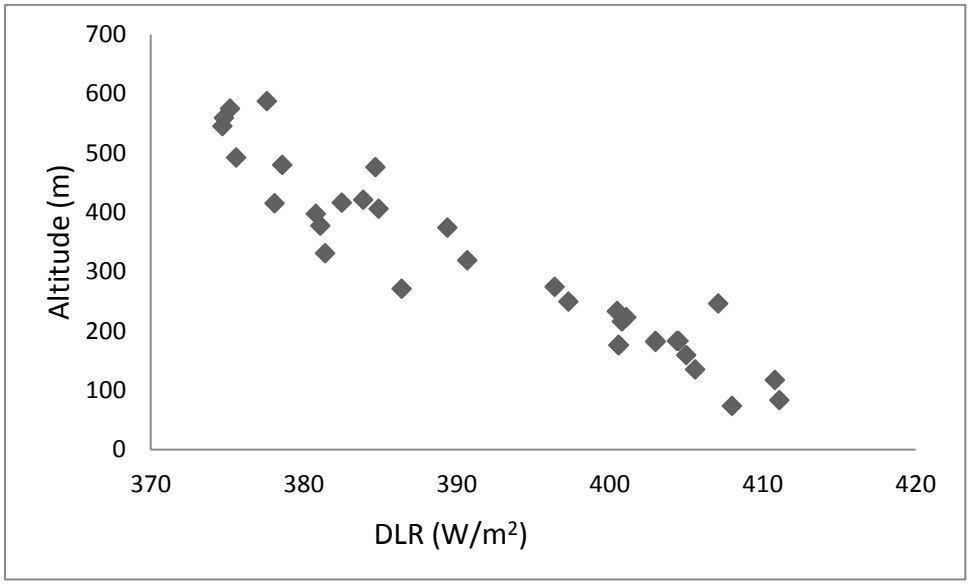

Fig 4.2.2: Scatter plot of altitude versus daily mean DLR, which shows that an increase in elevation corresponds to a decrease in daily mean DLR.

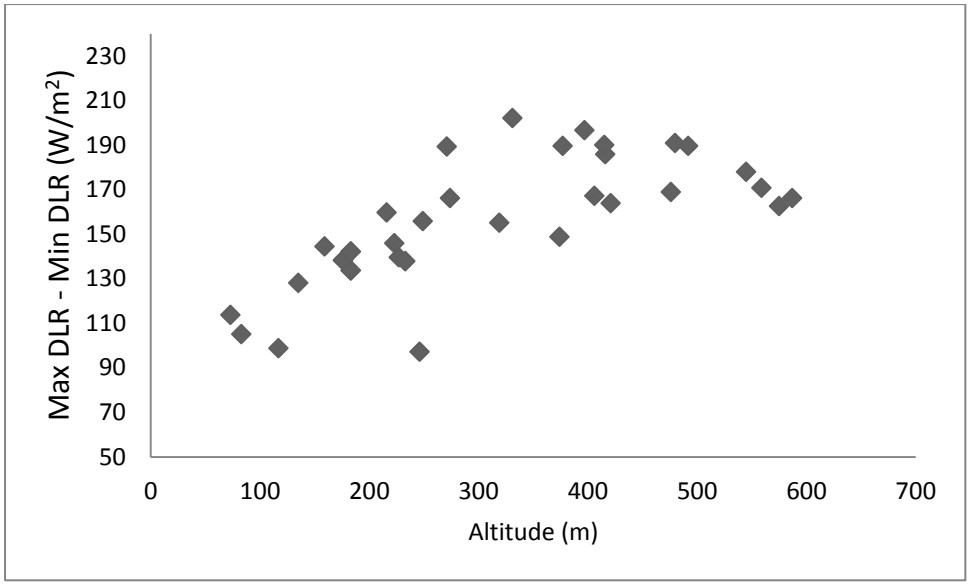

Fig 4.2.3: Scatter plot of DLR variability (max DLR–min DLR) versus altitude. The DLR range is directly proportional to the elevation.

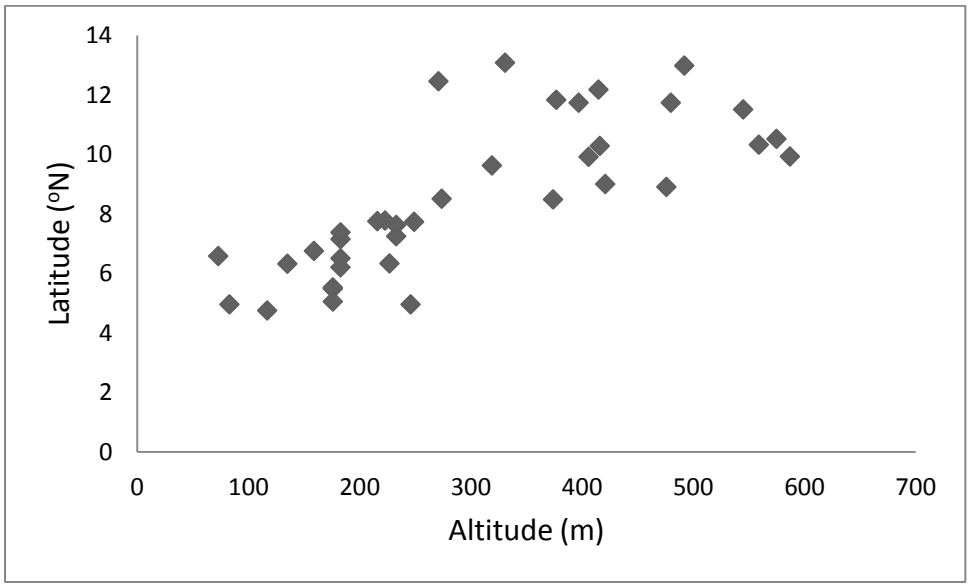

Fig 4.2.4: Scatter plot of latitude against altitude. The plot clearly indicates the direct proportionality between latitude and altitude over the whole study area.

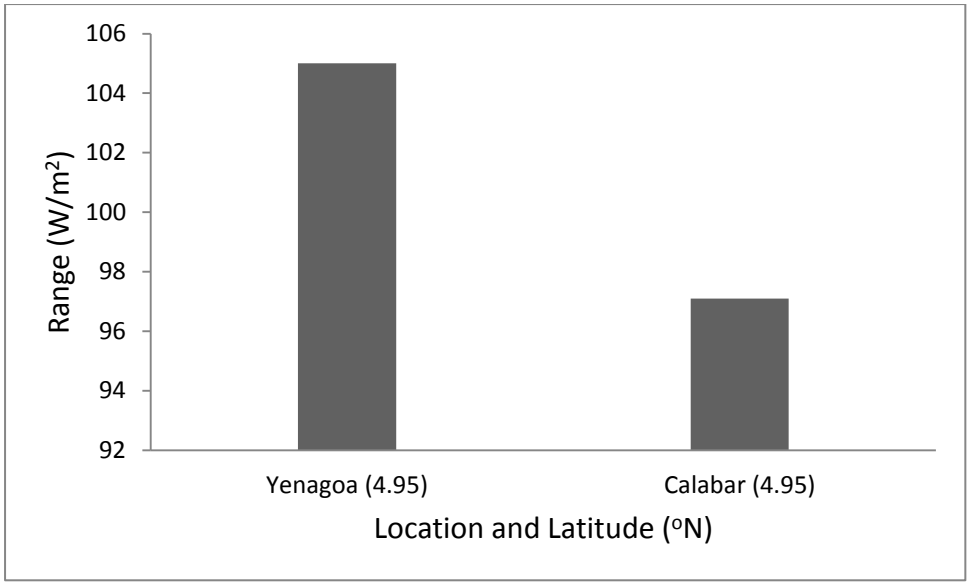

Fig 4.2.5 Histogram of DLR ranges for two locations on the same latitude. Calabar is closer to the Atlantic Ocean and has a narrower DLR range than Yenagoa.

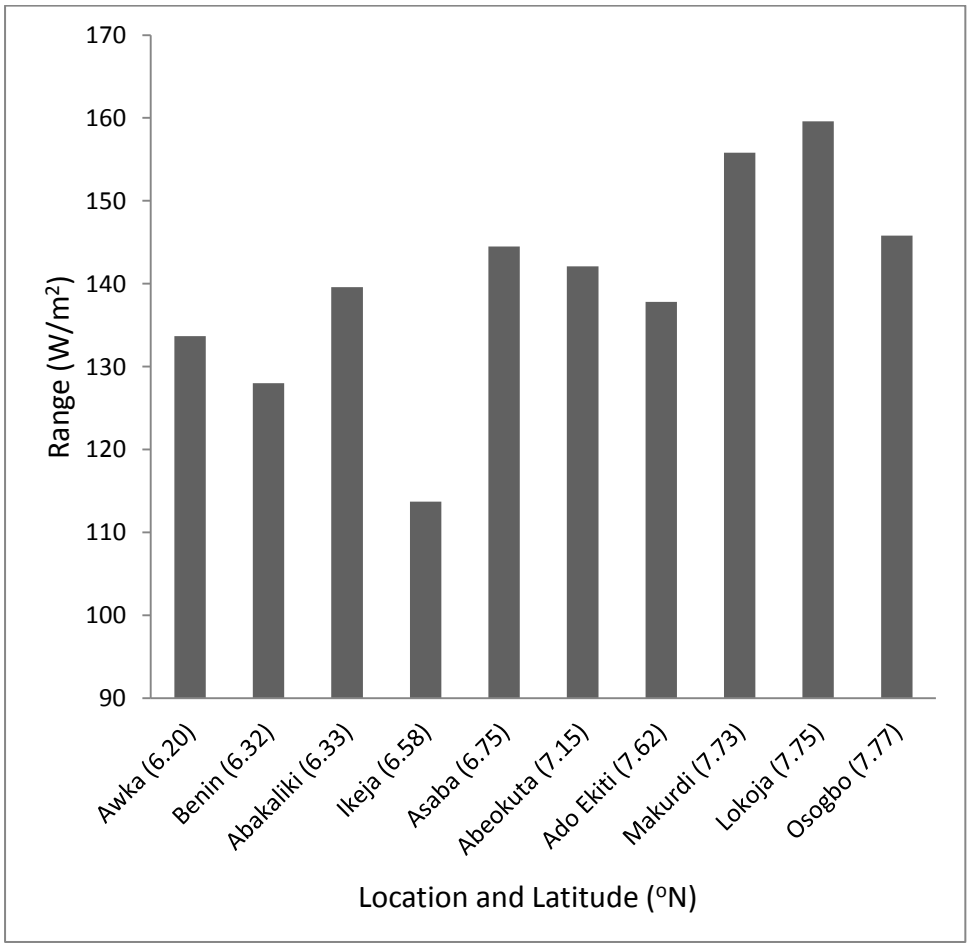

Fig 4.2.6: DLR ranges of ten locations between 6.20°N and 7.77°N. Twin cases such as Enugu and Ibadan (the same as Awka and Abeokuta) were not included.

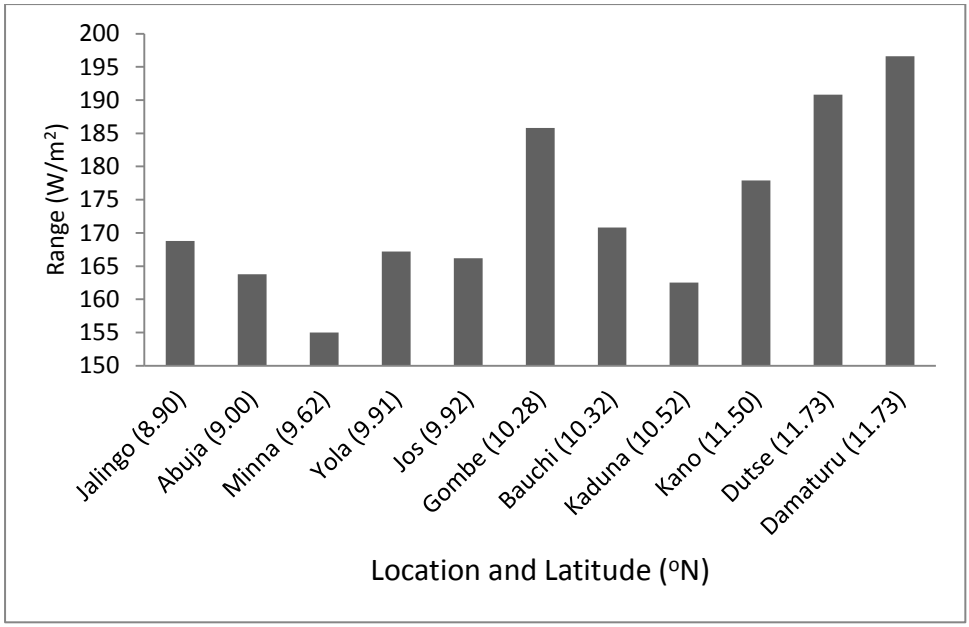

Fig 4.2.7: Histogram showing the DLR ranges of 11 locations between 8.90°N and 11.73°N. Narrow ranges are associated with water bodies.

4.2.3 Seasonal Trends of DLR

The seasonal pattern of the radiation is approximately the same from the south to the north, with some differences from one location to another; the results of the observed behavioural patterns are presented in Figs 4.3.1- 4.3.37. The common seasonal pattern shows the lowest radiation in January, and this value rises from February to its peak in either April or May. Afterwards, this high value is maintained with slight fluctuations until around September or October, before the value decreases throughout the rest of the year and then returns to the minimum in January. Based on increasing latitudes, the overall results within the seasonal evaluations show that the pattern of the monthly radiation can be used to segment the entire country into three characteristic types. The first group are those locations that have high values with little differences in DLR values between the months of the year, and such patterns are found for regions extremely close to the Atlantic Ocean, in the southern region of the country (Figs 4.3.1 - 4.3.3, 4.3.7 and 4.3.11). The third group is for locations that have

wide ranges but with small values of radiation and is typically for locations in the northern parts of the country (e.g. Figs 4.3.27 – 4.3.37), whereas the second group (for instance see Figs 4.3.12 - 4.3.19) is for locations exhibiting patterns that are between the first and the third groups and are regions at the middle section of the country. The second group has moderate amounts of DLR with corresponding moderate ranges, and the three seasonal trend groupings are latitude-dependent. Additionally, the quantities of rainfall from location to location are associated with the three established distinctive classes of radiation, which can be established by comparing Figs 4.3.1 – 4.3.37 with corresponding rainfall patterns where available in Figs 4.3.38a - 4.3.38v. Regions with heavy rainfall are associated with high radiation. In the south, the rainfall amount is largest, followed by the middle belt and, lastly by the north. It is noteworthy to state that the radiation is seasonally dependent; low during the dry season and high during the rainy season.

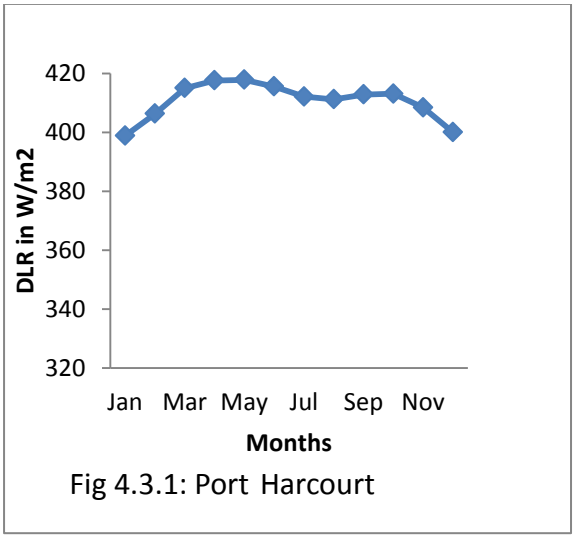

Fig 4.3.1: Port Harcourt

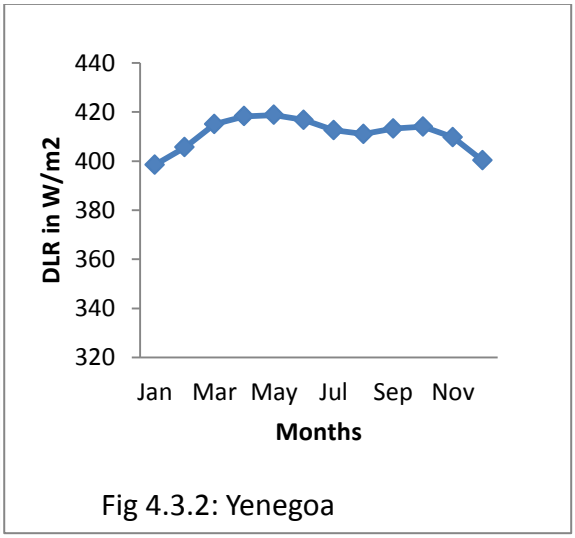

Fig 4.3.2: Yenegoa

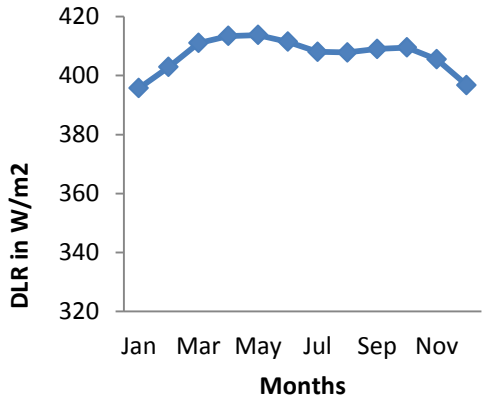

Fig 4.3.3: Calabar

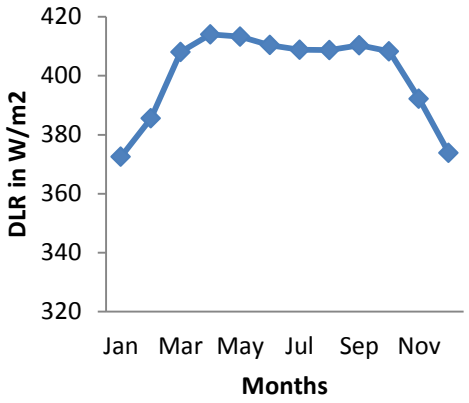

FIg 4.3.4: Uyo

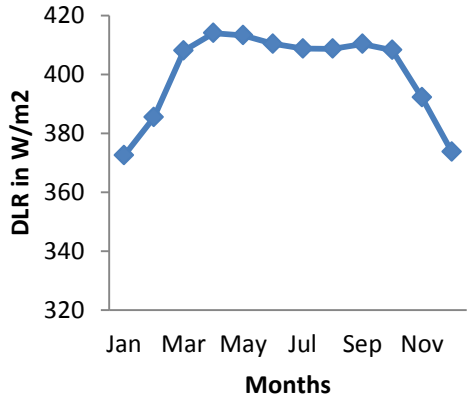

FIg 4.3.5: Owerri

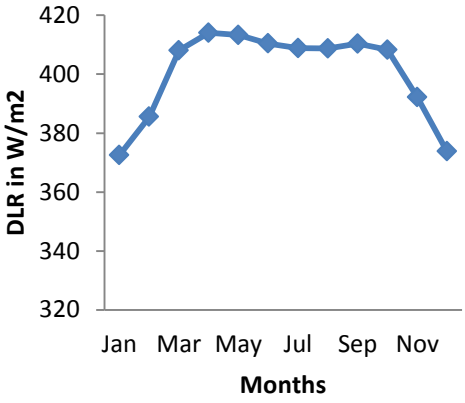

FIg 4.3.6: Umuahia

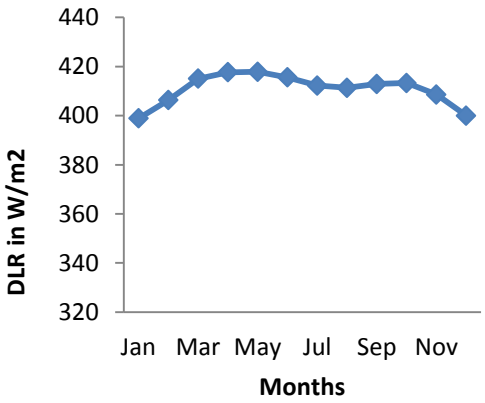

Fig 4.3.7: Awka

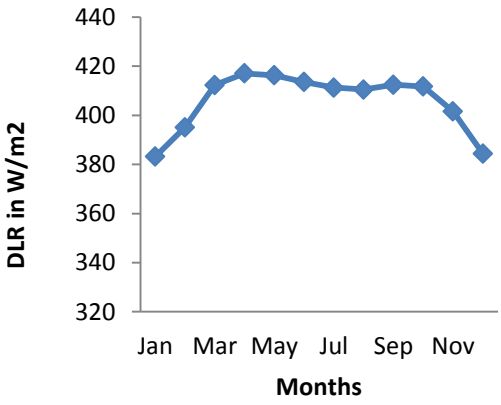

Fig 4.3.8: Benin

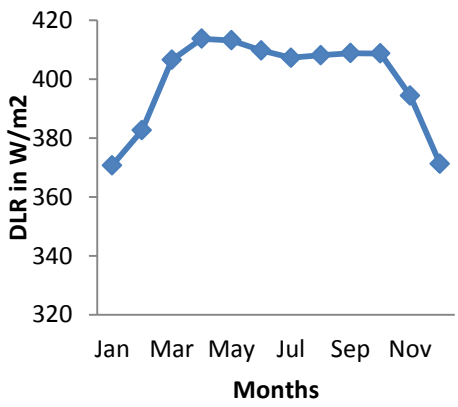

Fig 4.3.9: Abakaliki

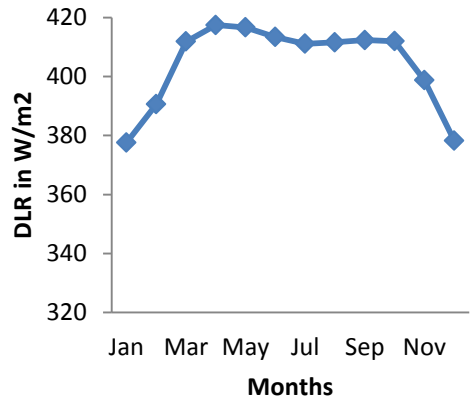

Fig 4.3.10: Enugu

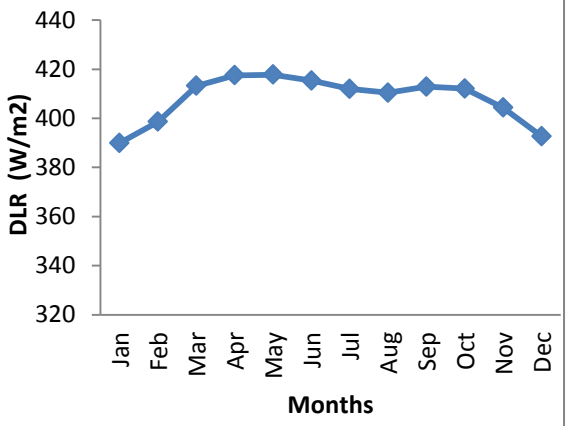

Fig 4.3.11: Ikeja

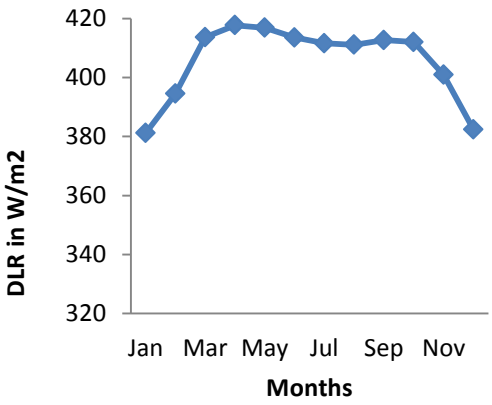

Fig 4.3.12: Asaba

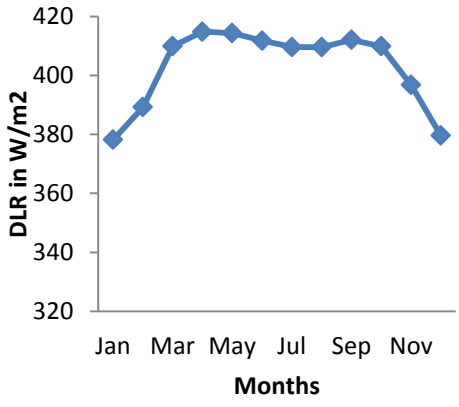

Fig 4.3.13: Abeokuta

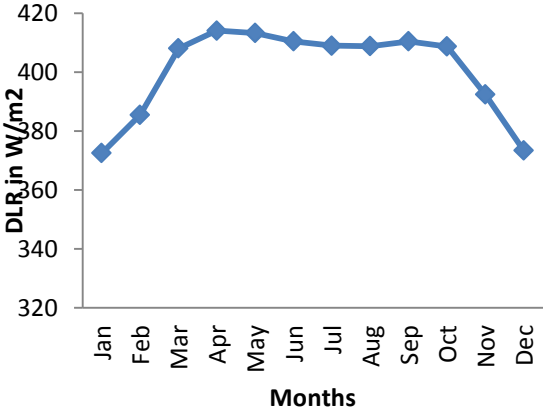

Fig 4.3.14: Akure

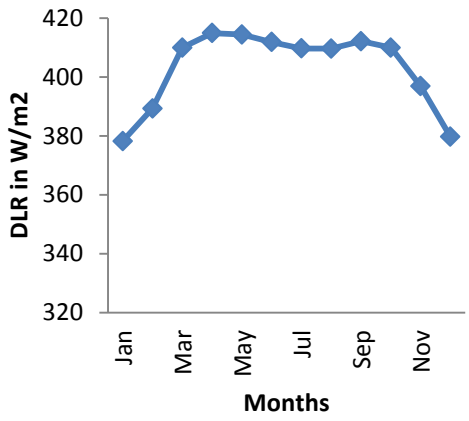

Fig 4.3.15: Ibadan

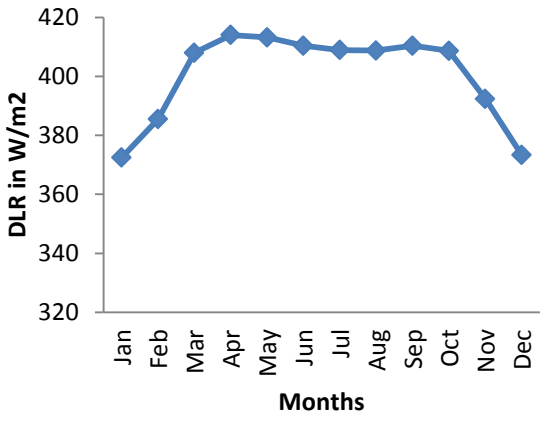

Fig 4.3.16: Ekiti

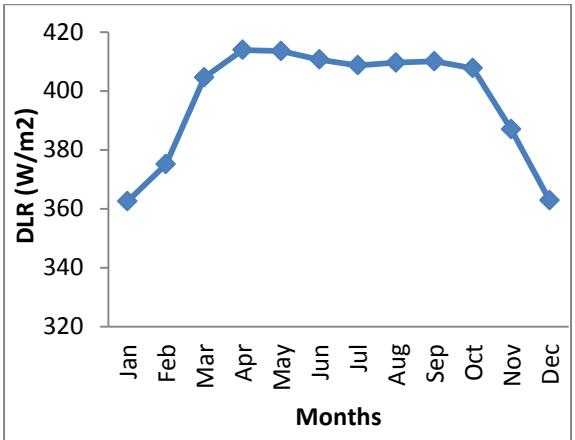

Fig 4.3.17: Makurdi

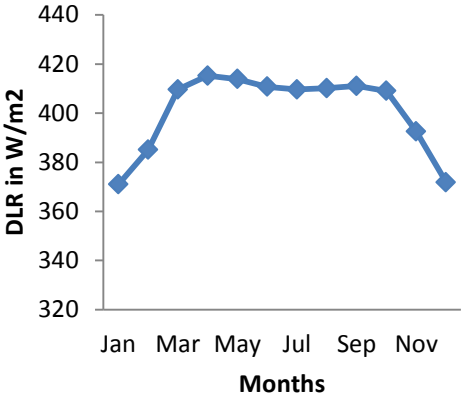

Fig 4.3.19: Lokoja

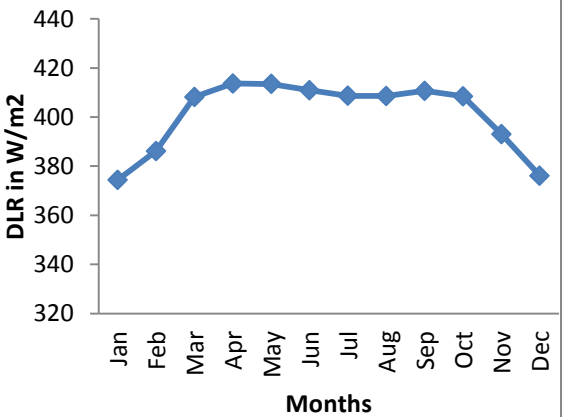

Fig 4.3.19: Osogbo

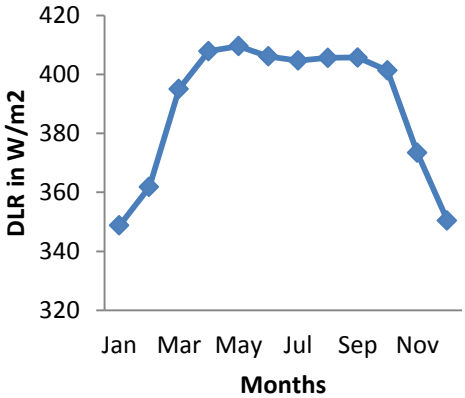

Fig 4.3.20: Lafia

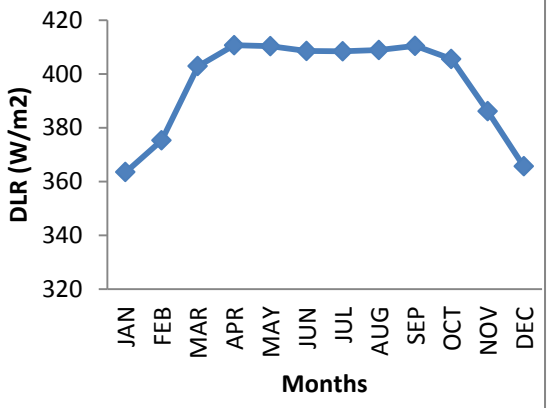

Fig 4.3.21: Ilorin

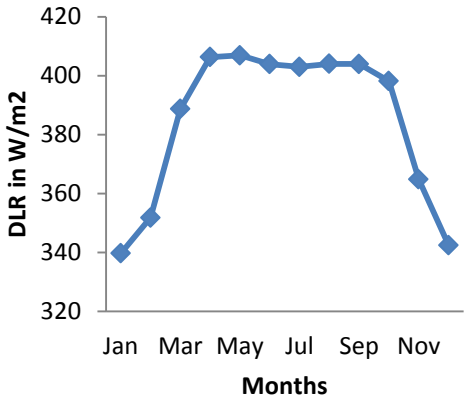

Fig 4.3.22: Jalingo

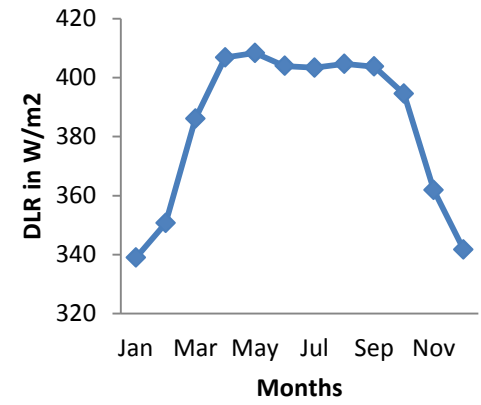

Fig 4.3.23: Abuja

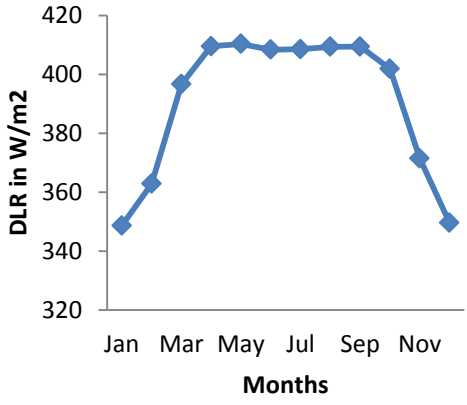

Fig 4.3.24: Minna

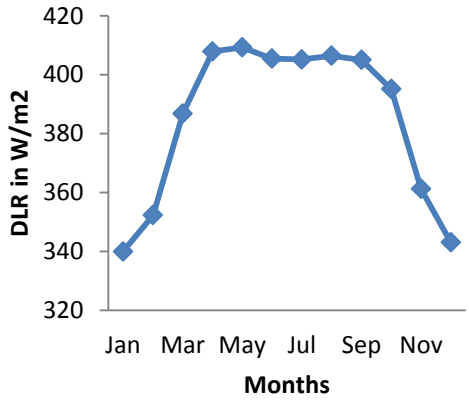

Fig 4.3.25: Yola

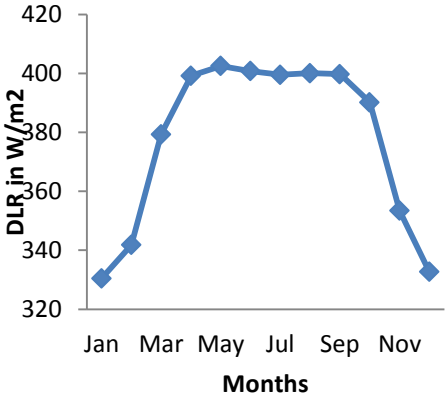

Fig 4.3.26: Jos

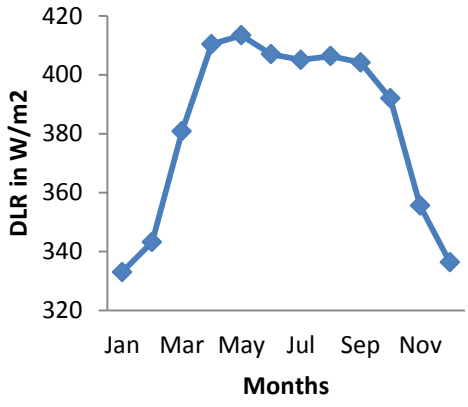

Fig 4.3.27: Gombe

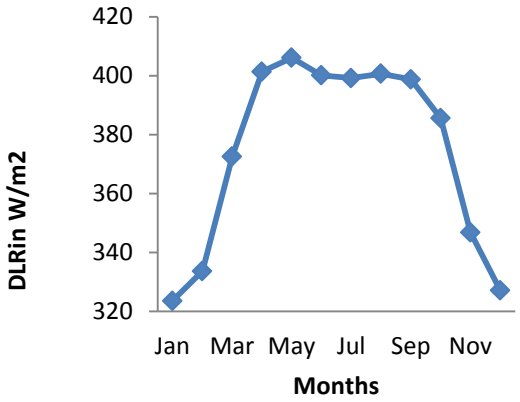

Fig 4.3.28: Bauchi

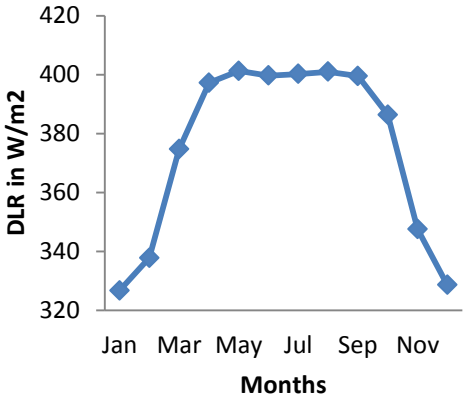

Fig 4.3.29: Kaduna

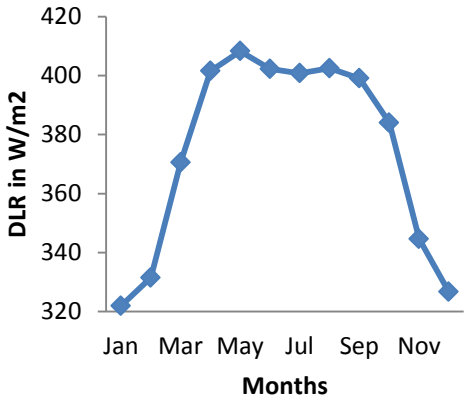

Fig 4.3.30: Kano

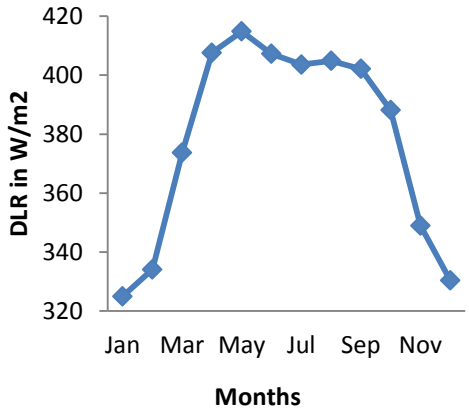

Fig 4.3.31: Dutse

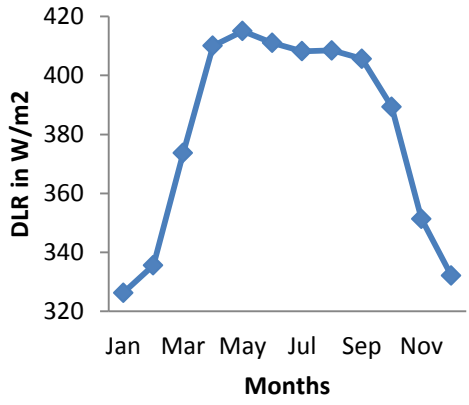

Fig 4.3.32: Damaturu

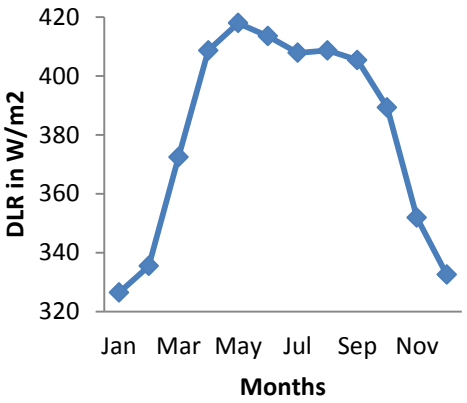

Fig 4.3.33: Maiduguri

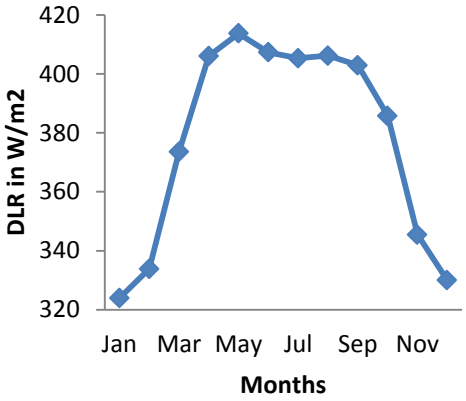

Fig 4.3.34: Gusau

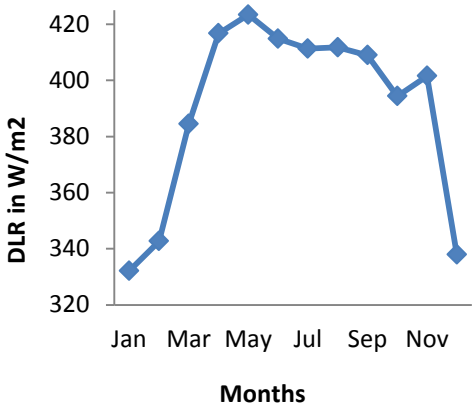

Fig 4.3.35: Birnin Kebbi

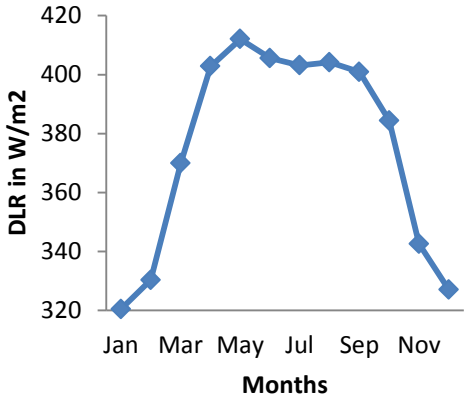

Fig 4.3.36: Katsina

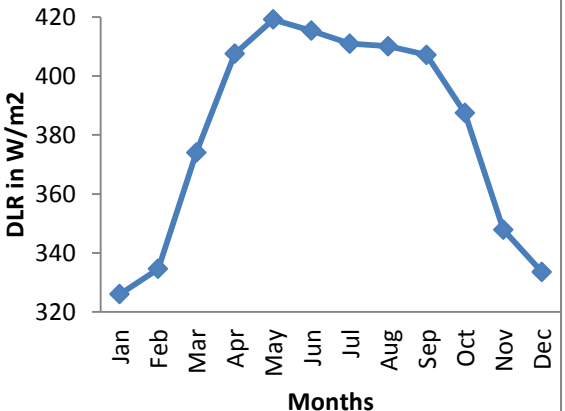

Fig 4.3.37: Sokoto

Fig 4.3.1 – 4.3.37: Seasonal patterns of DLR for all 37 locations which are the capital of the states and federal capital territory of Nigeria. The plots are monthly values of DLR from 1983 to 2005.

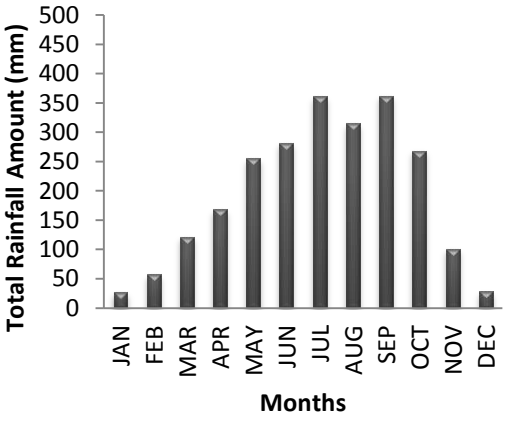

Fig 4.3.38a: Port Harcourt

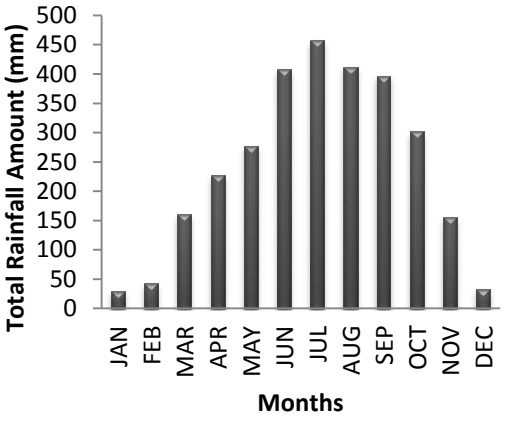

Fig 4.3.38b: Calabar

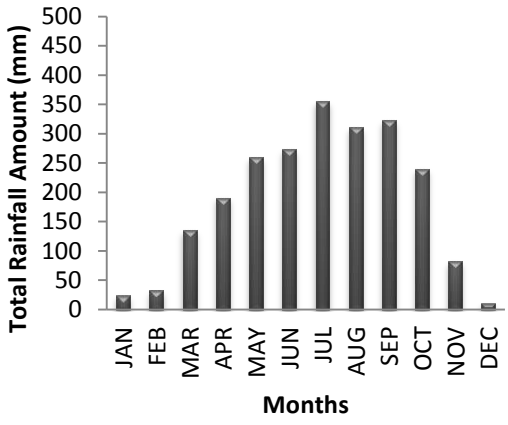

Fig 4.3.38c: Uyo

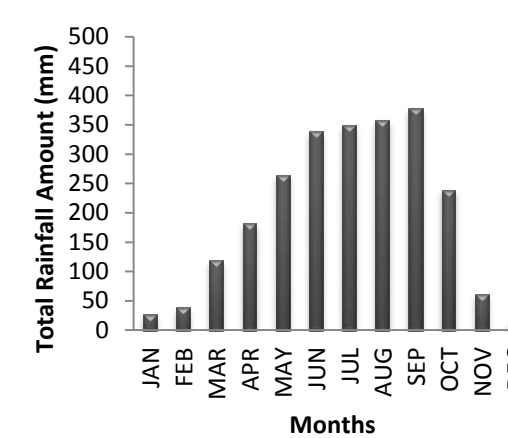

Fig 4.3.38d: Owerri

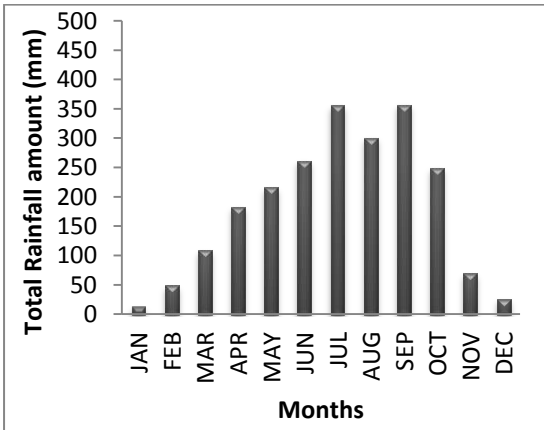

Fig 4.3.38e: Benin

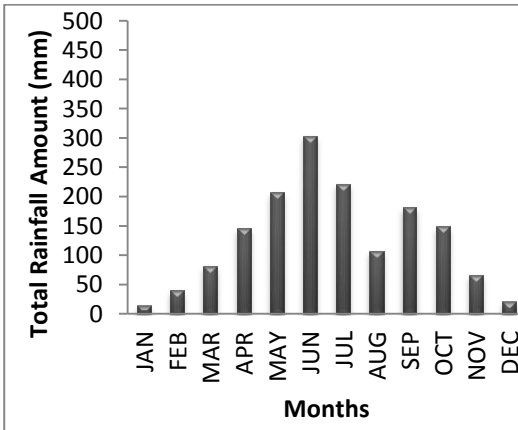

Fig 4.3.38f: Ikeja

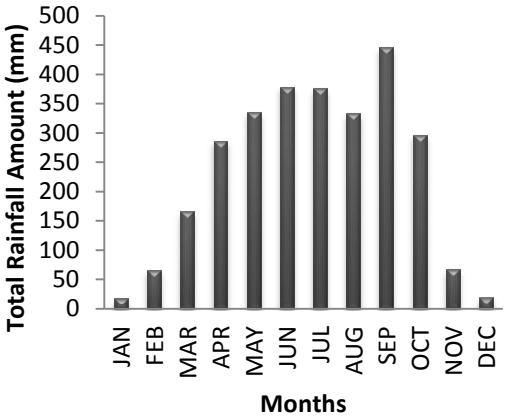

Fig 4.3.38g: Akure

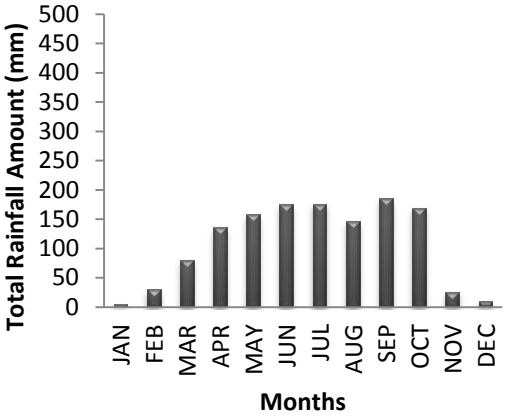

Fig 4.3.38h: Ibadan

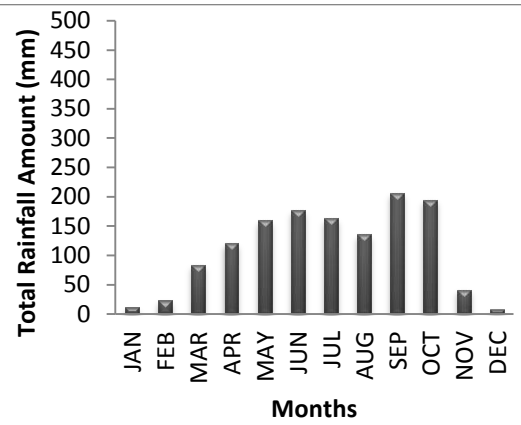

Fig 4.3.38i: Osogbo

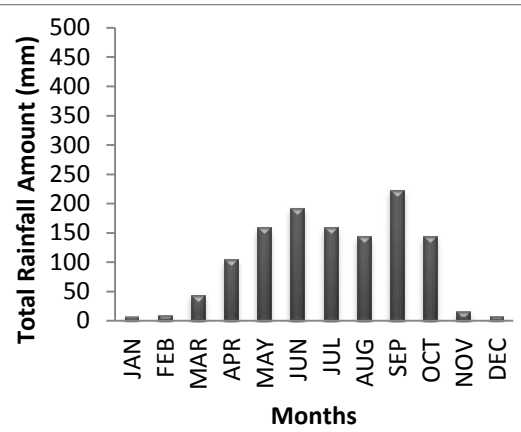

Fig 4.3.38j: Ilorin

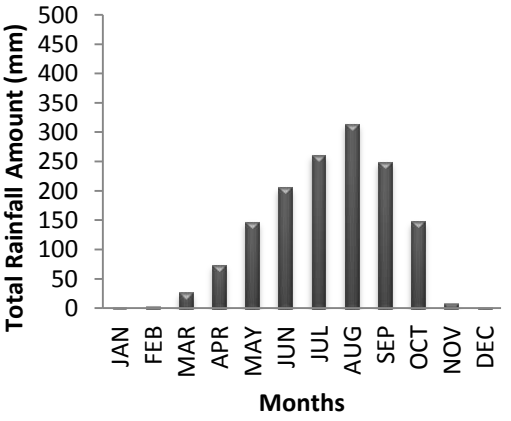

Fig 4.3.38k: Abuja

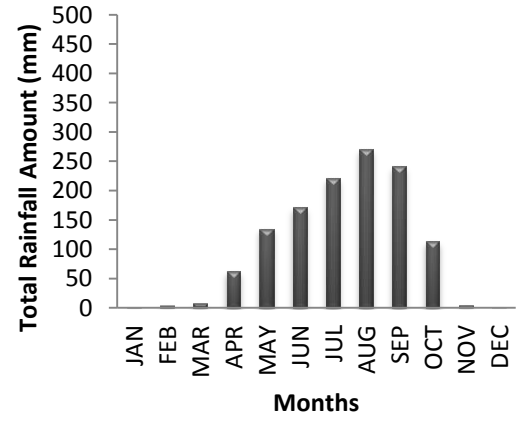

Fig 4.3.38l: Minna

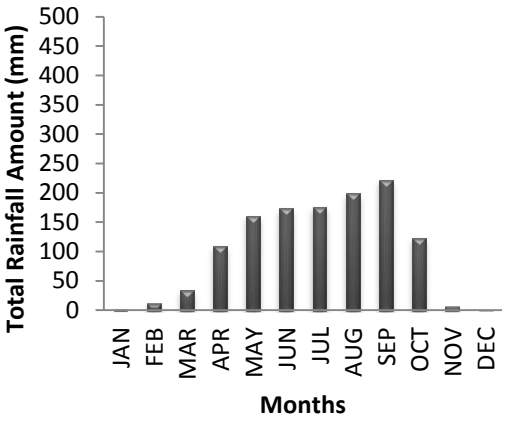

Fig 4.3.38m: Lokoja

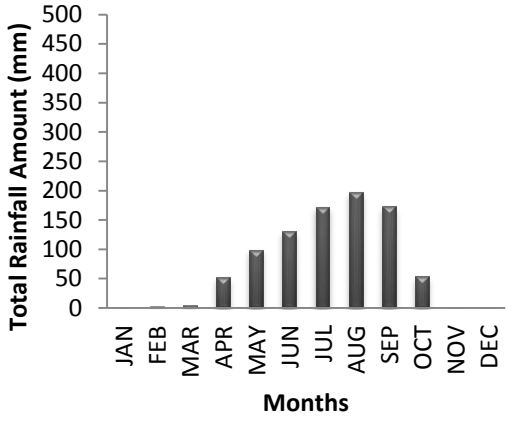

Fig 4.3.38n: Yola

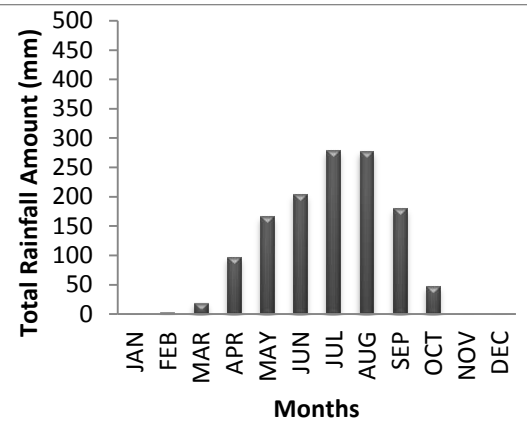

Fig 4.3.38o: Jos

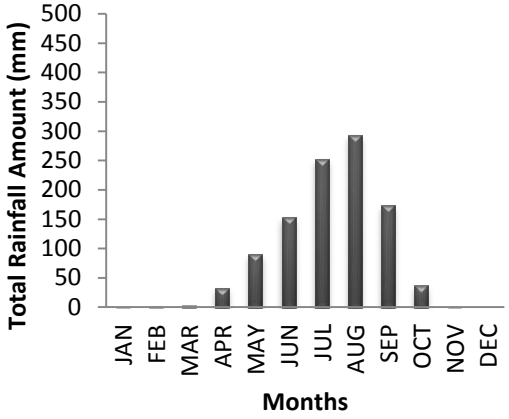

Fig 4.3.38p: Bauchi

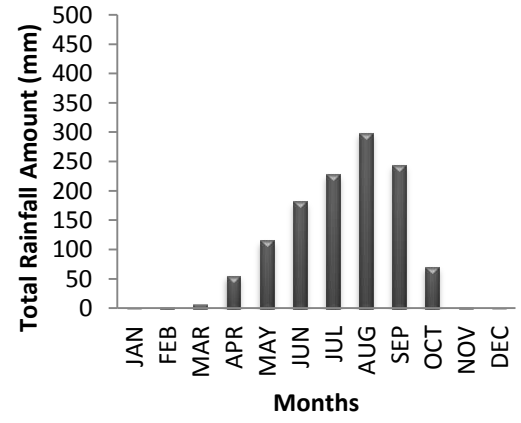

Fig 4.3.38q: Kaduna

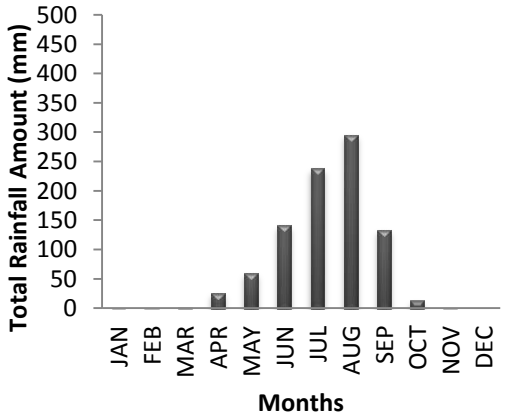

Fig 4.3.38r: Kano

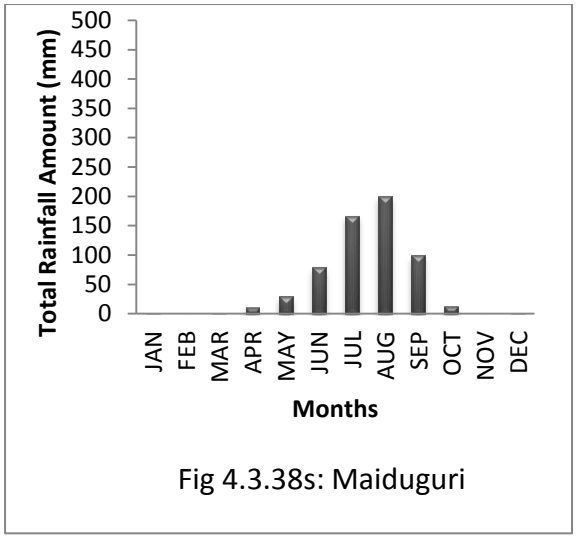

Fig 4.3.38s: Maiduguri

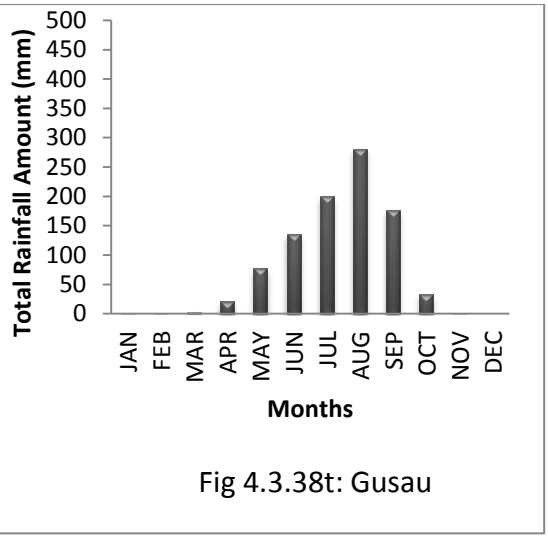

Fig 4.3.38t: Gusau

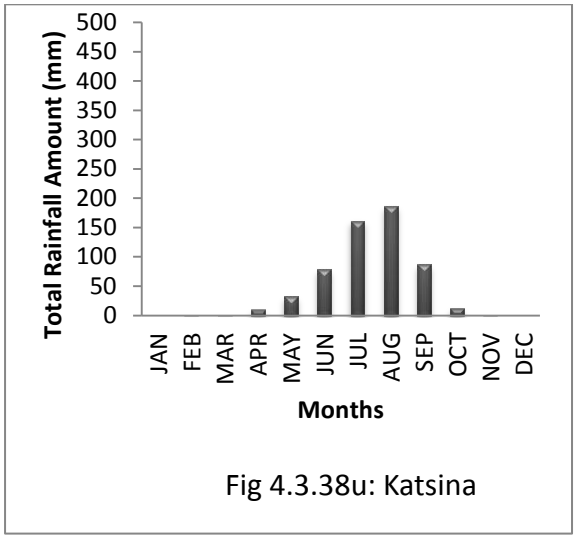

Fig 4.3.38u: Katsina

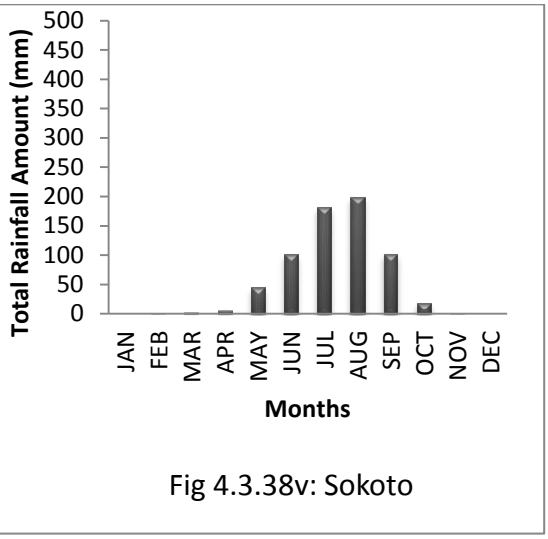

Fig 4.3.38v: Sokoto

Figs 4.3.38a- 4.3.38v: Rainfall patterns of some cities in Nigeria that their DLR have been studied. The period used to establish the rainfall patterns is from 1960 – 2010

4.2.4 Long Term Trends of DLR

The graphical outputs of the plots of DLR against the years of period from 1984 to 2005 (about two decades) for all 37 locations, all differ from each other (with the exception of the two twin cases). Throughout the graphs there are remarkable fluctuations (diming and brightening) for all the locations (Figs 4.4.1 – 4.4.37). Hence there is no remarkable influence

Table 4.4.1: Long term effects of DLR on the atmosphere

Location	Location	State	Latitude (^{o}N)	Longitude (^{o}E)	M	C	Mean	SD	Min	Max
Port Harcourt	Port Harcourt	Rivers	4.75	7.00	0.10	220.28	410.8	2.12	406.3	415.0
Yenagoa	Yenagoa	Bayelsa	4.95	6.26	0.10	211.35	411.3	2.28	406.3	415.8
Calabar	Calabar	Cross River	4.95	8.32	0.10	207.18	407.1	2.12	402.1	411.3
Uyo [S1]	Uyo	Akwa om	5.05	7.93	0.09	229.85	406.8	2.32	402.1	411.7
Owerri [S1]	Owerri	Imo	5.48	7.02	0.09	229.85	406.8	2.32	402.1	411.7
Umuahia [S1]	Umuahia	Abia	5.53	7.48	0.09	229.85	406.8	2.32	402.1	411.7
Awka [S2]	Awka2	Anambra	6.20	7.73	0.07	291.05	404.4	2.73	398.3	410.0
Benin	Benin	Edo	6.32	5.60	0.05	300.23	405.8	2.42	401.3	410.4
Abakaliki	Abakaliki	Ebonyi	6.33	8.10	0.07	255.58	399.6	2.82	393.3	406.3
Enugu [S2]	Enugu2	Enugu	6.50	7.50	0.06	291.05	404.4	2.73	398.3	410.0
Ikeja	Ikeja	Lagos	6.58	3.33	0.06	281.86	408.1	2.40	404.2	412.1
Asaba	Asaba	Delta	6.75	6.18	0.05	309.99	405.7	2.57	400.4	410.8
Abeokuta[S3]	Abeokuta3	Ogun	7.15	3.33	0.08	246.34	403.1	2.68	397.9	407.5
Akure[S4]	Akure	Ondo	7.25	5.20	0.03	346.62	400.6	2.81	394.6	405.8
Ibadan[S3]	Ibadan3	Oyo	7.38	3.90	0.08	246.34	403.1	2.68	397.9	407.5
Ado Ekiti[S4]	Ado Ekiti	Ekiti	7.62	5.22	0.03	346.62	400.6	2.81	394.6	405.8
Makurdi	Makurdi	Benue	7.73	8.53	0.05	288.86	397.3	2.93	390.8	404.2
Lokoja	Lokoja	Kogi	7.75	6.82	0.01	386.76	400.8	2.80	394.6	406.7
Osogbo	Osogbo	Osun	7.77	4.57	0.07	260.85	401.2	2.79	395.8	406.3
Lafia	Lafia	Nasarawa	8.48	8.52	-0.00	395.40	389.3	3.08	383.3	397.1
Ilorin	Ilorin	Kwara	8.50	4.55	0.06	279.13	396.4	3.00	390.4	402.1
Jalingo	Jalingo	Taraba	8.90	11.37	-0.12	625.29	384.6	3.21	377.1	390.8
Abuja	Abuja	Abuja	9.00	10.00	-0.18	744.25	383.9	3.55	376.7	391.7
Minna	Minna	Niger	9.62	6.55	-0.06	515.91	390.6	3.12	384.6	397.5
Yola	Yola	Adamawa	9.91	11.93	-0.16	704.43	384.9	3.26	377.1	390.8
Jos	Jos	Plateau	9.92	8.90	-0.04	455.00	377.6	3.32	371.7	384.6
Gombe	Gombe	Gombe	10.28	11.17	-0.16	692.17	382.5	3.50	374.6	388.8
Bauchi	Bauchi	Bauchi	10.32	9.83	-0.18	734.22	374.8	3.37	366.3	380.8
Kaduna	Kaduna	Kaduna	10.52	7.43	-0.11	591.04	375.2	3.27	367.5	380.8
Kano	Kano	Kano	11.50	8.50	-0.23	833.1	374.6	3.45	366.3	380.4
Dutse	Dutse	Jigawa	11.73	9.28	-0.27	913.92	378.5	3.57	370.0	385.0
Damaturu	Damaturu	Yobe	11.73	11.95	-0.26	890.78	380.7	3.83	373.3	388.3
Maiduguri	Maiduguri	Bornu	11.83	13.15	-0.33	1040.80	381.1	4.36	372.1	389.2
Gusau	Gusau	Zamfara	12.17	6.67	-0.27	912.45	378.0	3.54	369.2	383.8
Birnin Kebbi	Birnin Kebbi	Kebbi	12.45	4.20	-0.19	763.23	386.4	3.69	377.5	392.5
Katsina	Katsina	Katsina	12.98	7.60	-0.26	885.06	375.5	3.43	367.1	380.4
Sokoto	Sokoto	Sokoto	13.07	5.23	-0.21	792.39	381.3	3.58	372.5	385.8

[S1, S2, S3 S4]; Regions with the same grid and same values of meteorological parameters, where M is gradient and C is the intercept of the linearization of the DLR over the 22 years period

of the radiation over a long term period. If the period of five years is considered, probably a more remarkable increase or decrease in the radiation would be been noticed, however five years is hardly considered as long term. From Table 4.4.1, the rate of change of the radiation per year is from -0.25 to + 0.10. The change is mostly positive at the low end of the latitudes and negative at the high end of the latitudes and as the latitude increases the SD also increases.

As expected the same scenarios witnessed when the daily values were considered also manifested in the long term analysis. The yearly mean values of DLR of locations at low latitudes are higher than those of locations at higher latitudes. Also the range in yearly mean DLR increases as the latitude increases.

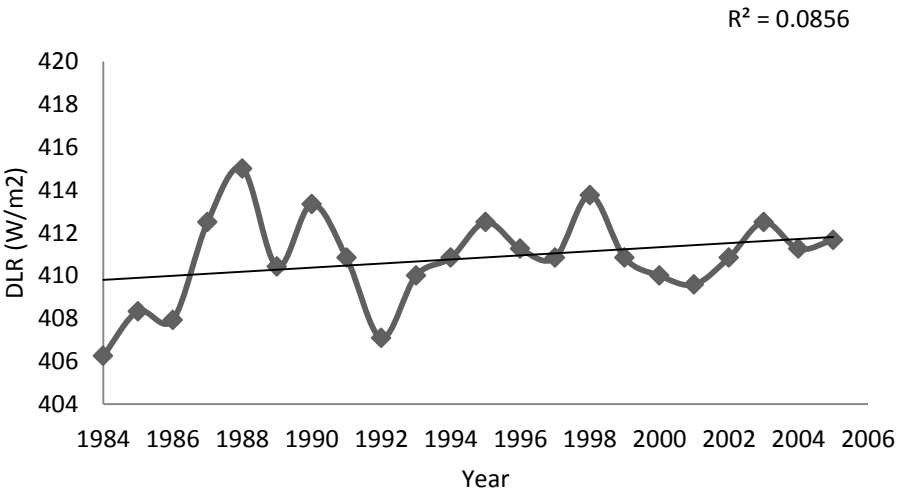

Fig 4.4.1: Port Harcourt

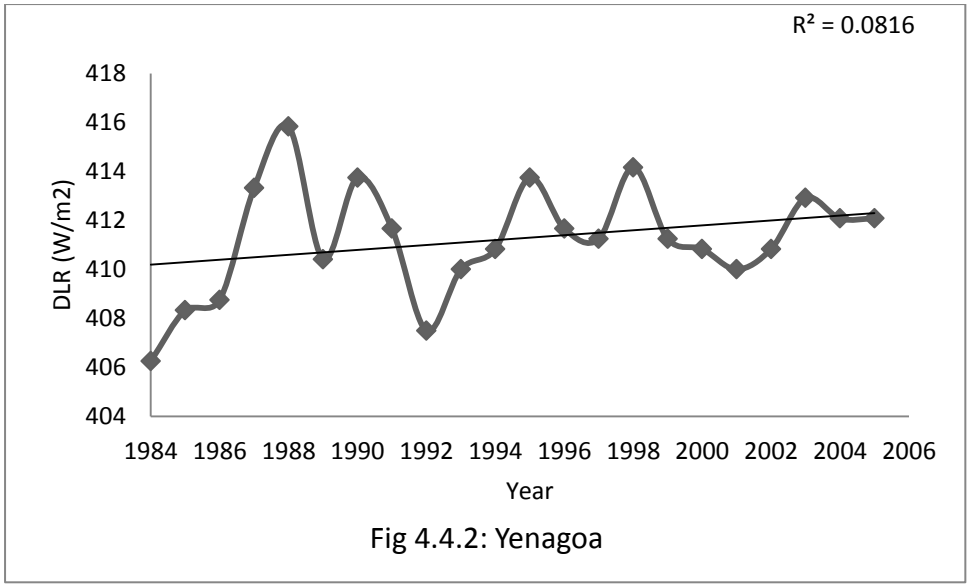

Fig 4.4.2: Yenagoa

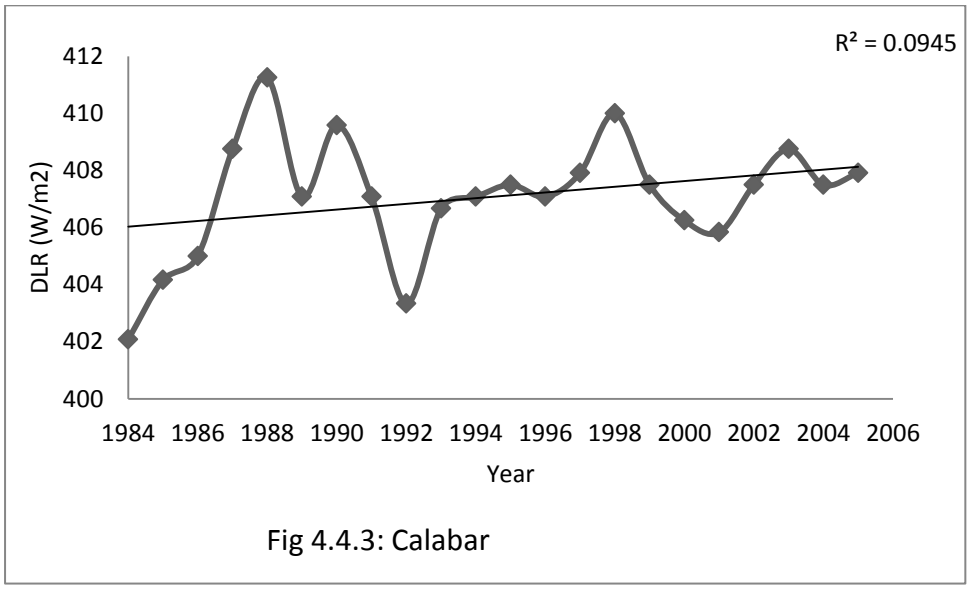

Fig 4.4.3: Calabar

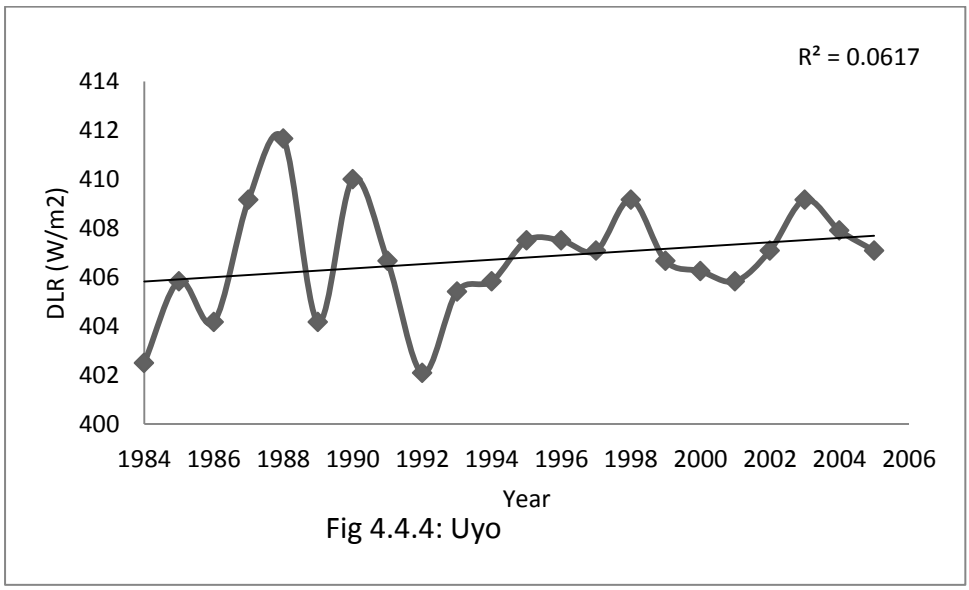

Fig 4.4.4: Uyo

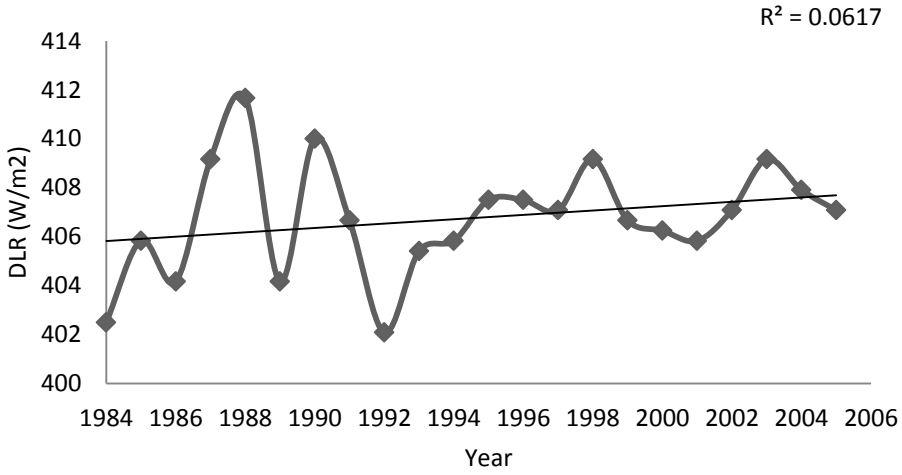

Fig 4.4.5: Owerri

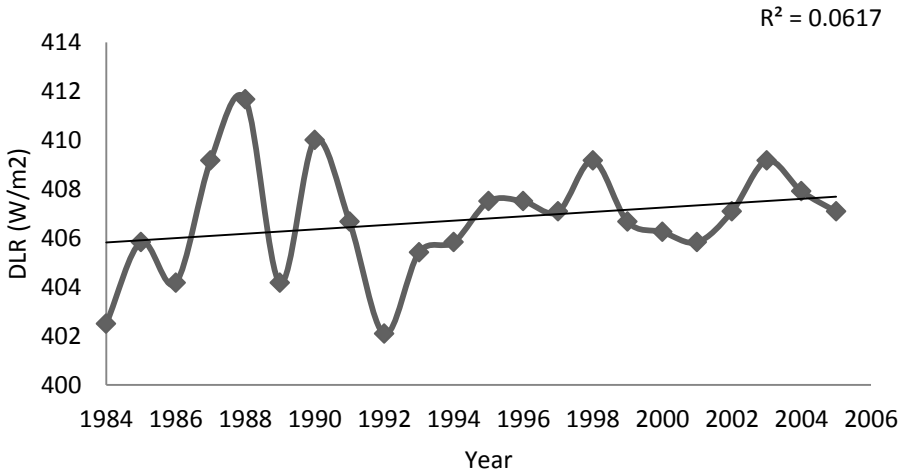

Fig 4.4.6: Umuahia

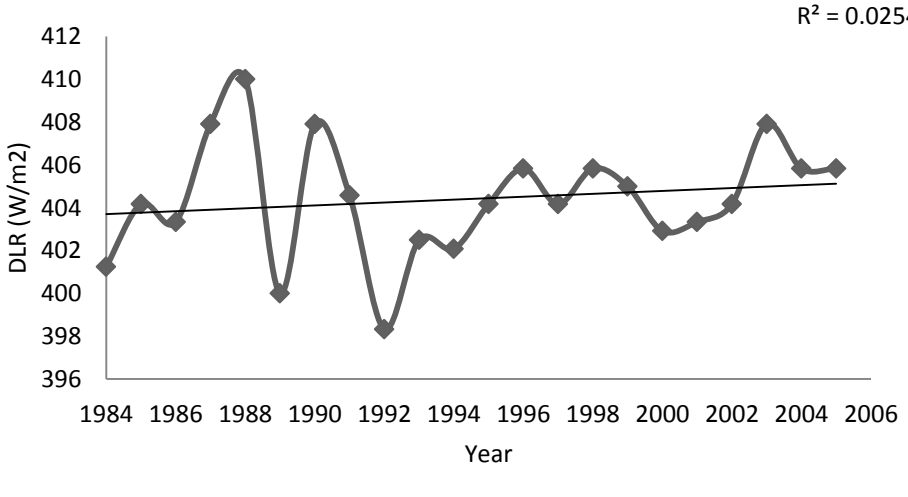

Fig 4.4.7: Awka

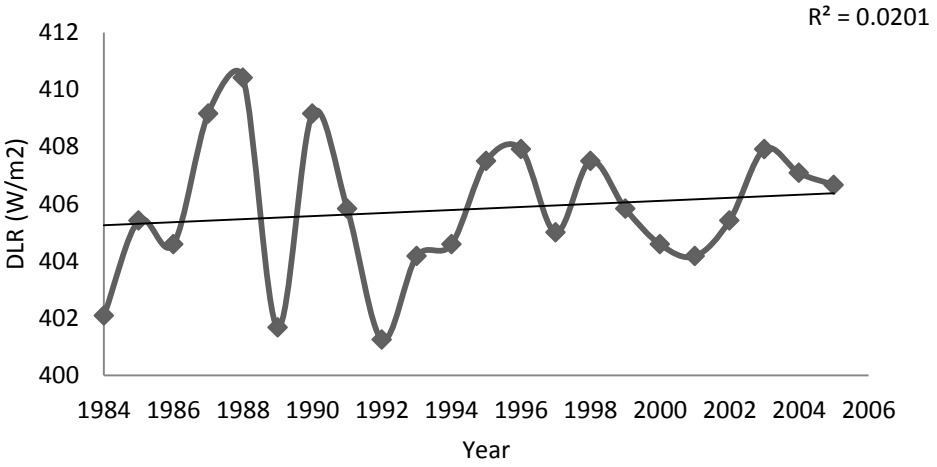

Fig 4.4.8: Benin

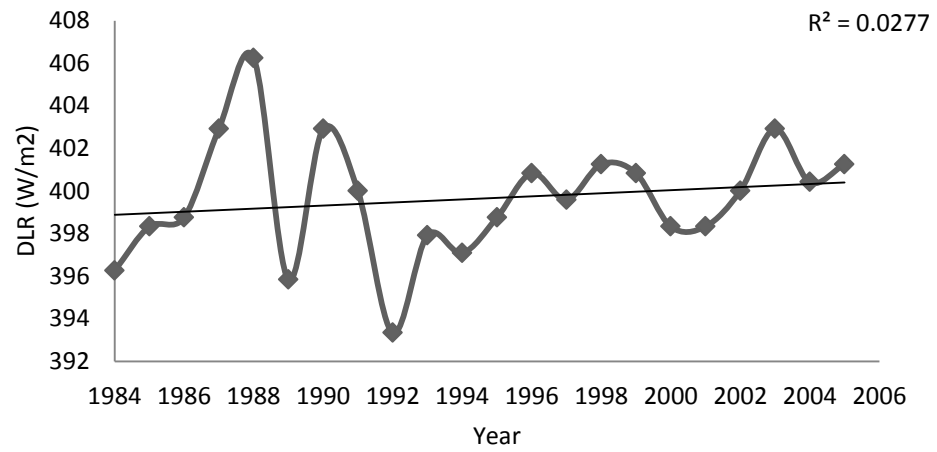

Fig 4.4.9: Abakaliki

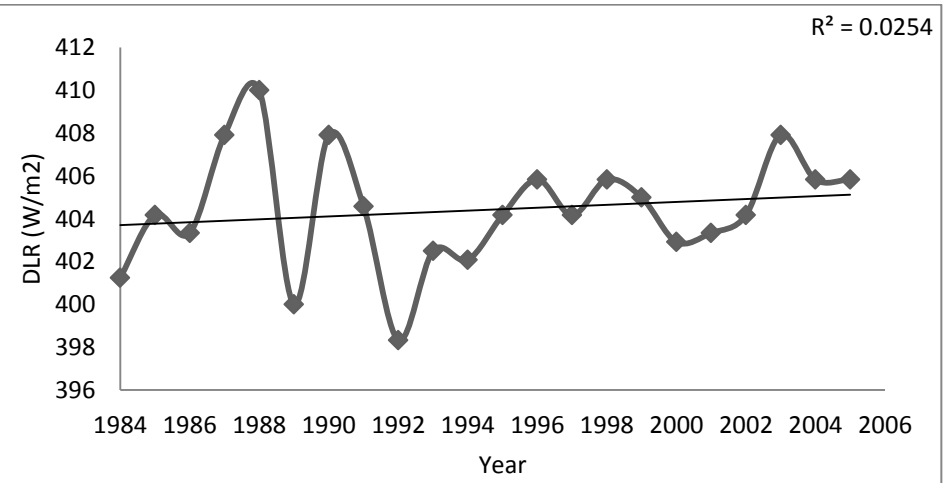

Fig 4.4.10: Enugu

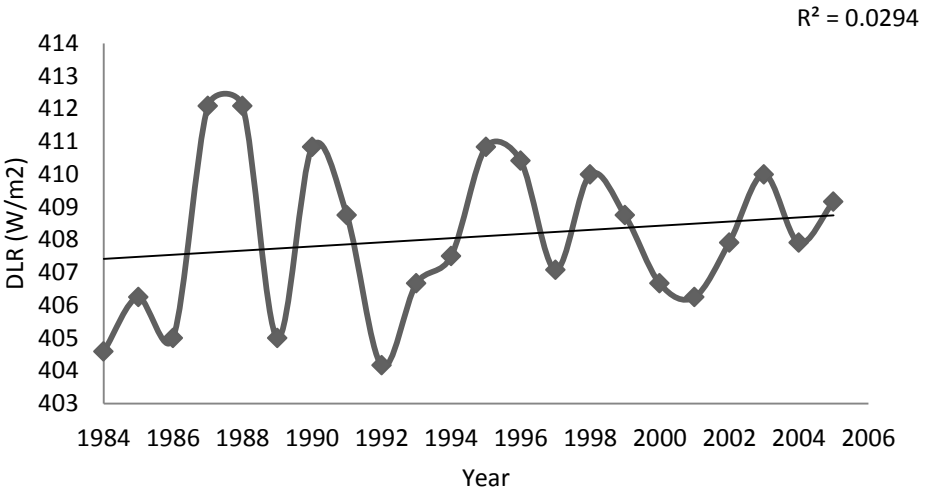

Fig 4.4.11: Ikeja

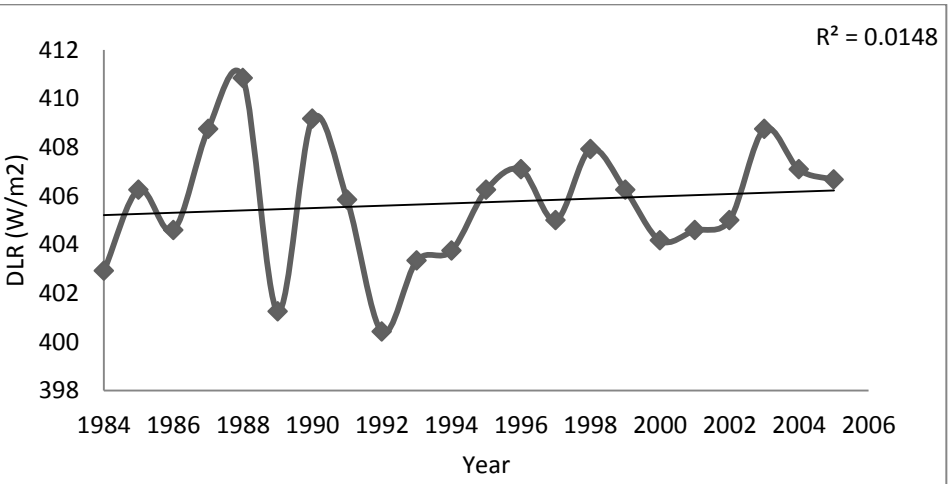

Fig 4.4.12: Asaba

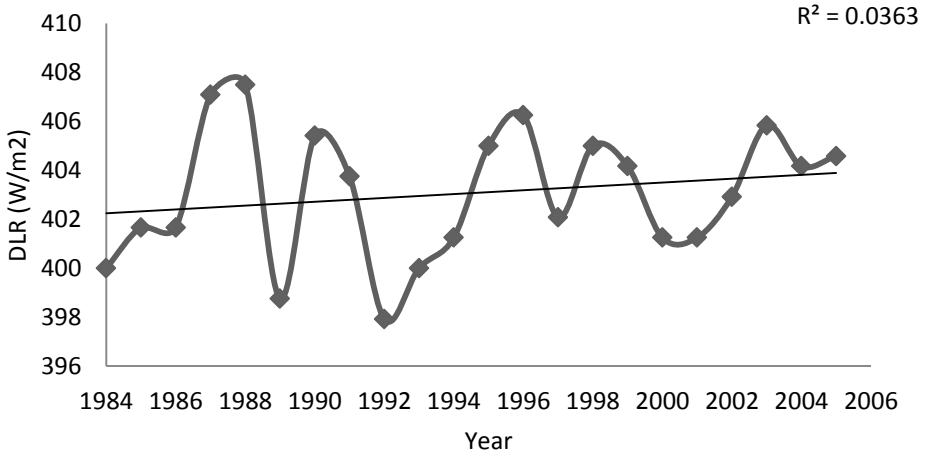

Fig 4.4.13: Abeokuta

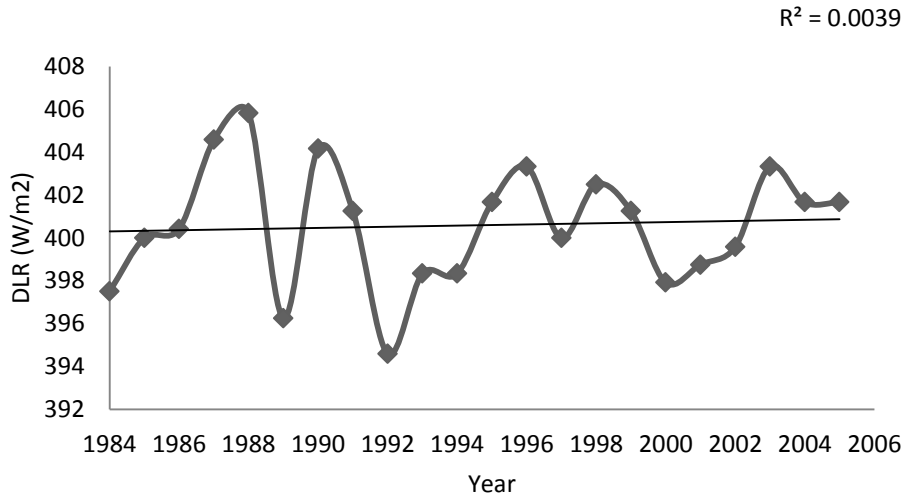

Fig 4.4.14: Akure

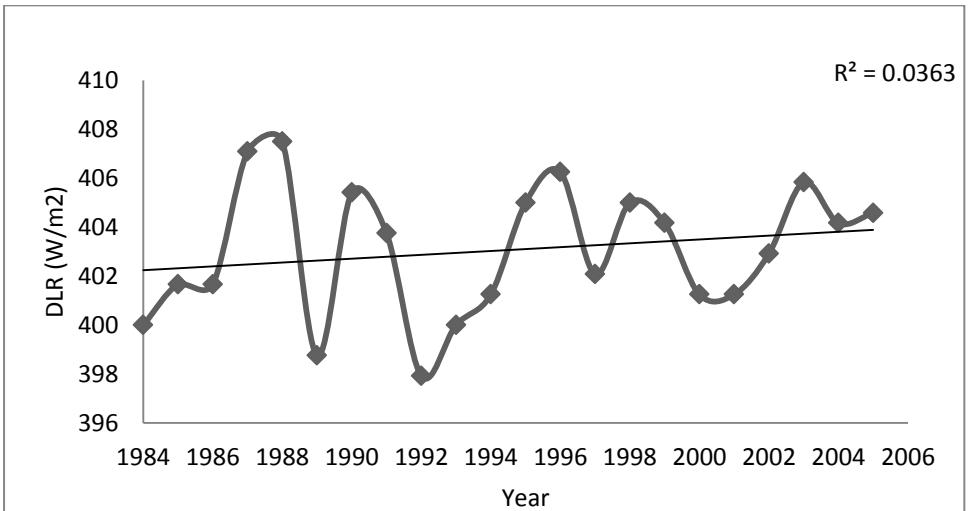

Fig 4.4.13: Abeokuta

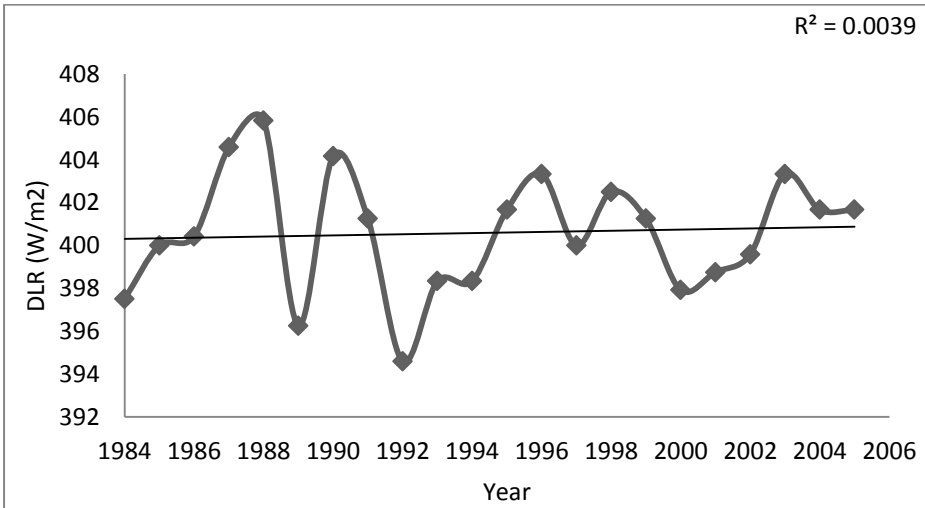

Fig 4.4.16: Ado Ekiti

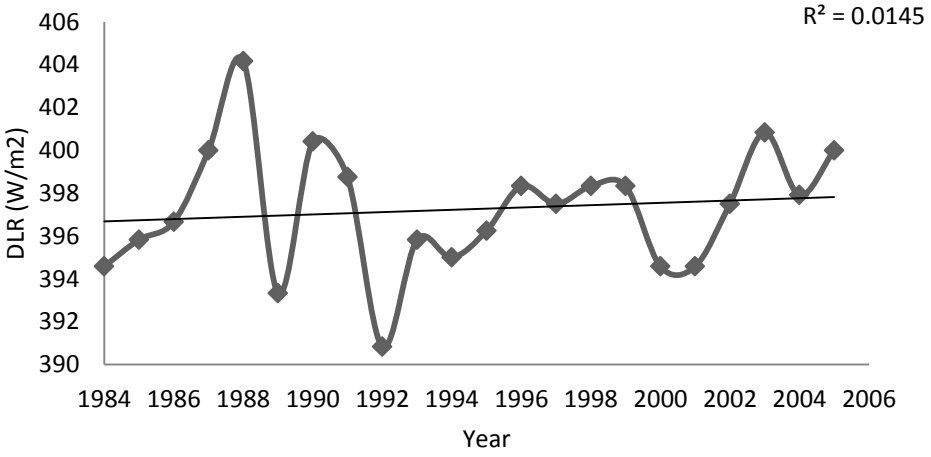

Fig 4.4.17: Makurdi

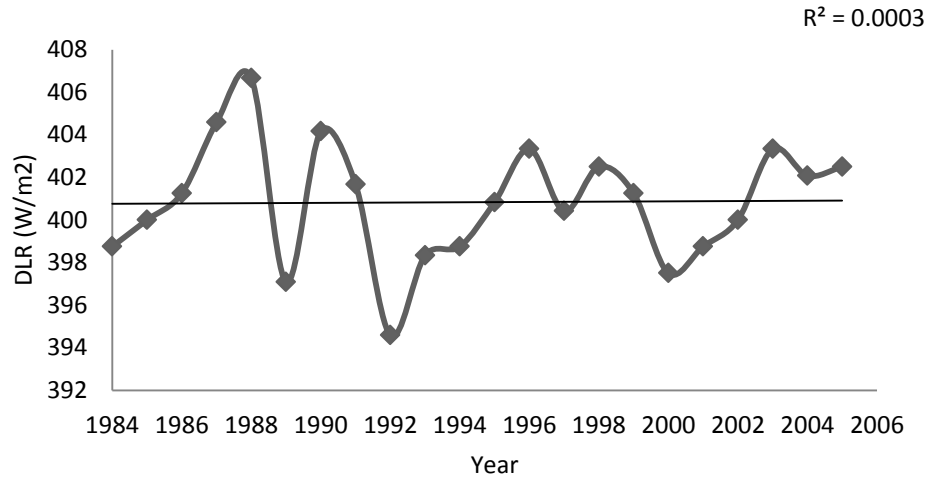

Fig 4.4.18: Lokoja

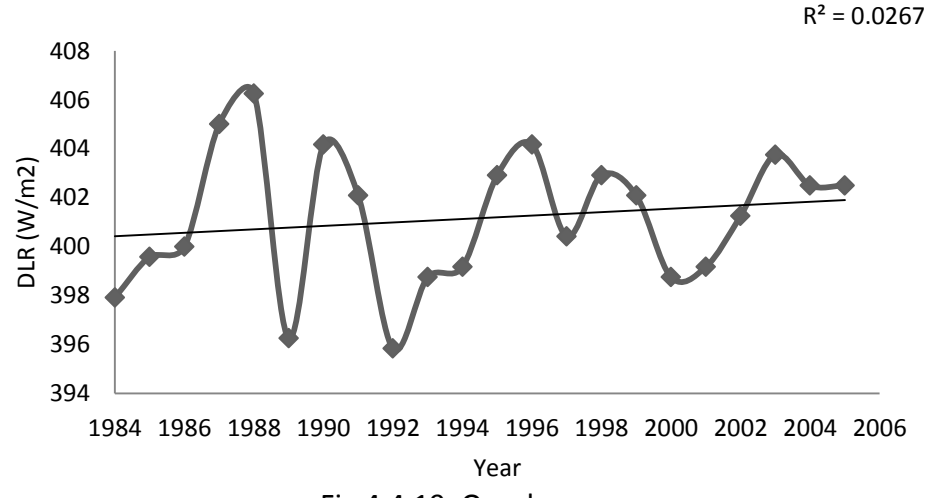

Fig 4.4.19: Osogbo

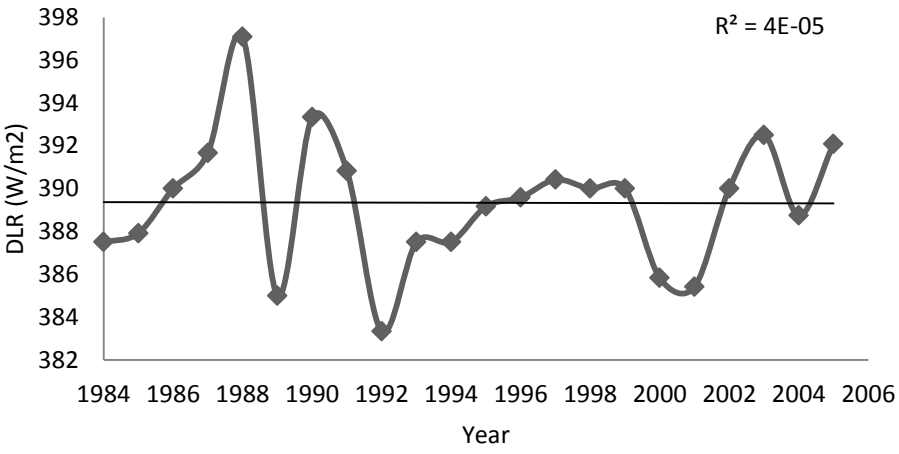

Fig 4.4.20: Lafia

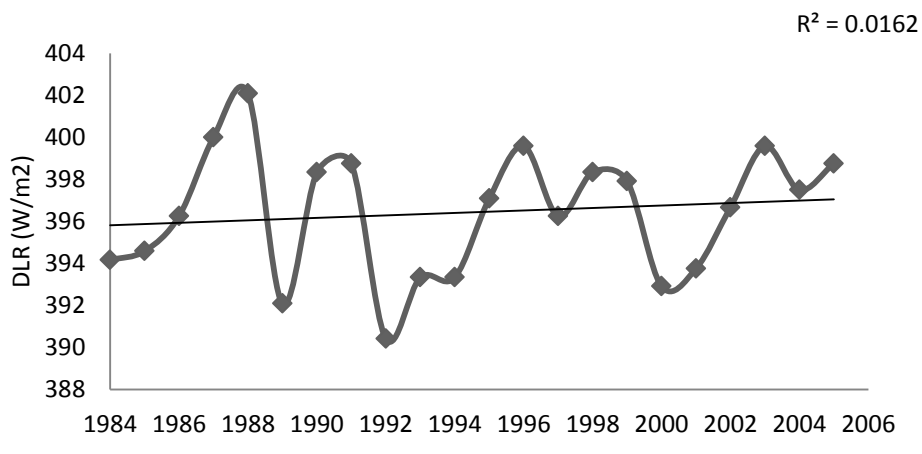

Fig 4.4.21: Ilorin

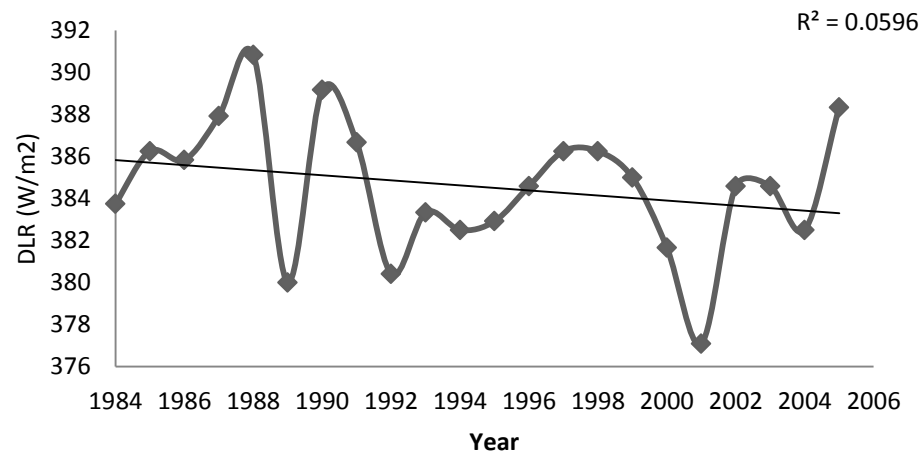

Fig 4.4.22: Jalingo

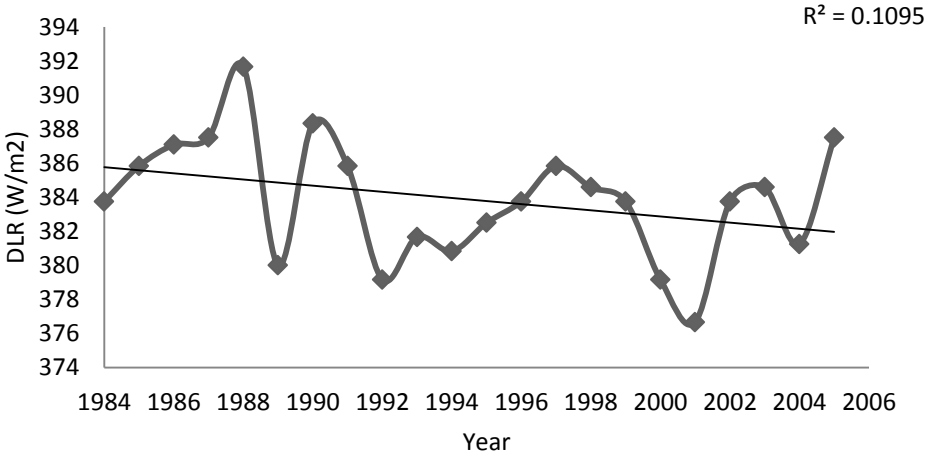

Fig 4.4.23: Abuja

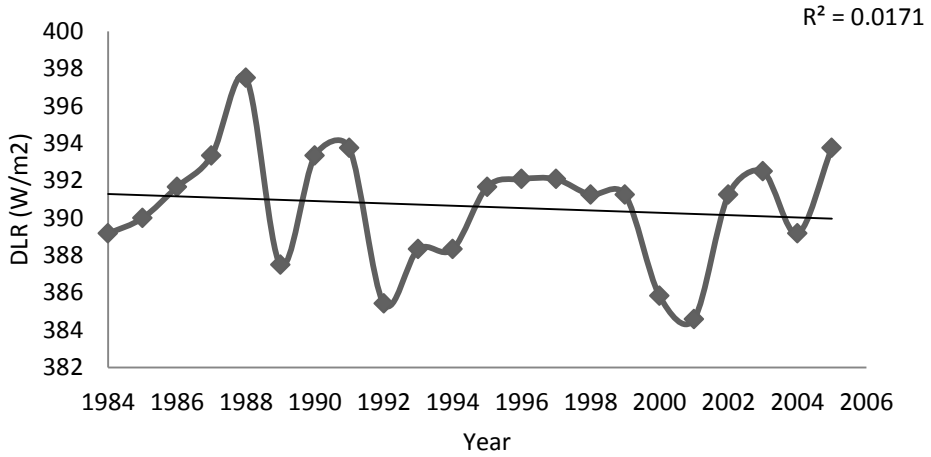

Fig 4.4.24: Minna

#

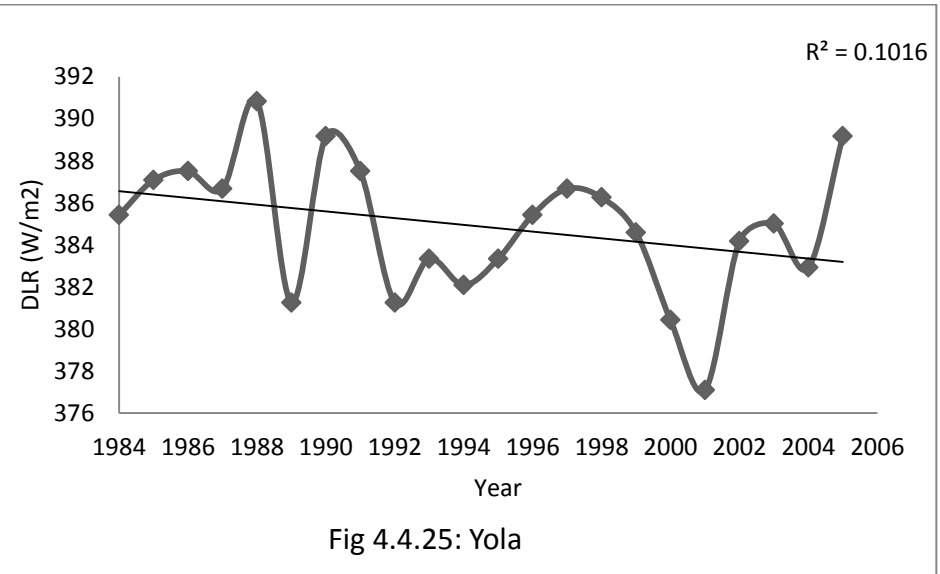

Fig 4.4.25: Yola

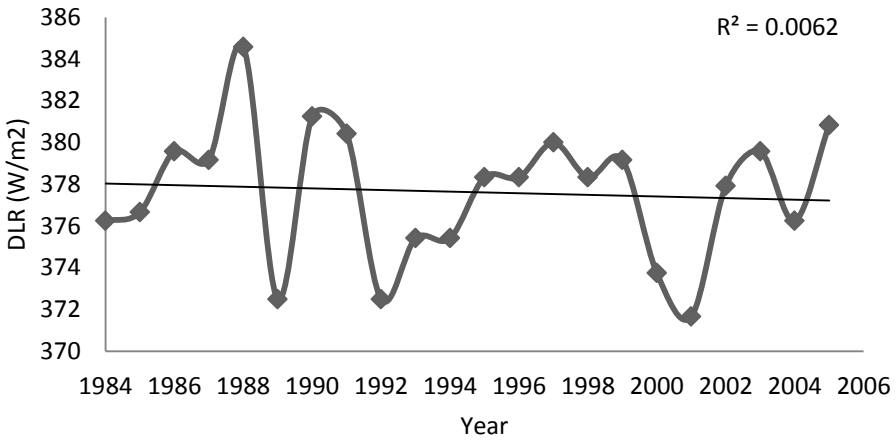

Fig 4.4.26: Jos

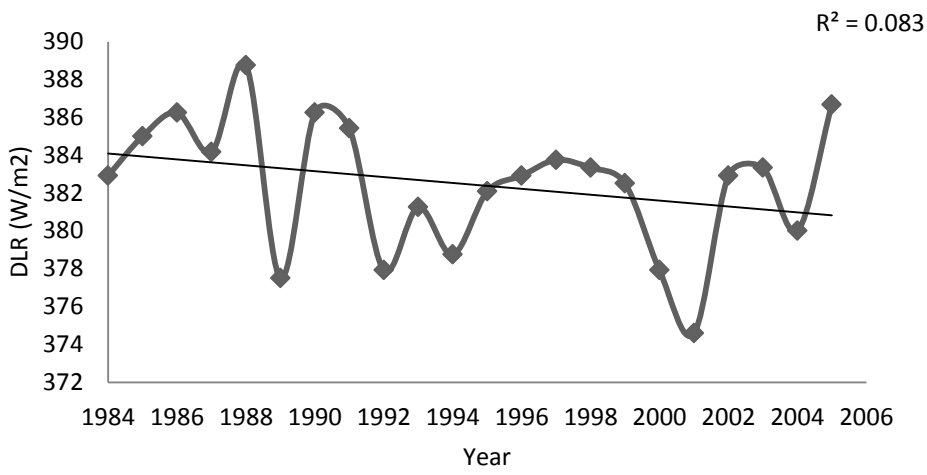

Fig 4.4.27: Gombe

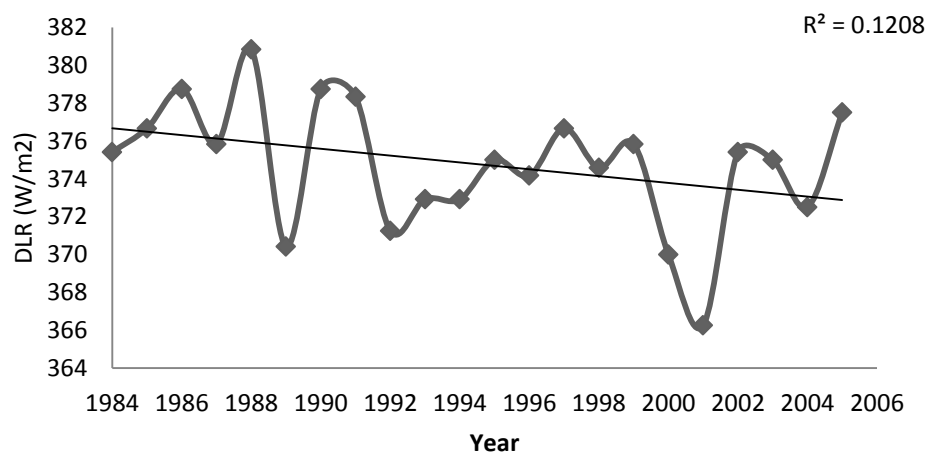

Fig 4.4.28: Bauchi

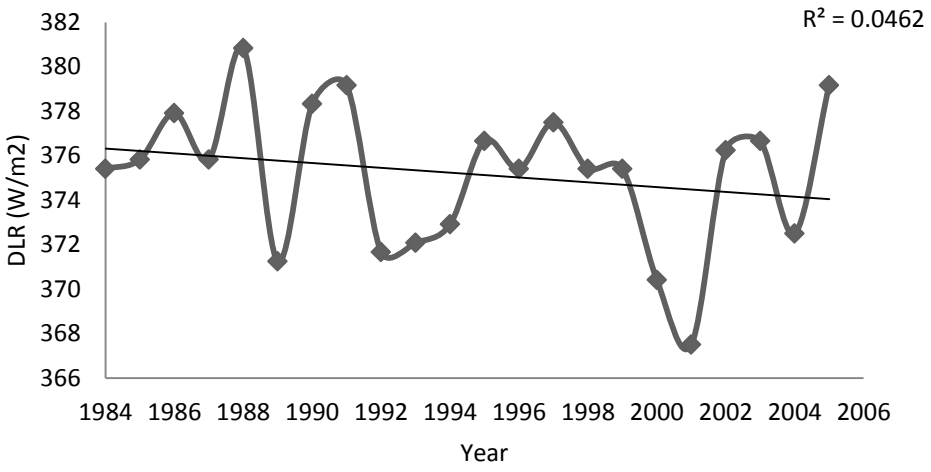

Fig 4.4.29: Kaduna

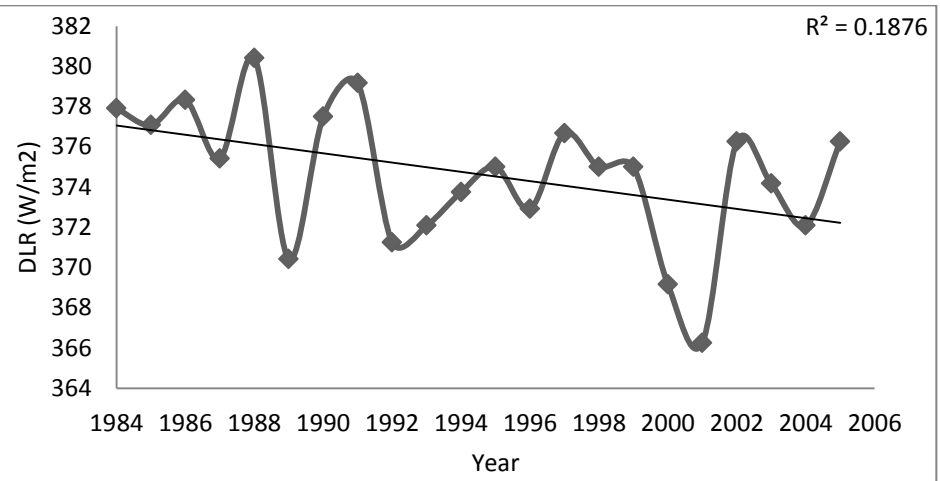

Fig 4.4.30: Kano

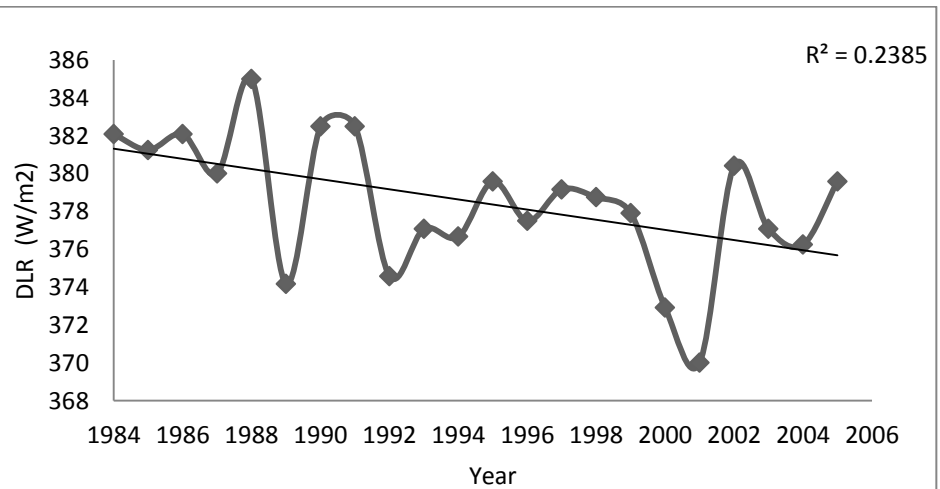

Fig 4.4.31: Dutse

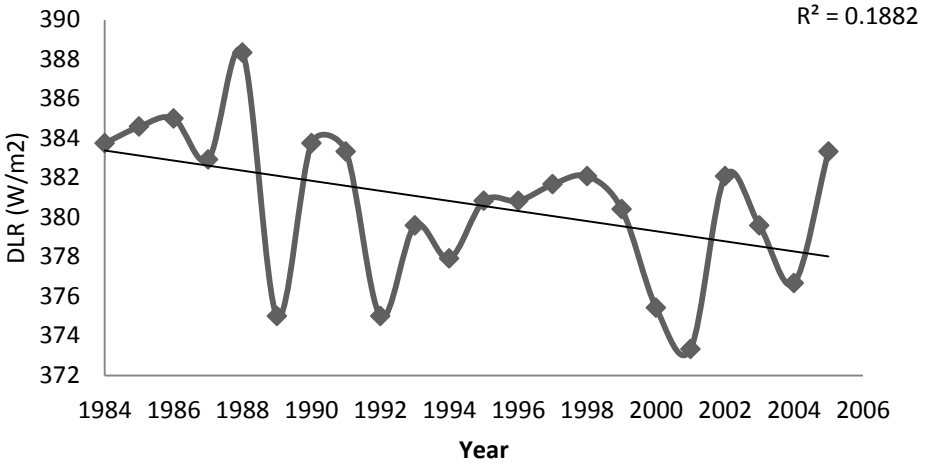

Fig 4.4.32: Damaturu

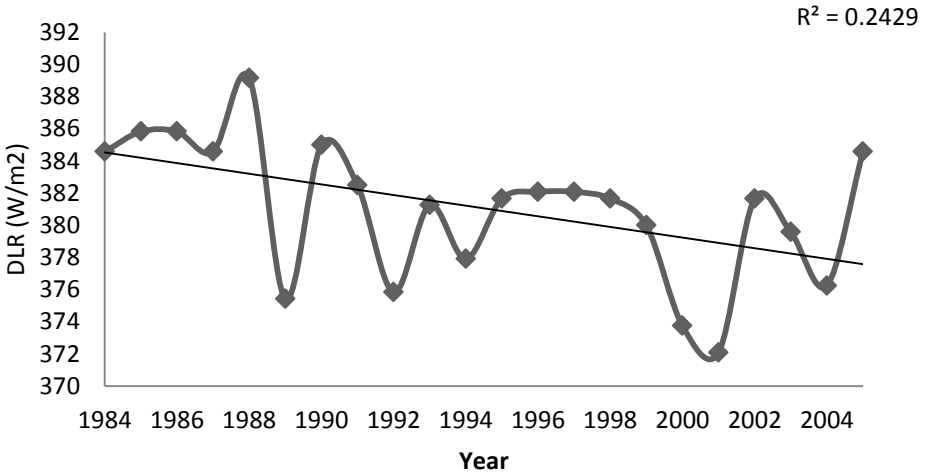

Fig 4.4.33: Maiduguri

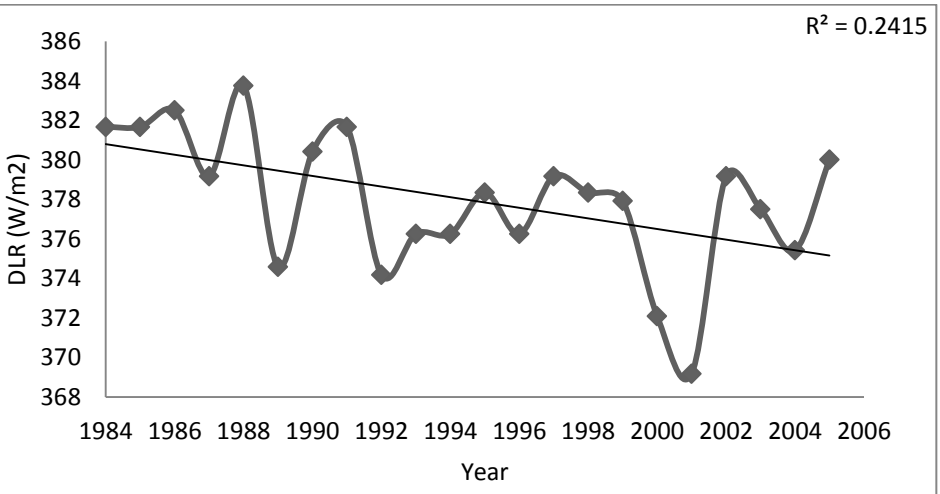

Fig 4.4.34: Gusau

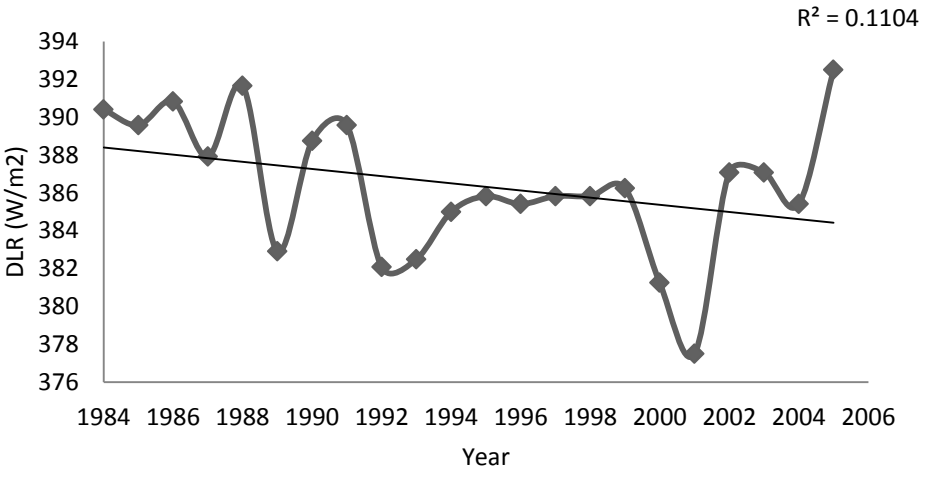

Fig 4.4.35: Birnin Kebbi

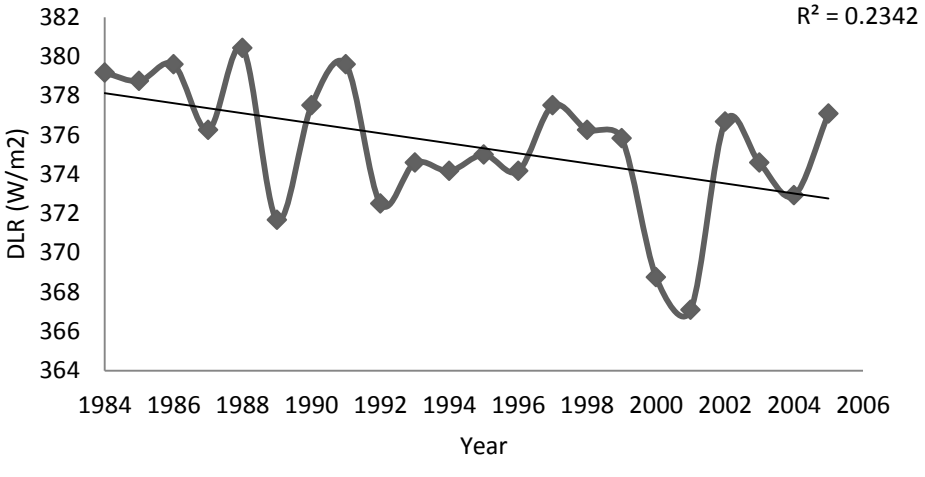

Fig 4.4.36: Katsina

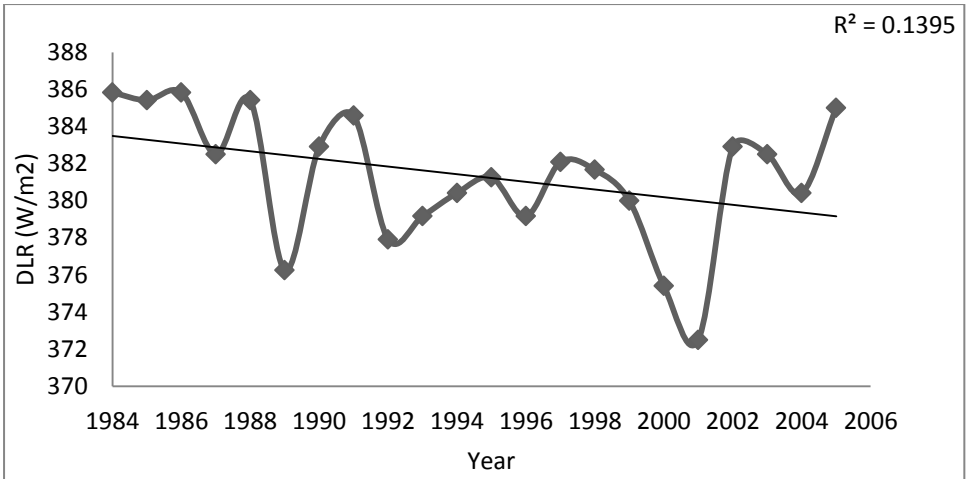

Fig 4.4.37: Sokoto

Figs 4.4.1 - 4.4.37: Long term trend of DLR for all 37 locations of the state capitals and federal territory of Nigeria for the period from 1984 to 2005.

4.3 Tested and Modelled Clear Skies DLR Equations at Ilorin

On the models that best describe the ground data for clear skies, it can be seen from Table 4.5.0 that no existing model at the same instance has correlation value from 0.90 upwards and also be statistically significant. Nonetheless the Swinbank (1963) model with a rather low correlation of 0.39 did estimate the ground measured DLR data with statistical significance. Thus it became necessary to put forward new ones and recalibration the Brunt (1932) model because it had the optimum performance based on the intercept and gradient values, apart from its high correlation coefficient.

Before embarking on the particular format any new model should take, different combinations of the water vapour and temperature were correlated against the emissivity and the result is as shown in Table 4.6.0. Even though the final output when multiplying the

emissivity, ε by σT^4 in equation 3.8 to obtain DLR will not entirely depend on the formal relationship between the emissivity and atmospheric parameters, yet it goes a long way to give a good estimation of the radiation if the correlation between emissivity and atmospheric parameters were high. Modelling based on the last two relationships between emissivity and atmospheric parameters in Table 4.6.0, though they had the highest values of correlation, were dropped due to the two reasons. Firstly, the combination of e/T (with a correlation of approximately 0.90) is the format of the Brutsaert (1975) model which is theoretical in form and needs profiles of water vapour and temperature even though it could be used without the profiles (Sedlar and Hock, 2009). There is no data for profiles of temperature and water vapour for the location. Secondly (that of water vapour pressure term also with a correlation of approximately 0.90), if only one parameter is used, any inconsistency in measurement could cause much deviation in the evaluation of the calculated term. So it could be more reliable if two parameters are used in modelling rather than one.

Table 4.7.0 shows the results of the new equations put forward (equation 3.22 or New 1 and equation 3.23 or New 2), the recalibrated Brunt (1932) model and the testing of one of the new models (equation 3.23) at a location (Barcelona) in Spain. As earlier mentioned the Brunt (1932) model was recalibrated because of its good fit based on its values on the gradient (V_m/V_c) and intercept columns. When considering the gradient value, a value of 1 is ideal and Brunt (1932) model's value for the gradient is 1. The intercept value of 0 is also ideal though that of Plata's model gives a lower value of 3.65 as against 5.53 of Brunt's model; however the Plata model is of a generalised nature so the idea of localising it was dropped. Eventually, it can be seen at the bottom parts of the table that the recalibrated Brunt (1930) that is equation 4.1, and the second new equation (equation 3.23) both met the desired statistical stipulations (i.e. having correlation values greater than or equal to 0.90 and being statistically significant). Even though the testing of New 2 at another location did not

produce the desired results, yet when it was localised it met the set out statistical standards. It should be pointed here that two new equations for Ilorin were put forward to show without doubt the extent that the exponential of temperature affect the radiation in this locality.

Table 4.5.0: The statistical results of the performance of the models for clear skies for ground measured data at Ilorin

Models	MBE	MABE	RMSE	R	t_s	V_m/V_c	Intercept
Brunt	-4.63	7.78	9.98	0.90[a]	4.71	1.00	5.53
Effimova	24.82	24.82	26.32	0.91[a]	25.51	0.89	19.05
Swinbank	2.77	15.87	19.57	0.39	1.29[b]	0.69	115.79
Idso and Jackson	6.99	16.07	20.68	0.39	3.23	0.67	123.41
Maykut and Church	24.31	27.40	31.14	0.39	11.25	1.12	-20.42
Brusaret	5.05	8.36	10.33	0.91[a]	5.04	0.87	44.04
Satterlund	8.10	11.72	14.93	0.81	5.82	1.27	-116.20
Idso 1	-22.79	22.79	24.39	0.92[a]	23.60	0.89	22.27
Idso 2	-22.51	22.51	27.53	0.93[a]	12.78	0.74	79.64
Konig-Langlo and Angstein	-34.07	34.91	39.05	0.39	16.07	1.15	-20.42
Plata	3.92	7.63	9.67	0.90[a]	4.00	0.98	3.65
Guest	-11.26	19.31	22.16	0.39	5.31	0.88	55.18

[a] correlation very high, [b] statistically significant

$$New\ 1 = (0.058\ \ln(eT^2) - 1.48\ x\ 10^{-4})\sigma T^4 \quad (3.22)$$

$$New\ 2 = (0.694 + \ 2.11\ x\ 10^{-5} eT)\sigma T^4 \quad (3.23)$$

$$Brunt\ (1932) = (0.605 + \ 0.048 e^{1/2})\sigma T^4 \quad (3.9)$$

$$Calibrated\ Brunt = (0.593 + 0.052e^{1/2})\sigma T^4 \quad (4.1)$$

Table 4.6.0: Correlation between the emissivity of clear skies DLR and different combinations of water vapour e and temperature T for the ground data of Ilorin between 1992 and 1994

Atmospheric Parameter	R	Standard Error	Intercept
$\log(eT^2)$, $\ln(eT^2)$	0.8722	0.0206	-0.6874
eT^2	0.8872	0.0194	0.6948
$\ln(e^{½}T^2)$	0.8480	0.0223	-3.9987
log(eT)	0.8758	0.0203	-0.0951
eT	0.8914	0.0190	0.6939
$e^{½}T^2$	0.8741	0.0223	0.5998
$e^{½}T$	0.8823	0.0197	0.5908
T	0.0240	0.0420	0.6313
e/T	0.8990	0.6922	0.6922
e	0.8954	0.0187	0.6930

Table 4.7.0: Statistical results of the performance of the new models for clear skies conditions at Ilorin

Models	MBE	MABE	RMSE	R	t_s	V_m/V_c	Intercept
New 1	-0.07	9.71	12.00	0.83	0.85 [b]	1.27	-103.64
New 2	0.20	6.75	8.65	0.91 [a]	0.21 [b]	0.92	29.40
Calibrated Brunt	-0.14	6.87	8.81	0.91 [a]	0.51 [b]	0.92	29.24
Jimenze et al. (1987) test with New 2	-6.63	9.90	13.50	0.95 [a]	5.07	0.97	15.17
New 2 localized on Jimenze et al. (1987)	-0.04	8.85	11.95	0.95 [a]	0.03 [b]	1.02	-6.28

[a] correlation very high, [b] statistically significant

4.4 Modelling with ANNs

Modelling of the radiation with ANNs obtained via Matlab® software gave some satisfactory results though not all the time. As seen from Table 4.8.0 except for just two input parameters, the set out statistical standards were met for the rest of the input parameters being from 3 to 8. Thus when the input parameters are more for the neural networks, the estimation is improved. When large data set were used for the neural networks, it was observed that it took quite a lot of time to produce the result (Table 4.9.0). In the first case time was not an issue

since it was fast. However the altering of default parameters only produced remarkable reduction in time used by ANNs in training and not much on the statistical result as shown in Table 4.9.0. It should be noted that the capability of the computer used has a role to play in this case. Contrary to Table 4.8.0 where the correlation was mostly very high (with just one exception of the case of two input parameters), in Table 4.9.0 the correlation values were not up to 0.90.

Again as seen from Table 4.10.0 when the ANNs were used at default, the correlations are not up to 0.90, even though as earlier shown in Table 4.8.0, where most times the correlations are from 0.90 upwards. The discrepancy can be attributed to the nature of data used as one set were taken at ground while the second set were obtained from satellite. That can be confirmed from Table 4.11.0 whereby a comparison of satellite derived data and ground measured data for the same location is made. It can therefore be concluded that for this particular case, ground measured data are better modelled with ANNs than satellite data. As another experimental modelling with ANNs were carried, it was observed that the higher the latitude the slightly better the correlation as seen in Table 4.12.0.

Comparing Tables 4.8.0 and 4.13.0 to Tables 4.9.0, 4.10.0 and 4.12.0 even though the correlation values are not always up to 0.90 (especially in Tables 4.9.0, 4.10.0 and 4.12.0), yet the t-statistic is okay for all cases. As earlier pointed out and clearly established by Table 4.11.0, the ground data have better correlation coefficient values than the satellite data. It is worthy to note that the ground measured data were obtained from different sources whereas in the case of the satellite data it came from one source. Throughout the experiments with ANNs, the satellite data did not have correlation values in the range of 0.9 – 1.0. In other places around the globe as seen in Table 4.13.0 ANNs perform well and those data are from the same source as the data of Ilorin (Table 4.8.0). Despite the fact that the ground data obtained for Ilorin in Table 4.8.0 were not all from the same source as against those of Table

4.13.0 which were all from BSRN, yet the performance of ANNs with regards to correlation coefficient remains high.

Table 4.8.0: Statistical results from ANNs for modelling ground-measured data carried out for the first experimental period of Sept 1992 – Aug 1994.

Input variables	MBE	MABE	RMSE	R	t_s
Vapour, temperature	-0.22	6.30	8.29	0.89	0.71 [b]
K_T, vapour, temperature	-0.24	5.49	7.01	0.93[a]	0.91[b]
K_T, vapour, declination	0.34	5.29	7.02	0.93 [a]	1.32 [b]
K_T, vapour, humidity, declination	0.30	5.42	7.07	0.93 [a]	1.21 [b]
K_T, vapour, humidity, declination, global radiation	0.12	5.30	6.70	0.93 [a]	0.47 [b]
Vapour, temperature, declination	0.29	6.04	8.05	0.90 [a]	0.95 [b]
K_T, vapour, temperature, humidity, declination, hour angle, zenith angle, azimuth angle	0.12	5.57	7.29	0.92 [a]	0.44 [b]

[a] correlation very high, [b] statistically significant

Table 4.9.0: Results obtained with neural networks for satellite data of July 1983- June 2005

Input Variables	Training Techniques	MBE	RMSE	R	t_s	Time (mins)
Ten input variables (day, month, year, declination angle, hour angle, zenith angle, temperature, vapour)	First six locations of lowest latitude of Table 4.3.0 using daily values for about 22 years at default	0.03	11.83	0.71	0.02 [b]	22
Ten input variables (day, month, year, declination angle, hour angle, zenith angle, temperature, vapour)	First six locations of lowest latitude of Table 4.3.0 using daily values about 22 years data with modified neuron parameters	0.01	9.87	0.72	0.01 [b]	5

[b] statistically significant

Table 4.10.0: Results obtained with neural networks for satellite data for some specific locations using the same input variables of Table 4.9.0

Location	Year	MBE	MASE	RMSE	R	t_s
Benin (Lat 6.32^o)	1985	0.94	8.92	13.05	0.55	0.65 [b]
Abakaliki (Lat 6.33^o)	1991	-0.90	9.07	13.05	0.76	0.59 [b]
Osogbo (Lat 7.77^o)	1998	-2.13	11.17	15.22	0.73	1.27 [b]
Sokoto (Lat 13.07^o)	2002	-2.74	18.54	23.91	0.86	1.04 [b]

[a] correlation very high, [b] statistically significant

Table 4.11.0: Two year (September 1992 to August 1994) satellite data modelling with ANNs at default with 10 hidden neurons of feed forward using ten inputs variables of Table 4.9.0

Type of Data	MBE	RMSE	R	t_s
Satellite	-0.10	15.59	0.83	0.06 [b]
Ground	0.24	10.40	0.92[a]	0.21 [b]

[a] correlation very high, [b] statistically significant

Table 4.12.0; Result obtained using 1984 satellite data for modelling with neural networks to test the effect of increasing latitude.

Input variable	Location	Latitude	R
Seven input variables (day, month, declination angle, hour angle, zenith angle, temperature, vapour)	Port Harcourt	4.74	0.75
	Awka	6.20	0.83
	Asaba	6.75	0.87
	Ado Ekiti	7.65	0.87
	Yola	9.91	0.88
	Dutse	11.73	0.88
	Sokoto	13.07	0.88

Table 4.13.0: Results of modelling with neural networks for other ground stations around the globe

Location	Year	MBE	MABE	RMSE	R	t_s
Barrow, USA (71.32°N, 156.60°S).	1996	3.11	9.16	14.90	0.92[a]	1.25[b]
Cabauw, Netherlands (51.97°N, 4.93°E)	2006	0.91	6.83	12.93	0.93[a]	1.34[b]
GOB, Namibia (23.56°S, 15.04°E).	2013	0.68	7.69	10.05	0.94[a]	1.30[b]
Georg von Neumayer, Germany (70.65°S, 15.04°E)	1996	1.42	8.12	12.41	0.94[a]	1.75[b]
South Pole (89.98°S, 24.80°W)	1996	-0.31	7.31	15.31	0.95[a]	0.33[b]

[a] correlation very high, [b] statistically significant

CHAPTER FIVE

DISCUSSION

5.1 Discussion of Results

The consistently good correlation between measured ground data and satellite data of DLR during the dry season as against the rainy season could be attributed to the clear skies more common during the dry season. Mostly the skies are cloudy during the rainy season. To improve on the data during the rainy season, it is imperative that the methods used to derive data of the radiation from satellite images need improvement particularly on water vapour molecules. At times, the inability for two models (i.e. ground measurement and satellite method) to be statistically significant points to the fact that there exists some detachment between both of them. Nonetheless using satellite data as surrogate for ground data is appropriate except in cases of extreme need for reliability.

With regard to the first period of ground measurement of DLR at Ilorin, the data were underestimated. However, for the second period, it can be concluded that the satellite data overestimate the ground data. If only the mean bias errors were considered, the shortcomings of the satellite data would not have been exposed. For instance, the correlation coefficient is very good if it is up to 0.90, yet all the values in this work are less than that. Contrary, Diak *et al.* (2000) found the RMSE between the daily values of DLR from pyrgeometer and developed parameterisation based on satellite image to be less than 5 W/m^2 as against the high values of the range between 9 to 22 W/m^2 found in this study (see Table 4.2.0). Also, given the inconsistency of statistical significance between the satellite-derived and the ground-measured data of DLR, thus there is the need to improve on the satellite method in this region.

Despite the fact that the Tropics are frequently characterised by cloudy skies, satellite estimates of DLR are better in the Tropics than in the Polar Regions that are otherwise characterised by clear skies (Nussbaumer and Pinker, 2012). Hence the quality of satellite data is down to the techniques of inferring the radiation from the water vapour properties of the cloud (Morcrette *et al.*, 2002), though the regional effect of clear skies cannot be ignored.

Based on the results obtained in this work for a single location, it could be misleading to generalise that satellites data do not have very high correlations with ground measurements. Nussbaumer and Pinker, (2012) showed that daily satellite data obtained from different organisations including BSRN when compared with ground truths produced yearly correlations of over 0.90 with small errors values. Their analyses of DLR data were done for about 33 BRSN stations from 2003 – 2007 although Ilorin was not included. Even though this present study clearly shows that an individual station could deviate from the general outlook, however from the global perspective, large discrepancies between satellites data and ground measurements of DLR fluxes do not exist. Furthermore in conformity with our work with regards to the magnitude of correlation between ground truth and satellite data is the work of Ba *et al.* (2001). They compared both the ground data and satellite data of downward surface irradiance (SW) for 11 African countries and found the overall correlation to be 0.75. While the least was Zaire with 0.33, the highest was Egypt with 0.98 and that of Nigeria was 0.83.

The amount of DLR is dependent on two main factors; the strength of solar radiation and the heaviness of the atmospheric gases which in turn translates to the level of cloudiness of the sky. The diurnal pattern is believed to probably synchronise with the sun's position in the sky particularly in this Equatorial region. Assuming a fixed amount of atmospheric gases, in the night hours when the sun is not in sight, DLR quantity is low and solely due to the atmospheric gases. As the sun rises, the intensity of the radiation increases and gets to

maximum when the sun is probably overhead. At that point the paths travelled by the sun's rays are shorter hence more radiation. Thus the sun is most likely overhead Ilorin at around 14hrs local time because it is the period of highest thermal energy of the day. On the other hand, assuming the solar intensity is fixed then as the content and nature of the gases in the atmosphere increase from time to time, the more the radiation and verse versa.

The extreme differing scenarios during June and December months when the sun-earth distance is either long or short could be responsible for those patterns. The average low values during the June solstices are probably due to the sun being the farthest away from the earth; therefore, even if there is much water vapour in the atmosphere, the incoming primary radiant energy is rather low. For the December case, the DRL loss during the day, where it typically increases, could probably be attributed to the intertwining effect of the earth's geomagnetic field and cosmic rays from the sun that are felt only when the distance between the sun and the earth is shortest. The DLR diurnal patterns been attributed to the sun-earth relationship is obviously form the facts that the sun is the primary source of radiation and its influence on the earth's climatic system is well recognized (Beer *et al.,* 2000; Kesseler and Jaeger 2003), especially the effects of the semiannual periodicity (Priester and Cattani, 1962; Harris and Priester, 1962). The phenomenal DLR diurnal variations during the mid and end of the year is not peculiar to this region alone as Hoch *et al.,* (2007) found others to occur in the polar region. For Ilorin as shown in this study the customary diurnal pattern of DLR in December is regular while that of June is vague and there are both likely to be due to Equatorial effects.

It has been established that the radiation is seasonal (Miskolczi *et al.,* 1997, Udo and Aro, 1999) and it is worthy to note that this present work has further confirmed the seasonality with different data set for the same location. It has been construed in previous studies that even though there are other contributory factors like cooler air and fewer clouds, the low

DLR during the dry season results from heavy dust particles in the atmosphere, which obstruct the radiation (Jimenez *et al.,* 1987; Miskolczi *et al.,* 1997; Dufresne *et al.,* 2002). Though not totally disagreeing with this notion, Jonsson *et al.* (2006) criticized it by showing that there is no coherent relationship between the change in DLR (predicted minus observed) residuals and the log of the total suspended particles (TSP) in three African cities. From the foregoing discussion, the low DLR during the dry season could be due to the dryness of the atmosphere because of the low concentration of water molecules, unlike the rainy season when the atmosphere is full of water molecules. The increased numbers of water molecules during the rainy season absorb radiation from the sun and later send it out to the atmosphere. Furthermore the analysis carried out by Morcrette (2002) gave a meager increment of about 1 W/m^2 as contribution from aerosols to the flux outside the Arctic and Antarctic regions. But rather than having more radiation during the dusty Harmarttan period which is a subset of the dry season (Miskolczi *et al.,* 1997) as the case should be, instead the radiation is lower. Therefore it is correct to state that the low DLR during the Harmarttan is due to the dry atmosphere (which lacks much of water molecules, a major gas of DLR) rather than insinuating that the dust particles (by blocking the radiation) are responsible for the low DLR during the dry season.

Also the fact of decreasing DLR away from low latitude is confirmed in this study (Jonsson *et al.,* 2006; Wild *et al.*, 2001). However in this work it is has shown that little variations in the latitude influences DLR, not only when the changes in latitudes much. Yet another confirmation of this study is the effect of closeness to water bodies which increases with DLR as observed by Choi *et al*., (2008). They measured DLR in Florida, USA over different land surfaces, such as water, wetland, urban, rangeland, forest and agriculture, and found that the radiation over open water was more than others and was consistent even when estimating the radiation using various models. In addition this work has shown that the influence of

water bodies can suppress the influence of either latitude or elevation on DLR between locations. The areas of high radiation are consistently relatively stable because these areas do not experience much variation, similar to areas of lower radiation. Large water bodies, such as oceans and lakes, may have a strong influence on downward longwave radiation because places that are closer to these water bodies have higher and more stable radiation than places farther away, even if these places lie on the same horizon.

The northern regions have harsh weather conditions, inferred from the fact that the differences between the minimum values and maximum values of DLR are higher in the north than in the south, although the southern regions generally have higher DLR values than the north. Uniquely, the north attains extremes of both high and low DLR radiation. Coupled with the fact that the north regions are at higher latitudes, these radiation values are also at higher altitudes. Apparently the distance the radiation from the sun travels to high altitude location is shorter than the path it transverses to low altitude location. In the absence of more atmospheric greenhouse gases responsible for locations of lower altitudes having greater mean valves of DLR than locations of high altitudes over time, since ray paths are shorter for high altitudes then very high valves of DLR are attainable. Because at the window region of DLR (DLR in the range of about 8-12μm) whereby DLR comes directly from the sun and reaches the earth, high values are not only attainable at high altitudes due to short ray path but also the window accounts for higher values of day time DLR when the sun is still up than night time. Again the side effect of lower concentration of DLR gases at high altitudes comes to play for the reason those locations record very low values of DLR. Whenever the sun's radiation is totally cut off, since there are less DLR gases filling the space at higher altitude regions then relatively small amount of contribution of DLR from gases is available hence very low valves of DLR are readily recorded at higher altitudes compared to lower altitudes.

The fact that there is a greater presence of atmospheric gasses in its space, such that a location at a lower altitude experience greater radiation by virtue of the longer blackbody clouds than a location at a higher altitude. Iziomon *et al.* (2003) showed that it was necessary to have two different sets of coefficients for a similar type of DLR equation for two locations because of the difference in their altitudes and due to the radiation dependency on altitude. Additionally, at a lower altitude, there is influence from other higher locations in the form of the reflection of radiation from the hilly locations (Pluss and Ohmura, 1997). DLR decreases moving from the south of Nigeria up to the north, and although from global perceptive the latitude change is relatively small (a difference of 8.32^{o} existing between the south and the north, see Table 4.3.0), the results remain in line with established findings that DLR decreases as the latitude increases (Wild et *al.,* 2001; Jonsson *et al.*, 2006). Moreover, Wild *et al.* (2001) established four different seasonal patterns of DLR at low latitudes where, incidentally, a location that falls between the far north and south of Nigeria, Ilorin, was established. Additionally, from both Wild *et al.* (2001) and this work, it would be concluded that not less than five different seasonal patterns for DLR have been found thus far for the low latitude regions.

Satellite data are relied upon for use in many applications, considering the problems that are associated with ground measurements, particularly in the case of downward longwave radiation. Such measurements averaged over 24 hrs are accompanied by a reasonably small magnitude of error less than 5 Wm^{-2}, and based on overall considerations; the data are useful for agricultural applications (Diak *et al.*, 2000).

Based on the mean statistic, the DLR regime over the country is of three main sections along latitudinal inclinations such that from latitude of about 4.75^{o} - $7\ .77^{o}$ the high, from 8.84^{o} – 10.28^{o} the moderate and from 10.32^{o} - 13.07^{o} the low. However other factors also like water bodies, altitude and the longitude are found collectively influence DLR. Most regions in the

northern Nigeria are at high altitude hence they receive lower DLR because of the low atmospheric length with corresponding DLR gases as compared to the south.

Given the fact that magnitude of the elevation of the northern zone is twice that of the south, the southern end of the country slops into the Atlantic Ocean; hence, the susceptibility to lose or gain landmass depends on the behaviour of the ocean. This region should not witness any major flooding, except flooding directly influenced by the ocean, because excess water on land should empty into the ocean.

Apart from satellite data, another method of DLR data acquisition in the face of rare ground measurements is to model using the Stefan Boltzmann equation, with three major input variables of temperature, water vapour pressure and cloud cover. Assuming that the atmosphere is a grey body, the emissivity of the atmosphere, as contained in the equation 3.1, can be further extended from only being constants to having either or both temperature and water vapour pressure terms. Moreover, cloud cover being another major factor in the equation, when introduced takes care of all skies conditions. There are various equations that estimate the radiation, and most of the equations are locality biased (Iziomon et *al.,* 2003), which has further being established in this study. In the field of radiant energy the range of temperature is in power of 4 to 6. Most models are tailored after the Stefan Boltzmann's model of σT^4. Obviously models with temperature term to the power of five to six fit better in this region with particular regards to statistical significance than models with power of 4 as evidenced by the two new equations for DLR put forward. The only existing model in its original form that was deemed statistically significant with the measured DLR was that of Swinbank (1965), which is of the form of power of 6 which lacks water vapour pressure term. In this region, water vapour pressure term is more important than temperature in relationship to the emissivity. Furthermore, notably, relative humidity is another atmospheric parameter that has been employed to model DLR such that, instead of including cloud cover in the

equation when extending from clear skies to all skies conditions as is primarily the case (for clear skies, cloud cover ratio is equal to 1), Gabathuler *et al.,* (2001) used the clearness index alongside relative humidity for their all sky models. Presumably, those equations that have only a temperature variable were derived from locations far away from water bodies; hence, those locations' DLR is influenced mostly by temperature rather than water vapour pressure. Additionally, in situations where water bodies are close by, the water vapour pressure becomes important (Alados-Arboledas, 1993). However, there are diverse and complex mechanisms responsible for the behaviour of atmospheric parameters, which vary from region to region across the globe, particularly during different seasons. These range from the physical atmospheric nature to the geographical composition, topology and vegetative interactions with different radiation transfers (Marthews *et al.,* 2012; Pomeroy *et al.,* 2003; Curry *et al.,* 1996).

Neural networks give better fits of how the DLR sought to be even in cases where correlation is not very high. Also it appears that the closer a location is to the Atlantic Ocean and the lower the latitude is, the worse the prediction. Ground data are better modelled than satellite data despite the fact that ground data parameters were not from the same source while satellite data were from the same source; implying satellite data is not a perfect substitute for ground data. Regarding the comparison between neural networks and traditional methods, the former predict the radiation better in this locality (Obot *et al.,* 2008). Various modelling using ANNs for DLR are attained and at all times the ANNs were statistically significant. However for large data set it took quite long time for ANNs to produce the result.

Many areas of application of this study abound, for instance, in the areas of agriculture, specifically in plant husbandry, such that if the radiation regime of a location is replicated via the greenhouse effect, then the plants that are found in that location can be cultivated elsewhere. Under unfavourable weather conditions, crop farming have been better practised

with adequate scientific techniques coupled with a knowledge of DLR (Lhomme and Vacher, 2002; Lhomme and Guilioni, 2004; Yin *et al.*, 2008). Weather conditioning can even be used by sports men and women. Another area is in the cooling of house and architectural design whereby selective absorption techniques imbedded in glasses can be deployed for space heating or cooling.

CHAPTER SIX

SUMMARY AND CONCLUSION

6.1 Summary

The findings in this study based on the five specific objectives that were set out, are hereby presented. Firstly, the relationship between ground data and satellite data of DLR at Ilorin was investigated. It was found that the correlations between ground data and satellite data at Ilorin for two ground measurements periods of DLR around 1992 - 1994 and 1995 - 1997 were 85% and 67% respectively, and that the dry season consistently had better correlations than the rainy season. Statistical significance between the ground-measured data and satellite-derived data of DLR was sometimes observed only at one season or the other.

Secondly, the inherent patterns in the daily, monthly and yearly data of the radiation in Nigeria were investigated. It was found that on the daily trends for Ilorin only, the radiation peaks at 14hrs local time and tends to show semi-annual periodicity with the sun, mostly during June and December (a six month cycle). Most times at the mid-year period the diurnal pattern is disordered while during the end of the year period, a double peaked diurnal pattern is mostly the case. The radiation is low in the dry season and high in the rainy season with varying degrees along the latitude and the low radiation is attributed to the effect of dry atmosphere during the dry season. Diverse yearly patterns were observed from the many locations examined but most locations in the south have slightly increasing trend of DLR as against slightly decreasing trend found in the northern section over a 22 year period of 1983 to 2005 of satellite data. Hence the study area of this work maintained steady state of DLR during the 22 years investigated. During the analysis of the daily mean DLR across Nigeria, this study confirmed that the latitude and elevation vary indirectly with DLR and that the closeness to water bodies increases the magnitude of DLR.

Thirdly, the intent of this study was to segment the country into appropriate DLR zones. Three major segments were observed such that from the south going up north (that is increasing latitude), on the average the first is a group that has high DLR values but small ranges, second is the group with moderate DLR values and corresponding ranges while the third group in the far north have low DLR values but large ranges. It can be concluded that the smaller the ranges the more stable the climate of the region.

The fourth of the fifth specified objectives of the study was to evaluate the performance of existing DLR equations under clear skies in Ilorin and put forward new ones using the data of the site. All the tested equations failed to meet the set out statistical standards. The stipulations were that the correlation coefficient R between the calculated DLR from the model and the ground measured DLR, should be up to 0.90 and also the calculated and the measured DLR should be statistical significance. It was found out none of the tested existing model met the standard. New models are put forward including the recalibration of Brunt (1930) model. One out of the two new models and the recalibrated Brunt (1930) model did meet the set out stipulations, which further establish the sensitivity of models to the locations they are derived from. It is opined that models with both temperature and water vapour terms are better such that the temperature preferably in the power range of T^5 to T^6 as against the Boltzmann model of T^4 fit better at Ilorin.

Lastly, modelling of DLR was attained using neural networks. The analysis of the estimation of DLR with ANNs were carried out under various conditions like testing the effect of the number of input parameters, effect of increasing latitude, the effect of large volume of data, comparisons of estimation of ground data against satellite data and the estimation of DLR elsewhere in the globe with that of Ilorin. It was found that a common factor throughout the diverse cases of modelling with ANNs is that statistical significance was attained, implying a reasonably fit of ANNs estimations. The more input parameters used the better the estimation

of DLR with ANNs, and the higher the latitude the slightly better the correlation coefficient for estimations of DLR with ANNs. Also ground measured DLR data were better estimated with ANNs than satellite derived data. ANNs were found to also meet the set out statistical standards when estimating ground measured DLR data from other parts of the world as it did in Ilorin. Generally, the time for training of large volume of data is quite long even though it is dependent on the capacity of the computer system used.

6.2 Conclusion

Seasonal effects contribute to satellite-derived data of downward longwave radiation (the satellite data of DLR are better derived during the dry season than the rainy season). Satellite data have moderate agreement with ground data and are deemed appropriate for use especially in cases where no ground measurements exist. It is found that there are significant deviations during the solstices' periods from the normal diurnal pattern of DLR. Nigeria has three distinctive seasonal patterns of DRL along latitudinal basis and generally the radiation is low during the dry season. It is confirmed that DLR vary indirectly with latitude and elevation but directly with closeness to water bodies and also that clear skies equations are sensitive to the locations they were derived from. Particularly in Ilorin, Nigeria, it is shown that clear skies DLR models of temperatures of the powers of 5 and 6 coupled with water vapour pressure term especially with regards to the t-statistic fit the radiation better. It is established that using ANNs to estimate the radiation have unique advantages over the traditional methods because ANNs are always statistically significant and can be extended to places where no data for DLR exist. The diurnal patterns of DLR at the middle and end of year periods should be further investigated even from a global scale.

6.3 Contributions to Knowledge

The contributions to knowledge from the work are as follows:

1. New equations of clear skies for downward longwave radiation for Ilorin in Nigeria have been developed. There are a total of three new equations whereby two are entirely new (to the best of my knowledge) while the third is the recalibration of an existing model of Brunt (1932). All the three models have good correlation values and are statistically significant.

2. Neural networks modelling of DLR in Nigeria have been attained and at all times, it was found to be statistically significant at 95% confidence level with the measured radiation, except with inappropriate number (only 2) of input parameters.

3. To the best of my knowledge this is the first work to establish uncommon diurnal patterns of the radiation during June and December in this locality. However the articulated reason for the uncommon patterns which is the sun-earth relationship was not quantitatively established. It may be a regional effect common at the Equator.

4. Three distinguished DLR categories across the country from the south to the north have been established, which could form a different zoning format for the country, apart from others like the exiting geopolitical and vegetation zones. The uniqueness of using DLR to zone the country is that the more the variation in DLR the less stable the climate of the region. Also DLR is known to depict the climate of a region better than atmospheric parameters like temperature and water vapour pressure (Soares *et al.,* 2004),

References

Aase, J. K. and Idso, S. B. (1978). A comparisons of two formulae types for calculating longwave radiation from the atmosphere. *Water Resources Research* **14**, 623-625

Alados-Arboledas, I. (1993). Estimation of hourly valves of downward atmospheric radiation under cloudless skies during day- and night- time conditions. *Theoretical and Applied Climatology* **48**, 127-131

Aliyu, A.S., Ramli, A.T., and Saleh, M.A. (2013). Nigeria electricity crisis: Power generation capacity expansion and environmental ramifications. *Energy* **61**, 354–367

Allan, R .P. (2006). Variability in clear-sky longwave radiative cooling of the atmosphere. *Journal of Geophysical Research* **111**, D22105, doi: 10.1029/2006JD007304

Allan, R. P. (2000). Evaluation of simulated clear-sky longwave radiation using ground-based observations. *Journal of Climate* **13**, 1951 – 1964

Allan, R. P. and Slingo, A. (1998). Simulated long-wave clear-sky irradiance over the ocean: spatial and temporal variability 1979-1993. *Physics and Chemistry of the Earth* **23**, 599 – 640

Anderson, E.R. (1954). Energy-budget studies, water-loss investigations: Lake Hefner studies. *US Geological Survey Professional Paper* **269**, 71–119

Angstrom, A. (1918). A study of the radiation of the atmosphere. *Smithsonian Institution Miscellaneous Collections* **65,** 159-161

Arnfield, A. J. (1979). Evaluation of empirical Expressions for the Estimation of Hourly and Daily totals of Atomospheric Longwave Radiation under all sky conditions. *Quarterly Journal of Royal Society* **105**, 1041 – 1052

Aro, T.O. (2007). Basic measurements of radiation at station Ilorin (eg1994-03). Department of Physics, University of Ilorin, doi:10.1594/PANGAEA.754653

Aubinet, M. (1994). Longwave sky radiation parameterization. *Solar Energy* **53**, 147-151

Ba, M. B., Frouin, R., Nicholson, S. E. and Dedieu, G. (2001). Satellite-derived radiation budget over the Africa continent, part 1: estimation of downward solar irradiance and albedo. *Journal of Climate* **14**, 45-58

Bar-Cohen, Y. (2006). Biomimetics-using nature to inspire human innovation. *Bioinspiration & Biommetric* **1**, 1-12

Bashahu, M. (2003). Statistical comparison of models for estimating the monthly average daily diffuse radiation at subtropical African site. *Solar Energy* **75**, 43-51.

Basheer, I. A. and Hajmeer, M. (2000). Artificial neural networks: fundamentals, computing, design, and application. *Journal of Microbiological Methods* **43**, 3 –31

Beale, M. H., Hogan, M. T. and Dermuth, H.B. (2014). Neural network toolbox user's guide R2014a. *The MathWork Inc. MA.*

Beer, J. Mende, W., Stellmacher, R. (2000). The role of the sun in climate forcing. *Quaternary Science Reviews* **19**, 403-415

Berdahl, P. and Fromberg R. (1982). The thermal radiance of clear skies. *Solar Energy* **29**, 229 - 314.

Berdahl, P. and Martin, M. (1984). Emissivity of clear skies. *Solar Energy* **32**, 663-664.

Berger, X., Bathiebo, J., Kieno, F. and Awanou, C. N. (1992). Clear sky radiation as a function of altitude. *Renewable Energy* **2**, 139-157

Berger, X., Cubizolles, B., and Donet, I. (1988). Radio-sounding data for the determination of the infrared sky radiation. *Solar and Wind Technology* **5,** 353-363.

Bocco, M., Orando, G. and Sayago, S. (2006). Development and evaluation of neural network models to estimate daily solar radiation at Cordoba, Argentina. *Pesquisa Agropecuária Brasileira* **41**, 179-184

Brunt, D. (1932). Notes on radiations in the atmospheres. *Quarterly Journal of the Royal Meteorological Society* **58**, 389-420

Brutsaert, W. (1975) On a derivable formula for long-wave radiation from clear skies. *Water Resources Research* **11**, 742–744

Budyko, M.I., (1974). Climate and Life. *Academic Press, New York.*

Catalanotti, S., Cuomo, V., Piro, G., Ruggi, D., Silverstrini, V. and Troise, G., (1975). Radiative Coolings of Selective Surfaces. *Solar Energy* **17**, 83-89.

Chevallier, F., Cheruy, F., Scott, N. A. and Chedin, A. (1998). A neural network approach to fast and accurate data assimilation. *Journal of Applied Meteorology* **40,** 1445 – 1461

Chevallier, F., Morcrette, J.-J., Cheruy F. and Scott, N.A. (2005). Use of a neural-network-based long-wave radiative-transfer scheme in the EMCWF atmospheric model. *Quarterly Journal of Royal Society* **126**, 761-776

Chineke T. C., Idinoba M. E. and Ajayi O. C. (2011). Seasonal evapotranspiration signatures under a changing landscape and ecosystem management in Nigeria: Implications for agriculture and food security. *American Journal of Scientific and Industrial Research* **2**: 191-204

Choi, M., Jacobs, J. M. and Kustas, W. P. (2008). Assessment of clear and cloud sky parameterizations for daily downwelling longwave radiation over different land surfaces in Florida, USA. *Geophysical Research Letters* **35**, L20402, doi:10.1029/2008GLS035731

Chou C and Neelin J.J. (1996). Linearization of longwave radiation scheme from intermediate tropical atmospheric models. *Journal of Geophysical Research* **101**, 15129 – 15145

Claquin T., Schulz M., Balkanski Y. and Boucher O. (1998). Uncertainties in assessing radiative forcing by mineral dust. *Tellus* **50B,** 491-505

Colarco P., Silva A da, Chin M., Diehl T. (2010). Online simulations of global aerosol distributions in the NASA GEOS-4 model and comparisons to satellite and ground-based aerosol optical depth. *Journal of Geophysical Research* **115**, D14207, doi:10.1029/2009JD012820

Cotton, W.R., Bryan, G., Heever, V.D., 2010. Storms and cloud dynamics. Academic Press.

Coulson, K. L. (1975). Solar and terrestrial radiation: methods and measurements. *Academic Press*

Crawford, T. M. and Duchon, C. E. (1999). An improved parameterization for estimating effective atmospheric emissivity for use in calculating daytime downwelling longwave radiation. *Journal of Applied Meteorology* **38**, 474–480

Culf, A. D. and Gash, J. H. C. (1993). Longwave radiations from clear skies in Niger; a comparison of observation with simple formulae. *Journal of Applied Meteorology* **32**, 539-547

Curry, J. A., Rossow, W. B., Randall, D., and Schramm, J. L. (1996) Overview of Arctic Cloud and Radiation Characteristics. *Journal of Climate* **9,** 1731–1764

DAO, (1996). Algorithm theoretical basis document version 1.01. *NASA's Goddard Space Flight Center*

David-Okoro, I.L., Chineke, T.C., Ihemmadu, V.E., Onyeuwaoma, W.D. and Dike, V.N., (2009). Solar electricity and optimal angles for mounting solar panels in the six geopolitical zones of Nigeria. *Nigeria Journal of Physics* **21,** 144-153

Demuth, H. and Beale, M. (2002). Neural Network Toolbox User's Guide. *The MathWork Inc. MA.*

Diak, G. R., Bland, W.L, Mecikalski, J. R. and Anderson, M. C. (2000). Satellite-based estimation of longwave radiation for agricultural applications. *Agricultural and Forest Meteorology* **103**, 349-355

Dilley, A.C. and O'Brien, D. M. (1998). Estimating downward clear sky long-wave irradiance at the surface from screen temperature and precipitable water. *Quarterly Journal of the Royal Meteorological Society* **124**, 1391–1401

Dorvlo, A. S. S., Jervase, J. A. and Al-Lawati, A. (2002). Solar radiation estimates for estimation using artificial neural networks. *Applied Energy* **7,** 307-319

Duarte H.F, Dias N.L., Maggiotto S.R. (2006). Assessing daytime downward longwave radiation clear and cloudy skies in Sourthen Brasil. *Agricultural and Forest Meteorology* **193**, 171-181

Duchon, C. E. and Wilk, G. E. (1994). Field comparisons of direct and component measurements of net radiation under clear skies. *Journal of Applied Meteorology* **33,** 245-255

Dufresne, J.-L., Gantier, C., Ricchiazzi, P. and Fouquart, Y. (2002). Longwave scattering effects of mineral aerosols. *Journal of Atmospheric Sciences* **59**, 1959-1966

Edwards, D. and Hamson, M. (1989). Guide to mathematical modelling. *London, Macmillian*

Efimova, N. A. (1961). On methods of calculating monthly values of net long wave radiation. *Meteorologiya Gidrologiya* **10**, 28–33

Ellington, R. G. (1995). Surface downward fluxes from satellite observations: a critical review. *Remote Sensing of Environment* **51**, 89-97

Enz, J. W., Klink, J. C. and Baker, D. G. (1975). Solar Radiation Effects on Pyrgeometer Performance. *Journal of Applied Meteorology* **14,** 1297-1302

Ezeabasili, A.C.C., Okoro, B.U., Ezeabasili, A.I., 2014. Water Resources: Management and Strategies in Nigeria. *AFRREV STECH: International Journal of Science and Technology* **3**, 35–54

Gabathuler, M., Marty, C.A., Hanselmann, K.W. (2001). Parameterization of incoming longwave radiation in high-mountain environments. *Physical Geography* **22**, 99-114

Guest, P.S. (1998). Surface longwave radiation conditions in the eastern Weddell Sea during winter. *Journal of Geophysical Research* **103**, 30761-30771

Harris, I. and Priester, W. (1962). Time-dependent structure of the upper atmosphere. *Journal of Atmospheric Science* **19**, 287-301

Heitor, A., Biga, A. J. and Rosa, R. (1991). Thermal Radiation Components of the Energy Balance at the Ground. *Agricultural and Forest Meteorology* **54**, 29 – 48.

Hoch, S.W., Calanca, P., Philipona, R. and Ohmura, A. (2007). Year-round observation of longwave radiation flux divergence in Greenland. *Journal of Applied Meteorology* **46**, 1469-1479

Idso, S. B. (1981). A set of equations for full spectrum and 8 to 14 um and 10.5 to 12.5 um thermal radiation from cloudless skies. *Water Resources Research* **17**, 295-304

Idso, S. B. and Jackson, R. D. (1969). Thermal radiation from the atmospheres. *Journal of Geophysical Research* **74,** 5397 – 5403.

IPCC, (1996). Climate change 1995. The science of climate change. *Cambridge University Press*

Iziomon, M. G., Mayerb, H. and Matzarakisb, A. (2003). Downward atmospheric longwave irradiance under clear and cloudy skies: measurement and parameterization. *Journal of Atmospheric and Solar-Terrestrial Physics* **65**, 1107– 1116

Jacobs, J.D. (1978). Radiation climate of Broughton Island. Energy budget studies in relation to fast-ice breakup processes in Davis Strait. *Institute of Arctic and Alpine Research Occasional Paper 26, University of Colorado, Boulder, United States*, 105–120.

Jain, A. K, Murty, M. N. and Flynn, P. J. (1996). Data clustering: a review. *ACM Computing Surveys* **31**, 264-323

Jalami B. S., Cheah S. C., Rajanaida, N. and Darus, A. (1997). Improvement of palm oil through breeding and biotechnology. *Journal of the American Oil Chemists' Society* **74**, 1451-1455

Jimenez, J. I., Alados-Arboledas, L., Castro-Diezy, Y. and Ballester, G. (1987). On the estimation of longwave radiation flux from clear skies. *Theoretical and Applied Climatology* **38**, 37 – 42

John, T. C., Carnell, R. E., Crossley, J. F., Gergory, J. M., Mitchell, J. F. B., Senior, C. A., Tett, S. F. B. and Wood, R. A. (1997). The second Hadley centre coupled ocean-atmosphere GCM: model description, spin up and validation. *Climate Dynasty* **10**, 103-134

Jonsson, P., Eliasson, I., Holmer, B and Grimmond, C.S.B. (2006). Longwave incoming radiation in the tropics: results from field work in three African cites. *Theoretical and Applied Climatology* **85**, 185 – 201

Kajisak, K., Maredai, M. and Boughton, D. (1997). Transportation versus stagnation in the oil palm industry: a comparison between Malaysia and Nigeria. *Department of Agricultural Economics Staff Paper 97-5. Michigan State University East Lausing*

Kalogiron, S. A. (2000). Applications of artificial neural-networks for energy systems. *Applied Energy* **67**, 17-35

Kalogiron, S.A. (2001). Artificial neural networks in renewable energy systems applications: a review. *Renewable & Sustainable Energy Review* **5**, 372-401

Kesseler, A. and Jaeger, L. (2003). Analysis of long time series of long-wave radiation fluxes above a pine forest. *Theoretical and Applied Climatology* **74**, 179-189

König-Langlo, G. Sieger, R. Schmithüsen H, Bücker A, Richter F, Dutton EG (2013). The Baseline Surface Radiation Network and its World Radiation Monitoring Centre at the Alfred Wegener Institute. *GCOS – 174 WCRP – 24/2013*

König-Langlo, G. and Augstein, E. (1994).Parameterization of the downward long-wave radiation of the earth's surface in the polar region. *Meteorologische Zeitschrift* **3,** 343-347

Konzelmann, T., Van De Wal, R.S.W., Greuell, W., Bintanja, R., Henneken, E.A.C. and Abeouchi, A. (1994). Parameterization of global and long-wave incoming radiation for the Greenland ice sheet. *Global Planet Change* **9**, 143–164

Krasnopolsky, V. M. Fox-Rabinovitz, M.S. and Chalikov, D.V. (2004). New approach to calculation of atmospheric model physics: accurate and fast neural network emulation of longwave radiation in a climate model. *Monthly Weather Review* **133**, 1370-1383

Kreyszig, E. (1999). Advanced Engineering mathematics. *John Wiley and Sons*

Kriesel D. (2005). An introduction to neural networks. *http//: www.dkriesel.com /en /science / neural_nekworks*

Krishnaiah, T., Srinivasa, R. S., Madhumurthy, K. and Reddy, K.S.(2007). Neural network approach for modelling global solar radiation. *Journal of Applied Sciences Research* **3(10),** 1105-1111

Krose, R. and Smart, van der P. (1996). An introduction to neural networks. (8th edition). *The University of Amsterdam*.

Krut N.S., Vendrome I.F., da Rocha H.R., Chou S.C. and Cabral O. (2010). Downward longwave radiation estimates for clear and all-sky conditions in the Sertaozinho region of Sao Paulo, Brazil. *Theoretical and Applied Climatology* **99**, 115-123

Kubuta M., Iwasaka N, Kizu S, Konda M and Kutsuwada K (2002). Japanese ocean flux data sets with the use of remote sensing observations (J-OFURO). *Journal of Oceanography* **58**, 231-225

Laë, R.,Williams, S., Malam Massou, A., Morand, P. and Mikolasek, O. (2003). Review of the present state of the environment, fish stocks and fisheries of the river Niger (West Africa). *Proceedings of the second international symposium on the management of large rivers for fisheries* **1**, 199–228

Lee H.T. and Ellington R. G. (2002). Development of nonlinear statistical method for estimating downward longwave radiation at the surface from satellite observation. *Journal of Atmosphere and Oceanic Technology* **19**, 1500 – 1515

Lehmann, F.-O. and Heymann, N. *(*2005*). Unconventional mechanisms control cyclic respiratory gas release in flying* Drosophila. *The Journal of Experimental Biology* **208**, 3645 *-3654*

Lhomme, J. P., Vacher, J. J. and Rocheteau, A. (2007). Estimating downward longwave radiation on the Andean Altiplano. *Agricultural and Forest Meteorology* **145**, 139 - 148

Lhomme, J.-P. and Guilioni, L. (2004). A simple model for minimum crop temperature forecasting during nocturnal cooling. Agriculture and Forest Meteorology **123**, 55–68

Lhomme, J.-P. and Vacher, J.-J. (2002). Modelling nocturnal heat dynamics and frost mitigation in Andean raised field system. Agriculture and Forest Meteorology **112**, 179 -193

Liang, S., Li, X. and Jindi, W. (edited) (2012). Advanced remote sensing: terrestrial information extraction and application. *Academic Press*

Lin, S.J. (2004). A "Vertically Lagrangian" Finite-Volume Dynamical Core for Global Models. *Monthly Weather Review* **132**, 2293–2307

Liu J., Curry J.A., Rossow W.b. Key J.R. and Wang X. (2005). Comparison of surface radiative flux data over the Arctic Ocean. *Journal of Geophysical Research* **110**, c02015, doi: 10.1029/2004JC002381

Liu Q, Simmer C and Ruprecht E (1997). Estimating longwave net radiation at the sea surface from special sensor microwave/imager (SSM/I). *Journal of Applied Meteorology* **36**, 919-930

Lopez, G., Batlles, F. J., Tovar-Pescador, J. (2005). Selection of input parameters to model direct solarirradiance by using artificial neural networks. *Energy* **30**, 1675–1684

Maksimovich, E. and Vihma, T. (2012). The effect of surface heat fluxes on interannual variability in the spring onset of snow melt in the central Arctic Ocean. *Journal Of Geophysical Research* **117**, C07012, doi:10.1029/2011JC007220,

Marthews, T.R., Malhi, Y., Iwata, H., (2012). Calculating downward longwave radiation under clear and cloudy conditions over a tropical lowland forest site: an evaluation of model schemes for hourly data. *Theoretical and Applied Climatology* **107**, 461–477

Marty, Ch., Philipona, R., Fröhlich, C., Ohmura, A., (2002). Altitude dependence of surface radiation fluxes and cloud forcing in the alps: results from the alpine surface radiation network. *Theoretical and Applied Climatology* **72**, 135–155

Maykut, G.A. and Church, P.F. (1973). Radiation climate of Barrow, Alaska, 1962–66. *Journal of Applied Meteorology* **12**, 620–628

Mc Millan, L.M. and Govindaraju, K. (1983). Retrieval of near surface temperatures from satellite data. *Journal of Climate Applied Meteorology* **22**, 364-368

McArthur, L.J.B. (2005). Baseline surface radiation network (BSRN), operations manual version 2.1. *WMO/TD. No **1274**, WCRP/WMO*

McCulloch, W. S. and Pitts, W. (1943). A logical calculus of ideas immanent in nervous activity *The Bulletin of Mathematical Biophysics* **5**, 115–133

Minsky, M. (1991). Logical versus analogical or symbolic versus connectionist or neat versus scruffy. *AI Magazine* **65**, 34-51

Minsky, M. and Papert, S. (1989) Perceptrons 2nd edn . *MIT Press Boston*, MA

Miskolczi, F., Aro, T. O., Iziomon, M. and Pinker, R. T. (1997). Surface radiative fluxes in Sub-Sahel Africa. *Journal of Meteorology* **36**, 521-530

Morcrette, J.-J. (*2002).* Assessment of the ECMWF model cloudiness and surface radiation fields at the ARM SGP site. *Monthly Weather Review* **130**, 257-277

Muller, B., Reinhardt, J. and Strickland, M.T. (1995). Physics of neural networks: an introduction. *Springer-Verlag, Berlin Heidelberg*

NASA, "Surface Meteorology and Solar Energy Data and Information," 2011, http://eosweb.larc.nasa.gov/sse.

Niemela, S., Raisanen, P. and Savijarvi, H. (2001). Comparison of surface radiative flux parameterizations Part 1: longwave radiation. *Atmospheric Research* **58,** 1-18

Nussbaumer, E. A. and Pinker, R. T. (2012). Estimating surface long-wave radiative fluxes at global scale. *Quarterly Journal of the Royal Meteorological Society* **138**, 1083-1093

Nwokocha, C.O., Chineke, T.C. and Fagbenro, A.B., (2012). Renewable energy potentials for Nigeria: making the transition from oil and gas to solar. *Prime Journal of Physical Science* **1**, 31-39

Obot, N., Chendo, M., Erusafe, E. and Olutayo, O. (2008). Comparison of clear skies downward longwave radiation obtained through equations with that obtained from artificial neural networks. *10th World Renewable Energy Congress and Exhibition, Scotland*, 2023-2027

Ohmura, A. (2001). Physical Basis for the Temperature-Based Melt-Index. *Journal of Applied Meteorology* **40,** 753-761

Ojoina O.A. (2014). Hydrogeophysical Investigation for Groundwater in Lokoja Metropolis, Kogi State, Central Nigeria. *Journal of Geography and Geology* **6**, 81-87

Olukanni, D.O. and Salami, A.W. (2012). Assessment of Impact of Hydropower Dams Reservoir Outflow on the Downstream River Flood Regime–Nigeria's Experience. *Hydropower-Practice and Application* **Chapter 4**, 61–82

Okonkwo, G.I. and Mbajiorgu, C.C. (2010). Rainfall intensity-duration-frequency analyses for south eastern Nigeria. *CICR ejournal, manuscript* **1304**, 1-15

Omotosho J.B. and Abiodun B.J. (2007). A numerical study of moisture build-up and rainfall over West Africa. *Meteorological Application* **14**, 209 - 225

Parker, D. B. (1985). Learning logic Technical Report TR-47 Center for Computational Research in Economics and Management Science. *Massachusetts Institute of Technology, Cambridge, MA*

Pluss, C. and Ohmura, A., (1997). Longwave radiation on snow-covered mountainous surfaces. *Journal of Applied Meteorology* **36**, 818 - 824

Pomeroy, J.W., Toth, B., Granger, R.J., Hedstorm, N.R. and Essery, R.I.H. (2003). Variation in Surface Energetics during Snowmelt in a Subarctic Mountain Catchment. *Journal of Hydrometeorology* **4**, 702-791

Prata, A. J. (1996) A new long-wave formula for estimating downward clear-sky radiations at the surface. *Quarterly Journal of the Royal Meteorological Society* **122**, 1127–1151

Quinn, M.F., Alameddines, O. and Al-Jamal, K. (1984). Experimental measurements of the infra red sky radiation in Kuwait. *Applied Optics* **23**, 419-424

Reddy, K. S. and Ranjan, M. (2003). Solar resources estimation using artificial neural networks and comparison with other correlation models. *Energy Conversion and Management* **49**, 2519-2530

Rosenblatt, F. (1962). Principles of Neurodynamics. *New York Spartan*

Rumelhart, D. E. and McClelland, J. L. (1986). Parallel Distributed Processing. *Boston, MA: MIT Press*

Satterlund, D. R. (1979). An improved equation for estimating longwave radiation from the atmosphere. *Water Resources Research* **15**, 1649-1650

Sedlar, J. and Hock, R. (2009). Testing longwave radiation parameterizations under clear and overcast skies at Storglaciaren, Sweden. *The Cryosphere* **3,** 75-84

Sellers, W.D.(1965). Physical Climatology. *University of Chicago Press, Chicago*.

Sfetsos, A. and Coonick, A. H. (2000). Univariate and multivariate forecasting of hourly solar radiation with artificial intelligence techniques. *Solar Energy* **68**, 168-179

Soares, J., Oliveira, A. P., Boznar, M. Z., Mlakar, P., Escobedo, J. A., and Machado, A. J. (2004). Modelling hourly diffuse solar-radiation in the city of Sao Paulo using neural-network technique. *Applied Energy* **79**, 201-214

Sridhar, V. and Elliott, R. L., (2002). On the development of a simple downwelling longwave radiation scheme. *Agriculture and Forest Meteorology* **112**, 237–243

Stone, R. J. (1993). Improved Statistical procedure for the evaluation of solar radiation estimation models. *Solar Energy* **51**, 289-291

Suarez, M. J. (Ed) (2005). Documentation and Validation of the Goddard Earth Observing System (GEOS) Data Assimilation System–Version 4. *NASA/TM–104606,* Vol. 26

Sugita, M. and Brutsaert, W.H. (1993). Cloud effect in the estimation of instantaneous downward longwave radiation. *Water Resources Research* **29**,599–605

Swinbank, W. C. (1963). Long-wave radiation from clear skies. *Quarterly Journal of the Royal Meteorological Society* **89**, 339–348

Udo S.O. (2000). Quantification of solar heating of the dome of a pyrgeometer for a tropical location: Ilorin, Nigeria. *Journal of Atmospheric and Oceanic Technology* **17**, 995-1000

Udo, S. O. (1997). Measurement and analysis of global solar atmospheric radiation at Ilorin, Nigeria. A PhD thesis. *University of Ilorin*

Udo, S. O. (2003). Modeling of infrared radiation radiation for all skies from easy-to-measure meteorological parameters at tropical location: Ilorin, Nigeria. *Turkey Journal of Physics* **27**, 61-68

Udo, S. O. and Aro, T. O. (1999). Measurement of global solar global photosynthetically active and downward infrared radiations at Ilorin, Nigeria. *Renewable Energy* **17**, 113–122

Wang K. Wan Z. Wang P. Sparrow M. Liu J., Zhou X and Haginoya S. (2005). Estimation of surface longwave radiation and broadband sensitivity using moderate resolution imaging spectroradiometer (MODIS) land surface temperature/emissivity products. *Journal of Geophysical Research* **110**, D11109 doi:10.1029/2004JD005566

Wang, K. C. and Dickinson, R. E. (2013), Global atmospheric downward longwave radiation at the surface from ground-based observations, satellite retrievals, and reanalyses. *Reviews of Geophysics* **51**, 150–185

Wang, W. and Liang S. (2009a). Estimation of high spatial resolution clear-sky longwave downward and net radiation over land surfaces from MODIS data. *Remote Sensing of Environment* **113**, 745-754

Wang, K., and Liang, S. (2009b). Global atmospheric downward longwave radiation overland surface under all-sky conditions from 1973 to 2008. *Journal of Geophysical Research* **114**, D19101

Weldon P. J, Aldrich J. R., Klun J. A., Oliver J. E. and Debboun M. (2003). Benzoquinones from millipedes deter mosquitoes and elicit self-anointing in capuchin monkeys *(Cebus* spp.). *Naturwissenschaften* **90**, 301-304

Wendler, G and Eaton, F. (1990). Surface radiation budget at Barrow, Alaska. *Theoretical and Applied Climatology* **41**, 107-115

Wild M., Ohmura A., Gilden H., Morcrette J.-J. and Slingo A. (2001). Evaluation of downward longwave radiation in the general circulation models. *Journal of Climate* **14,** 3227-3239

WMO (1981). Meterological aspects of the utilization of solar radiation as energy source. Technical note no.172, WMO No.557

World Bank, (2006). Technology, adaptation and exports: how some developing countries got it right. *The World Bank, Washington DC*

Wu, T.Y., Mohammad, A.W., Jahim, J. Md. and Anuar, N. (2007). Palm oil mill effluent (POME) treatment and bio resources recovery using ultrafiltration membrane: effect of pressure on membrane fouling. *Biochemical Engineering Journal* **35**, 309–317

Yin, Y., Shaohong, W., Du, Z. and Qinye, Y. (2008). Radiation calibration of FAO56 Penman–Monteith model to estimate reference crop evapotranspiration in China. *Agricultural Water Management* **95**, 77 – 84

Yusoff, S. (2006). Renewable energy from palm-oil-innovation on effective utilization of waste. *Journal of Cleaner Production* **14**, 87-93

Zarzalejo, L. F., Ramirez, L. and Polo, J. (2005). Artificial intelligence techniques applied to hourly global irradiance estimation from satellite-derived cloud index. *Energy* **30**, 1685-1697

Zhang, T., Bowling, S. A. and Stamnes, K. (1997). Impact of the atmosphere on surface radiative fluxes and snowmelt in the Arctic and Subarctic. *Journal of Geophysical Research* **102**, 4287- 4302

Zhou Y. Kratz D.P., Wilber A.C. Gupta S.K. and Cess R.D. (2007). An improved algorithm for retrieving surface downwelling longwave radiation from satellite measurements. *Journal of Geophysical Research* **112**, D15102. Doi:10.1029/2006JD008159